

An-Najah National University
Faculty of Graduate Studies

**HPLC Determination of Four Textile Dyes and
Studying Their Degradation Using
Spectrophotometric Technique**

By

Safwat Mohammad Abdul Azeez Saleh

Supervisors

Dr. Nidal A. Za'tar
Prof. Maher A. Abu-Eid

*Submitted in Partial Fulfillment of the Requirements for the Degree of
Master of Science in Chemistry, Faculty of Graduate Studies, at An-Najah
National University, Nablus, Palestine.*

2005



HPLC Determination of Four Textile Dyes and Studying Their Degradation Using Spectrophotometric Technique

By

Safwat Mohammad Abdul Azeez Saleh

This Thesis was defended successfully on 22/5/2005 and approved by:

Committee Members

1. Dr. Nidal Za'tar - Advisor
2. Prof. Maher A. Abu-Eid - Advisor
3. Dr. Raqi M. Shubietah - Internal examiner
4. Dr. Nizam A. Diab - External examiner

Signature

Nidal Za'tar

~~M. Natsel~~

Raqi M. Shubietah

M. Diab

III

DEDICATION

To

My Mother

My Father

My Brothers and Sister

With Great Love

ACKNOWLEDGMENT

After thanking Allah, who granted me the power to finish this work, I would like to express my great thanks and gratitude to my supervisors Dr. Nidal Za'tar and Prof. Maher A. Abu-Ebu-Eid for their supervision, encouragement and guidance throughout this study.

I really appreciate the help of all the staff members of the chemistry labrotary especially, Mr. Mahmoud Al-Shammaly. I thank also the staff of Chemical, Biological and Drugs Analysis Center.

At last my great thanks, gratitude and love to my mother, father, brothers and sister and to all my friends for their support, and their sincere encouragement.

List of Contents

	Content	Page No.
	Committee Members	II
	Dedication	III
	Acknowledgment	IV
	List of Contents	V
	List of Tables	VII
	List of Figures	VIII
	Abstract	XV
	Chapter One: Introduction	1
1.1	History of Dyestuffs and Dyeing	2
1.2	Textile dyes	2
1.3	Dyes classification	3
1.4	Dyes, environmental concern	3
1.5	Quantitative determination of textile dyes	4
1.5.1	Chromatographic determination of textile dyes	5
1.5.2	Spectrophotometric determination of textile dyes	8
1.5.3	Voltammetric determination of textile dyes	10
1.5.4	Capillary electrophoresis determination of textile dyes	12
1.5.5	Other Spectroscopic techniques used for determination of textile dyes	13
1.6	Dyes removal techniques	14
1.6.1	Sorption and ion exchange	14
1.6.2	Advanced oxidation processes	16
1.6.3	Biological techniques	18
1.6.4	Coagulation / Flocculation	20
1.6.5	Electrolysis	20
1.6.6	Membrane filtration	21
1.6.7	Removal of textile dyes by metals	23
1.6.8	Ultra sonic methods	24
1.7	Aims of this work	25
	Chapter Two: Experimental	26
2.1	Chemicals and reagents	27
2.2	Standard dyes solutions	27
2.3	Mobile phase	27
2.4	Instrumentation	27
2.5	HPLC analysis	28
2.6	Identification	28
2.7	Degradation of textile dyes using metals	29
	Chapter Three: Results and Discussion	31

	Part I : HPLC analysis	32
3.1	Absorption spectra	32
3.2	HPLC Results	32
3.2.1	Retention time	32
3.2.2	Effect of CTAB concentration in the mobile phase on the retention time	35
3.2.3	Effect of pH on the retention time	36
3.2.4	Effect of acetonitrile: water ratio in the mobile phase on the retention time	37
3.3	Calibration curves	37
3.4	Quantitative determination of Direct Red 81, Direct Blue 15, Direct Black 22 and Direct Orange 34 dyes in presence of each other using HPLC technique	40
3.5	The resolution (R_s) of the method	45
3.6	Analysis of real water samples	46
	Part II: Kinetic results of degradation	
3.7	Kinetic results of degradation	48
3.7.1	Effect of amount of iron and aluminum on degradation of Direct dyes in aqueous solution	48
3.7.2	Effect of concentration of dye on degradation of aqueous Direct dyes	53
3.7.3	Effect of temperature on degradation of Direct dyes	60
3.7.4	Effect of pH on degradation of Direct dyes	65
3.7.5	Effect of agitation speed on degradation of Direct dyes	70
3.7.6	Effect of metals nature on degradation of aqueous Direct dyes	75
3.8	Degradation mechanism of Direct azo dyes	78
3.9	Results of degradation of Direct azo dyes	79
	References	85
	Abstract in Arabic	ب

List of Tables

Table		Page No.
Table 1	Characterization of dyes studied in this work.	29
Table 3.2.2	Effect of CTAB concentration in the mobile phase on the retention time of dyes.	36
Table 3.2.3	Effect of pH on the retention time of dyes	36
Table 3.2.4	Effect of acetonitrile: water ratio in the mobile phase on the retention time of dyes.	37
Table 3.3.1	Details of conditions for HPLC analysis	40
Table 3.5	Resolution (R_s) in the separation of the four Direct dyes	46
Table 3.7.2.1	Observed reaction rate constants for the four Direct dyes degradation in Fe^0 - H_2O system	55
Table 3.7.2.2	Observed reaction rate constants for the four Direct dyes degradation in Al^0 - H_2O system.	55
Table 3.7.3.1	Thermodynamic parameters for degradation of Direct dyes in Fe^0 - H_2O system.	
Table 3.7.3.2	Thermodynamic parameters for degradation of Direct dyes in Al^0 - H_2O system.	61
Table 3.7.6	Standard oxidation potentials ($25^\circ C$)	
Table 3.9	The -N=N- absorption band of the four Direct dyes before degradation.	79

List of Figures

Figure		Page No
Figure 3.1	Absorption spectra a, b, c and d of Direct Red 81, Direct Blue 15 Direct Black 22 and Direct Orange dyes, respectively.	32
Figure 3.2.1.a	HPLC chromatogram for 20ppm Direct Red 81 dye, [wavelength 510 nm, mobile phase 0.45 M CTAB in acetonitrile: water (60: 40, v/v)].	33
Figure 3.2.1.b	HPLC chromatogram for 20ppm Direct Blue 15 dye, [wavelength 607 nm, mobile phase 0.45 M CTAB in acetonitrile: water (60: 40, v/v)].	34
Figure 3.2.1.c	HPLC chromatogram for 50ppm Direct Black 22 dye, [wavelength 484 nm, mobile phase 0.45 M CTAB in acetonitrile: water (60: 40, v/v)].	34
Figure 3.2.1.d	HPLC chromatogram for 20 ppm Direct Orange 34 dye, [wavelength 411 nm, mobile phase 0.45 M CTAB in acetonitrile: water (60: 40, v/v)].	35
Figure 3.3.a	Calibration curve for HPLC determination of Direct Red 81 [wavelength (510 nm), mobile phase acetonitrile: water (60: 40, v/v) containing 0.45 CTAB].	38
Figure 3.3.b	Calibration curve for HPLC determination of Direct Blue 15 [wavelength (607 nm), mobile phase acetonitrile: water (60: 40, v/v) containing 0.45 CTAB].	38
Figure 3.3.c	Calibration curve for HPLC determination of direct Black 22 [wavelength (484 nm), mobile phase acetonitrile: water (60: 40, v/v) containing 0.45 CTAB].	39
Figure 3.3.d	Calibration curve for HPLC determination of Direct Orange 34 [wavelength (411 nm), mobile phase acetonitrile: water (60: 40, v/v) containing 0.45 CTAB].	39
Figure 3.4.a	HPLC Chromatogram for 20ppm Direct Red 81 dye, [Wavelength 510 nm, 607 nm, 484 nm and 411 nm, mobile phase 0.45 M CTAB in acetonitrile: water (60: 40, v/v)].	41
Figure 3.4.b	HPLC Chromatogram for 20ppm Direct Blue 15 dye, [Wavelength 510 nm, 607 nm, 484 nm and 411 nm, mobile phase 0.45 M CTAB in acetonitrile: water (60: 40v/v)].	42

Figure 3.4.c	HPLC chromatogram for 50ppm Direct Black 22 dye, [wavelength 510nm, 607nm, 484nm, and 411nm, mobile phase 0.45 M CTAB in acetonitrile: water (60: 40, v/v)].	42
Figure 3.4.d	HPLC Chromatogram for 20ppm Direct Orange 34 dye, [wavelength 510 nm, 607nm, 484nm and 411nm, mobile phase 0.45 M CTAB in acetonitrile: water (60: 40, v/v)].	43
Figure 3.4.e	HPLC quantitative determination of 20ppm Direct Red 81, 20ppm Direct Blue 15, 50ppm Direct Black 22 and 20ppm Direct Orange 34 in the presence of each other at the conditions recommend for Direct red 81	43
Figure 3.4.f	HPLC quantitative determination of 20ppm Direct Red 81, 20ppm Direct Blue 15, 50ppm Direct Black 22 and 20ppm Direct Orange 34 in the presence of each other at the conditions recommend for Direct Blue 15.	44
Figure 3.4.g	HPLC quantitative determination of 20ppm Direct 81, 20ppm Direct Blue 15, 50ppm Direct Black 22 and 20ppm Direct Orange 34 in the presence of each other at the conditions recommend for Direct Black 22.	44
Figure 3.4.h	HPLC quantitative determination of 20ppm Direct Red 81, 20ppm Direct Blue 15, 50ppm Direct Black 22 and 20ppm Direct Orange 34 in the presence of each other at the conditions recommend for Direct Orange 34.	45
Figure 3.6.A -C	Typical chromatograms for detection and quantitative determination of the four dyes (Direct Red 81, Direct Blue 15, Direct Black 22 and Direct Orange 34) in three real samples of ground water collected from Wad Assajor, Khallet Asenan and Khallet Issa wells. Conditions: [wavelength 510 nm, 607nm, 484nm and 411 nm, mobile phase 0.45 M CTAB in acetonitrile : water (60: 40, v/v)].	47
Figure 3.7.1	Absorption spectra of 20ppm Direct Blue 15 solution containing 1 gm iron metal at pH 6.1 and at different reaction time (a-h) curves after (0,3,6,9,12,15,18,21) min respectively	49
Figure 3.7.1.a	Effect of changing the amount of iron on the rate of degradation of Direct Red 81 dye [[dye] =20ppm, temperature (25±2°C)].	49
Figure 3.7.1.b	Effect of changing the amount of iron on the rate	50

	of degradation of Direct Blue 15 dye [[dye] =20ppm, temperature (25±2°C)].	
Figure 3.7.1.c	Effect of changing the amount of iron on the rate of degradation of Direct Black 22 dye [[dye] =50ppm, temperature (25±2°C)].	50
Figure 3.7.1.d	Effect of changing the amount of iron on the rate of degradation of Direct Orange 34 dye [[dye] =20ppm, temperature (25±2°C)].	51
Figure 3.7.1.e	Effect of changing the amount of aluminum on the rate of degradation of Direct Red 81 dye [[dye] =20ppm, temperature (25±2°C)].	51
Figure 3.7.1.f	Effect of changing the amount of aluminum on the rate of degradation of Direct Blue 15 dye [[dye] =20ppm, temperature (25±2°C)].	52
Figure 3.7.1.g	Effect of changing the amount of aluminum on the rate of degradation of Direct Black 22 dye [[dye] =50ppm, temperature (25±2°C)].	52
Figure 3.7.1.h	Effect of changing the amount of aluminum on the rate of degradation of Direct Orange 34 dye [[dye] =20ppm, temperature (25±2°C)].	53
Figure 3.7.2	Langmuir adsorption of direct Black 22 dye.	54
Figure 3.7.2.a	Effect of changing the dye concentration on the rate of degradation of Direct Red 81 dye [Fe amount =1 g, temperature (25±2°C)].	56
Figure 3.7.2.b	Effect of changing the dye concentration on the rate of degradation of Direct Blue 15 dye [Fe amount =1 g, temperature (25±2°C)].	56
Figure 3.7.2.c	Effect of changing the dye concentration on the rate of degradation of Direct Black 22 dye [Fe amount =1 g, temperature (25±2°C)].	57
Figure 3.7.2.d	Effect of changing the dye concentration on the rate of degradation of Direct Orange 34 dye [Fe amount =1 g, temperature (25±2°C)].	57
Figure 3.7.2.e	Effect of changing the dye concentration on the rate of degradation of Direct Red 81 dye [Al amount =0.5g, temperature (25±2°C)].	58
Figure 3.7.2.f	Effect of changing the dye concentration on the rate of degradation of Direct Blue 15 dye [Al amount =0.5g, temperature (25±2°C)].	58
Figure 3.7.2.g	Effect of changing the dye concentration on the rate of degradation of Direct Black 22 dye [Al amount =0.5 g, temperature (25±2°C)].	59
Figure 3.7.2.h	Effect of changing the dye concentration on the rate of degradation of Direct Orange 34 dye [Al amount =0.5 g, temperature (25±2°C)].	59

Figure 3.7.3.a	Effect of temperature on degradation of Direct Red 81 dye. Conditions: Fe amount = 1 g, pH =6.1 and [dye] =20ppm.	61
Figure 3.7.3.b	Effect of temperature on degradation of Direct Blue 15 dye. Conditions: Fe amount = 1 g, pH =6.1 and [dye] =20ppm	62
Figure 3.7.3.c	Effect of temperature on degradation of Direct Black 22 dyes. Conditions: Fe amount = 1 g, pH =6.1 and [dye] =50ppm.	62
Figure 3.7.3.d	Effect of temperature on degradation of Direct Orange 34 dye. Conditions: Fe amount = 1 g, pH =6.1 and [dye] =20ppm	63
Figure 3.7.3.e	Effect of temperature on degradation of Direct Red 81 dye. Conditions: Al amount = 0.5 g, pH =6.1 and [dye] =20ppm.	63
Figure 3.7.3.f	Effect of temperature on degradation of Direct Blue 15 dyes. Conditions: Al amount = 0.5 g, pH =6.1 and [dye] =20ppm.	64
Figure 3.7.3.g	Effect of temperature on degradation of Direct Black 22 dye. Conditions: Al amount = 0.5 g, pH =6.1 and [dye] =50ppm.	64
Figure 3.7.3.h	Effect of temperature on degradation of Direct Orange 34 dye. Conditions: Al amount = 0.5 g, pH =6.1 and [dye] =20ppm. Effect of variable pH on degradation of Direct Red 81 dye. Conditions: Fe amount = 1 g, [dye] = 20ppm and temperature ($25 \pm 2^{\circ}\text{C}$).	65
Figure 3.7.4.a	Effect of variable pH on degradation of Direct Blue 15 dye. Conditions: Fe amount = 1 g, [dye] = 20ppm and temperature ($25 \pm 2^{\circ}\text{C}$).	66
Figure 3.7.4.b	Effect of variable pH on degradation of Direct Black 22 dye. Conditions: Fe amount = 1 g, [dye] = 50ppm and temperature ($25 \pm 2^{\circ}\text{C}$).	67
Figure 3.7.4.c	Effect of variable pH on degradation of Direct Orange 34 dye. Conditions: Fe amount = 1 g, [dye] = 20ppm and temperature ($25 \pm 2^{\circ}\text{C}$).	67
Figure 3.7.4.d	Effect of variable pH on degradation of Direct Red 81 dye. Conditions: Al amount = 0.5 g, [dye] = 20ppm and temperature ($25 \pm 2^{\circ}\text{C}$).	68
Figure 3.7.4.e	Effect of variable pH on degradation of Direct Blue 15 dye. Conditions: Al amount = 0.5 g, [dye] = 20ppm and temperature ($25 \pm 2^{\circ}\text{C}$).	68
Figure 3.7.4.f	Effect of variable pH on degradation of Direct Black 22 dye. Conditions: Al amount = 0.5 g, [dye] = 50ppm and temperature ($25 \pm 2^{\circ}\text{C}$).	69

Figure 3.7.4.g	Effect of variable pH on degradation of Direct Orange 34 dye. Conditions: Al amount = 0.5 g, [dye] = 20ppm and temperature ($25\pm 2^{\circ}\text{C}$).	69
Figure 3.7.4.h	Effect of agitation speed on degradation of Direct Red 81 dye. Conditions: Fe amount = 1 g, [dye] = 20ppm and temperature ($25\pm 2^{\circ}\text{C}$).	70
Figure 3.7.5.a	Effect of agitation speed on degradation of Direct Blue 15 dye. Conditions: Fe amount = 1 g, [dye] = 20ppm and temperature ($25\pm 2^{\circ}\text{C}$).	71
Figure 3.7.5.b	Effect of agitation speed on degradation of Direct Black 22 dye. Conditions: Fe amount = 1 g, [dye] = 50ppm and temperature ($25\pm 2^{\circ}\text{C}$).	71
Figure 3.7.5.c	Effect of agitation speed on degradation of Direct Orange 34 dye. Conditions: Fe amount = 1 g, [dye] = 20ppm and temperature ($25\pm 2^{\circ}\text{C}$).	72
Figure 3.7.5.d	Effect of agitation speed on degradation of Direct Red 81 dye. Conditions: Al amount = 0.5 g, [dye] = 20ppm and temperature ($25\pm 2^{\circ}\text{C}$).	72
Figure 3.7.5.e	Effect of agitation speed on degradation of Direct Blue 15 dye. Conditions: Al amount = 0.5 gm, [dye] = 20ppm and temperature ($25\pm 2^{\circ}\text{C}$).	73
Figure 3.7.5.f	Effect of agitation speed on degradation of Direct Black 22 dye. Conditions: Al amount = 0.5 g, [dye] = 50ppm and temperature ($25\pm 2^{\circ}\text{C}$).	73
Figure 3.7.5.g	Effect of agitation speed on degradation of Direct Orange 34 dye. Conditions: Al amount = 0.5 gm, [dye] = 20ppm and temperature ($25\pm 2^{\circ}\text{C}$).	74
Figure 3.7.5.h	Effect of metals on degradation of Direct Red 81 dye. Conditions: metal amount = 1 g, [dye] = 20ppm, pH = 6.1 and temperature ($25\pm 2^{\circ}\text{C}$).	74
Figure 3.7.6.a	Effect of metals on degradation of Direct Blue 15 dye. Conditions: metal amount = 1 gm, [dye] = 20ppm, pH = 6.1 and temperature ($25\pm 2^{\circ}\text{C}$).	76
Figure 3.7.6.b	Effect of metals on degradation of Direct Black dye. Conditions: metal amount = 1 g, [dye] = 50ppm, pH = 6.1 and temperature ($25\pm 2^{\circ}\text{C}$).	76
Figure 3.7.6.c	Effect of metals on degradation of Direct Orange 34 dye. Conditions: metal amount = 1 g, [dye] = 20ppm, pH = 6.1 and temperature ($25\pm 2^{\circ}\text{C}$).	77
Figure 3.7.6.d	Degradation mechanism of direct Red 81 dye in $\text{Fe}^{\circ}\text{-H}_2\text{O}$ system.	77
Figure 3.8	IR spectrum for Direct Red 81 dye before degradation and after degradation by iron.	79
Figure 3.9.a	IR spectrum for Direct Red 81 dye before degradation and after degradation by iron.	80

Figure 3.9.b	IR spectrum for Direct Blue 15 dye before degradation and after degradation by iron.	81
Figure 3.9.c	IR spectrum for Direct Black 22 dye before degradation and after degradation by iron.	82
Figure 3.9.d	IR spectrum for Direct Orange 34 dye before degradation and after degradation by iron.	83
Figure 3.9.e	Absorption spectrum for Direct Red 81 dye before degradation and after degradation by iron.	84

**HPLC Determination of Four Textile Dyes and
Studying Their Degradation Using
Spectrophotometric Technique**

By

Safwat Mohammad Abdul Azeez Saleh

Supervisors

Dr. Nidal Za'tar

Prof. Maher A. Abu-Eid

Abstract

In the present work, a simple and a sensitive HPLC method was developed for quantitative determination of four Direct textile dyes (Direct Red 81, Direct Blue 15, Direct Black 22 and Direct Orange 34).

The maximum absorbance value for the above mentioned dyes were found to be at 510 nm, 607 nm, 484 nm and 411 nm, with retention times of 15.4, 8.8, 5.8 and 12.7 min, respectively.

The mobile phase used was consisting of acetonitrile: water (60:40, v/v) containing 0.45 M N-cetyl-N,N,N-trimethyl ammonium bromide (CTAB). RP C₁₈ column was used with a flow rate of 0.5ml/min.

Calibration graphs were found to be linear over the ranges of 0.3–10ppm, 10–30ppm, 0.5–10ppm and 1–12ppm for Direct Red 81, Direct Blue 15, Direct Black 22 and Direct Orange 34, respectively, with limit of detection 0.3ppm, 10ppm, 0.5ppm and 1ppm. The relative standard deviations (RSD%) were found to be 0.92 %, 0.83 %, 1.13 % and 0.34 %, respectively (n=3) with concentrations of 10ppm of each dye. The effect of pH, CTAB concentration and acetonitrile: water ratios (v/v) in the mobile phase on the determination of the four Direct azo dyes were investigated.

The reducing degradation kinetics of the four Direct dyes; Direct Red 81, Direct Blue 15, Direct Black 22 and Direct Orange 34 by zero– valent

iron and aluminum metals in aqueous solutions were studied. Effective degradation was achieved when using Al compared to Fe. The results show that the rate of degradation is affected by acidity, amount of iron and aluminum, temperature and speed of solution agitation.

The effect of metals nature on degradation of the four Direct azo dyes was studied. The following metals were used in this study (Mn, Ni, Co, Zn, Mg and Cu). The obtained results showed that using Cu do not effects on degradation rate, where using Al, Mg give a higher degradation rate compared to iron.

Chapter One
Introduction

1.1 History of dyestuffs and dyeing

Ever since primitive people could create, they have been endeavoring to add color to the world around them. They used natural matter to stain hides, decorate shells and feathers, and paint their story on the walls of ancient caves. Scientists have been able to date the black, white, yellow and reddish pigments made from ochre used by primitive man in cave paintings to over 15,000 BCE. With the development of fixed settlements and agriculture around 7,000-2,000 BCE man began to produce and use textiles, and would therefore add color to them as well (Grierson, 1989). Organic natural colorants have a timeless history of application, especially as textile dyes.

The first synthetic dye was discovered by William Henry Perkin, a student at the Royal College of Chemistry. He tried to make the drug quinine from aniline (a chemical found in coal). The experiment produced a thick dark sludge. Instead of throwing it away, Perkin tried diluting it with alcohol and found that the solution was purple. He discovered that it would dye silk and that it was a 'fast' dye, resistant to washing and to the fading effects of light.

This concept of research and development was soon to be followed by others and new dyes began to appear on the market, a process that was strongly stimulated by Kekule's discovery of the molecular structure of benzene in 1865. In the beginning of the 20th century, synthetic dyestuffs had almost completely supplanted natural dyes (Welham, 2000).

1.2 Textile dyes

Synthetic dyes are extensively used in textile dyeing, paper printing, color photography, pharmaceutical, food, cosmetics and other industries

(Rafi, Franklin and Cerniglia, 1990). Approximately, 10,000 different dyes and pigments are used industrially, and over 7×10^5 tons of synthetic dyes are produced annually worldwide. In 1991, the world production of dyes was estimated 668,000 tons (Ollgaard *et al.*, 1998) of which azo dyes contributed 70% (ETAD, 1997). During dying process, a substantial amount of azo dye is lost in wastewater (Ollgaard *et al.*, 1998). Zollinger, (1987) reported that about 10-15% of dyes were lost in effluent during dyeing process.

Major classes of synthetic dyes include azo, anthraquinon and triaryl-methane dyes, and many of them are toxic or even carcinogenic compounds with long turnover times. With the increased use of a wide variety of dyes, pollution by dye's wastewater is becoming increasingly alarming.

1.3 Dyes classification

All aromatic compounds absorb electromagnetic energy but only those that absorb light with wavelengths in the visible range (~350-850 nm) are colored. Dyes contain chromophores (delocalized electron systems with conjugated double bonds) and auxochromes (electron-withdrawing or electron-donating substituents that intensify the color of the chromophore by altering the overall energy of the electron system). Usual chromophores are $-\text{C}=\text{C}-$, $-\text{C}=\text{N}-$, $-\text{C}=\text{O}$, $-\text{N}=\text{N}-$, $-\text{NO}_2$ and quinoid rings, usual auxochromes are $-\text{NH}_3$, $-\text{COOH}$, $-\text{SO}_3\text{H}$ and $-\text{OH}$ (Zee, 2002).

Based on chemical structure of chromophores, 20-30 different groups of dyes can be discerned. Azo (monoazo, diazo, triazo, polyazo), anthraquinone, phthalocyanine, and triarylmethane dyes are quantitatively the most important groups.

Most of the commercial available azo dyes are in fact formulations of several components in order to improve the technical properties of the dyeing process. The majority of industrial important azo dyes belong to the following classes: Acid dyes, Basic dyes, Direct dyes, Disperse dyes, Mordant dyes, Reactive dyes and Solvent dyes. The Acid, Basic, Direct and Reactive azo dyes are ionic dyes (Anliker, Clarke and Moser, 1981).

1.4 Dyes, environmental concern

Wastewater from the textile industry is a complex mixture of many polluting substances ranging from organochlorine-based pesticides to heavy metals associated with dyes or the dyeing process (Correia, Stephenson and Judd, 1994). Many dyes are visible in water at concentrations as low as 1mg l^{-1} . Textile-processing wastewaters, typically with dye content in the range $10\text{-}200\text{mg l}^{-1}$ (O'Neill *et al.*, 1999) are therefore usually highly colored and discharge in open waters presents an aesthetic problem. As dyes designed to be chemically and photolytically stable, they are highly persistent in natural environments.

The majority of dyes pose a potential health hazard to all forms of life (Prakash and Solank). These dyes may cause allergic responses, skin dermatoses, eczema (Su and Horton, 1998), and may affect the liver (Jaskot and Costa), the lungs, the vasco-circulatory system, the immune system and the reproductive system (Nikulina, Deveikis and Pyshnov, 1995) of experimental animals as well as humans.

Textile dyes have found to be toxic, genotoxic and mutagenic in various test systems. Dyes with azo bonds nitro- or amino-groups are carcinogenic, causing tumors of liver and urinary bladder in experimental animals (Dipple and Bigger, 1991). However, reduction of azo dyes, i.e.

cleavage of the dye's azo linkage(s), leads to formation of aromatic amines and several aromatic amines are known mutagens and carcinogens. In mammals, metabolic activation (reduction) of azo dyes is mainly due to bacterial activity in the anaerobic parts of the lower gastrointestinal tract. Various other organs, especially the liver and the kidneys, can, however, also reduce azo dyes (Zee, 2002). The toxicity of aromatic amines depends on the nature and location of other substituents. As an example the substitution with nitro, methyl or methoxy groups or halogen atoms may increase the toxicity; whereas substitution with carboxyl or sulphonate groups generally lower the toxicity (Chung and Cerniglia, 1992). As most soluble commercial azo dyestuffs contain one or more sulphonate groups, insight in the potentials danger of sulphonated aromatic amines is particularly important. Sulphonated aromatic amines, in contrast to some of their unsulphonated analogues, have generally no or very low genotoxic and tumorigenic potential (Jung, Steinle and Ankliker, 1992).

1.5 Quantitative determination of textile dyes

Several methods have been reported for determination of textile dyes, such as chromatographic, spectrophotometric, voltammetric and capillary electrophoresis.

1.5.1 Chromatographic determination of textile dyes

In 1991 Yinon and Saar, used HPLC technique to analyze series of disperse dyes extracted from polyester and cellulose fibers, a basic dye from orlon fiber and a vat dye from denim. Molecular characterization of each dye was obtained from the extract of a single fiber, 5-10 mm long. This was achieved by HPLC separation followed by mass spectrometry identification of the separated dyes.

Davila-Jimenez *et al.*, (2000) exposed individually several textile dyes to electrochemical treatment. Chromaticity variation and the formation of degradation products were followed using UV spectrophotometer and HPLC techniques. The dyes studied belong to the azo, methine, indigo, and natural and arylmethane classes.

Rafols and Barcelo (1997) developed new method for determination of the disulphonated azo dyes (Acid Red 1, Mordant Red 9, Acid Red 13, Acid Red 14, Acid Red 73, Acid Yellow 28, Direct Yellow 28, and Acid Blue 113) and of the monosulphonated azo dyes (Mordant Yellow 8, Mordant Black 11 and Mordant Black 17). The method is based on using liquid chromatography- atmospheric pressure chemical ionization (APCI), mass spectrometry (MS) with positive ion (PI) and negative ion (NI) modes of operation and liquid chromatography- high flow pneumatically assisted electrospray (ES) mass spectrometry with negative mode.

High fragmentation was observed when using APCI with losses of one or two SO_3Na groups, either attached to one ring or two different rings. Losses of Na and 2Na are common to all techniques used high flow ES was the most sensitive technique for all the dyes studied, except for Mordant Red 9 with a linear range varying from 1-3 to 700-800 ppb. APCI using negative ion mode was one order of magnitude less sensitive than ES, with a linear range varying from 50-70 to 2000-3000 ppb, whereas, positive ion mode APCI-MS showed the poorest linear range and sensitivity. The determination of Direct Yellow 28 and Acid Blue 113 in water samples was also reported by pre-concentrating 500ml of water with solid- phase disk extraction followed by LC-high flow pneumatically assisted ES-MS.

Novotna *et al.*, (1999) developed a reversed-phase HPLC technique for identification and quantization of nine natural quinone dyes applied to

historical textile fibers. A purospher RP18e column was used with a convex gradient of methanol in a mobile phase of 0.1M aqueous citrate buffer (pH 2.5) and diode-array detection at 270 nm. For identification of alizarin, purpurin and xanthopurpurin, occurring together in the madder plant, an isocratic method was used with a methanol- 0.2M acetate buffer (pH 4.3) (75: 25) as the mobile phase. After an acid extraction of textile fibers and the analysis of the extracts, alizarin and purpurin were identified and quantitated in three fibers. The limits of detection obtained are similar, ranging from 0.6 ppb (xanthopurpurin – isocratic separation at 254 nm) to 12 ppb (carminic acid – gradient separation at 270 nm). The repeatability is satisfactory, as typical RSDs (n=6) amount to 3.3% for the isocratic and 6.6% for the gradient elution separation.

Perez-Urquiza, Prat and Beltran (2000) presented an ion-interaction high- performance liquid chromatographic method for quick separation and determination of the sulphonated dye Acid Yellow 1, and the sulphonated azo dyes Acid Orange 7, Acid Orange 12, Acid Orange 52, Acid Red 2, Acid Red 26, Acid Red 27, and Acid Red 88. RP-ODS stationary phase is used, and the mobile phase contains an acetonitrile-phosphate buffer (27: 73) mixture at pH 6.7, containing 2.4mM butylamine as ion interaction reagent. Good separations were obtained using isocratic elution and spectrophotometric detection at 460 nm. The detection limits for the eight dyes ranged from 7 - 28ppb for an injection volume of 100 μ l. This method allows the quantification of the studied dyes in spiked tap water samples in conjunction with solid-phase extraction. It allows the analysis of water samples containing between 0.3 and 1.2ppb of the studied dyes.

Fisher, Bischof and Rabe (1990) investigated the separation and identification of complex mixtures of natural and synthetic textile dyes

using HPLC with diode array detection. Separation was carried out on a reversed phase column with acetonitrile-phosphoric acid gradient elution. The results showed that the anthraquinones from madder root and the insect dye cocheneal present in ancient red dyes can easily be distinguished from azo – dyes present in later textile fibers.

Tayem, (2002) developed a simple HPLC method for quantitative determination of three dyes (Blue R Special, Red RB 198 and Yellow RNL 107). The HPLC method is based on using a mobile phase consisting of acetonitrile: water (60:40, v/v) containing 0.45M N-Cetyl-N,N,N-trimethylammonium bromide (CTAB) and buffered to pH=7.92, RP-C18 column was used with a flow rate of 0.6mL/min. The retention times for Blue R Special, Red RB 198 and Yellow RNL 107 were found to be 5.4 min, 7.8 min and 2.3 min with a range of a linear of 0.10-5.00ppm, 0.10-1.20ppm and 0.05-1.50ppm for the three mentioned dyes, respectively. The relative standard deviations were found to be (5.21%, 4.75% and 3.10%) for these dyes, respectively (n=3).

Zubi, (2003) investigated the HPLC method for the determination of three dyes (Acid Orange 7, Acid Orange 10 and Acid Orange 12) and their retention times were found to be 2.8 min, 4.8 min and 3.1 min, respectively. Calibration graphs for the determination of the studied dyes were linear in the range 0.05-4.0ppm, 0.10-4.0ppm and 0.10-4.0ppm with relative standard deviation of 3.8%, 4.1% and 4.2% (n=3) and detection limit of 0.03, 0.05 and 0.05ppm, respectively.

1.5.2 Spectrophotometric determination of textile dyes

Bae, Motomura and Morita (1997) investigated the adsorption of three anionic dyes (Reactive Red 120, a monochlorotriazinyl red dye and Direct

Blue 1) on cellulose from a neutral dye bath at 80°C over a wide concentration range of sodium sulfate using UV-Spectrophotometric technique. The standard chemical potential differences between the cellulose and solution phases, or the standard affinity, for these dyes were calculated on the basis of the Donnan equilibrium model. Reactive red 120 and Direct Blue 1 showed saturation in the adsorption isotherm, while Red E had a likeness to other dyes when a high salt concentration was used.

Harbin, Going and Breen, (1990) developed a novel spectrophotometric method to estimate the total amounts of textile dyes on air monitoring filters in industrial hygiene applications. The method was developed in response to the complexity of the samples and the low levels of dyes which were anticipated to be present. By measuring the total sample absorbance over the wavelength interval, an estimate of the quantity of dyes present can be determined from a Beer's law calculation using the average spectral absorptivity constant. Feasibility of the method was demonstrated on dye mixture solutions containing both 10 and 20 dyes, with as many as five different dye classes being present simultaneously. Dye recovery experiments established that the air filter extraction procedure produced recoveries in the 78-101% range for 40 to 160 µg total amounts. Simulated textile plant air filters were prepared which contained 18 dyes from three dye classes at levels ranging from 40 to 180 µg total amounts. After correcting for dye recovery, the total dye estimates were observed to have relative errors ranging from 0 to 24%. The primary factors affecting the accuracy of the total dye estimation method are the number of dyes in the mixture, the standard deviation, the spectral absorptivity constants, and the levels of dyes present on the air filter.

1.5.3 Voltammetric determination of textile dyes

Govert, Temmerman and Kiekens, (1999) reported a linear sweep and cyclic voltammetric studies of indigo, indanthrene dye and sodium dithionite in alkaline solutions. The results were applied to develop amperometric determination methods for these Vat dyes and reducing agent. On different electrode materials (Au, glassy carbon, Pd, Pt) the reduced dyes give an anodic voltammetric signal. This reaction referring to the oxidation of dyestuff is concentration, rotation and potential scan rate dependent. In a concentration range from detection limit up to 1 g l^{-1} , indigo gives oxidative currents at potentials more positive than -0.85 V vs SCE . The voltammetric wave of indigo is characterized by repeatable limiting currents measured at a potential of -0.6 V vs SCE in the plateau. Up to a concentration of 1 g l^{-1} the limiting anodic currents are dependent on concentration and rotation rate for a rotating disc electrode. Adsorption of oxidized dyestuff on the electrode surface was found to impede the chronoamperometric determination. By introduce potential steps, in situ cleaning of the electrode surface leads to a repetitive renewal and activation of the electrode surface. The use of multi-pulse amperometric technique allows to measure in a semicontinuous way a voltammetric signal that is proportional to the dye concentration.

Zanoni *et al.*, (1997) determined two anthraquinone based chlorotriazine reactive dyes, Protion Blue Mx-R (PB) and Cibacorn Blue 3GA (CB) at nanomolar level using cathodic stripping voltametry. When the differential pulse Voltammetric stripping mode is used no peak is obtained for the reduction of the anthraquinone moiety in these dyes, although the signal is present when the linear sweep mode is used. The absence of this peak in the differential pulse mode is believed to occur

because, when this group is reduced in the adsorbed state on application of the potential pulse, it is reduced so rapidly that reduction is complete before the current is monitored at the end of the pulse.

The differential pulse signal is present for the reduction of the chlorotriazine active groups. The differential pulse peak for the anthraquinone reduction process does appear when boric acid is present in the supporting electrolyte, and it is also present when the chlorotriazine groups are hydrolysed or reacted with other hydroxyl compounds. The reproducibility of the differential pulse cathodic stripping voltammetric response was evaluated for PB and CB for the peak corresponding to reduction of the chlorotriazine moiety at pH 4.5 acetate and pH 10.0 carbonate buffer with an accumulation time of 120s. For pH 4.5 acetate buffer the relative standard deviations for the determination of CB and PB at the 1×10^{-7} M level were calculated to be 3.5% and 3.7%, respectively, ($n=7$). For pH 10.0 carbonate buffer these relative standard deviations were 2.1% and 2.3%, respectively. At pH 4.5 the use of the peak at - 0.9 V is recommended. The calibration plots given for pH 10.0 allow a detection limit of 3×10^{-10} M. Thus, both PB and CB can be determined with good precision and a low detection limit by differential pulse cathodic stripping voltammetry in both acidic and alkaline solution based on the chlorotriazine peaks.

Tayem, (2002) developed a simple and sensitive voltammetric method for the determination of three dyes (Blue R Special, Red RB 198 and Yellow RNL 107). The voltammetric method for trace determination of dyes is based on adsorption and accumulation of dyes at a hanging mercury drop electrode (HMDE) using differential pulse-adsorptive cathodic stripping voltammetry (DP-AdCSV) technique. Experimental and

operational parameters for the quantitative analysis of dyes are optimized. Calibration graph for determination of Blue R Special, Red RB 198 and Yellow RNL 107 dyes were constructed and were found to be linear over the range 0.10-1.00 ppm, 0.05-1.00 ppm and 0.05-1.00 ppm with relative standard deviation (RSD) of 2.21%, 2.36%, and 1.95%, respectively (n=3).

Zu'bi, (2003) developed a voltammetric method for quantitative determination of three dyes (Acid Orange 7, Acid Orange 10 and Acid Orange 12). The voltammetric method for determination of trace amount of dyes is carried out by DP-AdCSV technique at HMDE. The effects of different parameters that influence the DP-AdCSV were studied. These parameters include pH, accumulation potential, accumulation time, pulse amplitude, scan rate, drop size and interference by other ions. The calibration graphs for the determination of the studied dyes were linear in the range 0.004-0.105ppm, 0.009-0.180ppm and 0.0070-0.140ppm with detection limit of 0.002ppm, 0.005ppm and 0.004ppm and relative standard deviation of 1.96%, 2.10% and 2.15%, respectively (n=3).

1.5.4 Capillary electrophoresis determination of textile dyes

Siren and Sulkava, (1995) developed a capillary zone electrophoresis (CZE) method for routine screening of black reactive dyes and black acid dyes isolated from cotton and wool materials; detection was based on UV absorption. The electrolyte solution was 3-[Cyclohexylamino]-1- propane sulphonic acid buffer (pH 10.8), which was chosen to maintain the current at a low level under high voltages. Pretreatment of the cotton and wool samples involved extraction with NaOH or NH₃. With the CZE technique the dyes were detected at very low concentration levels. The dye components were identified using a newly developed marker technique. The marker components for the calculations were UV-absorbing

phenylacetic acid, benzoic acid and meso-2, 3-diphenylsuccinic acid. The marker technique proved effectiveness in determining the electrophoretic mobilities of the analytes, since the relative standard deviations of the migration indices and the electrophoretic mobility for the analyte were below 0.6%.

Perez-Urquiza, Ferrer and Beltran, (2000) developed a method based on capillary electrophoresis coupled with photodiode-array detection to determine several sulfonated dyes including a sulfonated dye (acid yellow 1), and the sulfanated azo dyes acid orange 7, acid orange 12, acid orange 52, acid red 26, acid red 27 and acid red 88. A CElect- FS75 CE column is used. The electrophoresis buffer contains a 1:5 dilution of 10 mM phosphoric acid and tetrabutylammonium hydroxide buffer (pH 11.5), and 25 mM of diethylamine, the final pH being 11.5. The detection limits for the seven dyes ranged from 0.1 - 4.53 μ g/ml.

1.5.5 Other spectroscopic techniques used for determination of textile dyes

Preiss *et al.*, (2000) developed techniques using LC/NMR and LC/MS to characterize the organic constituents of industrial waste water with emphasis on polar, nonvolatile compounds. In the effluent of textile company, various compounds such as anthraquinone dyes and their by-products a fluorescent brightener, a by- product from polyester production and auxiliaries such as anionic and nonionic surfactants and their degradation products were identified. Zhang, Hou and Tan, (1997) investigated six violet acid dyes derived from bromaminic acid. The samples were prepared and their structures were determined via UV-visible, IR, H-NMR and MS techniques. The color fastness and dyeing rate of these dyes were also measured and compared. It was found that the dyes had excellent coloration properties on wool, silk and polyamide fibers with

excellent fastness to light wet treatment rubbing and high dye uptake, having intense brilliant bluish violet.

1.6 Dyes removal techniques

Color is the first contaminant to be recognized in wastewater and has to be removed before discharging into water bodies or on land. The removal of color from wastewater is often more important than the removal of the soluble colorless organic substances, which usually contribute the major fraction of the biochemical oxygen demand (BOD) (Fewson, 1988; Seshadri *et al*, 1994). Many methods have been reported for removing textile dyes from wastewater, among which are membrane filtration, coagulation/flocculation, precipitation, flotation, adsorption, ion exchange, ion pair extraction, ultrasonic, mineralization, electrolysis, advanced oxidation (chlorination, bleaching, ozonation, Fenton oxidation and photocatalytic oxidation) and chemical reduction. Biological techniques include bacterial and fungal biosorption and biodegradation in aerobic, anaerobic or combined anaerobic/aerobic treatment processes (Cooper, 1993). The use of one individual process may often not be sufficient to achieve complete decolorization. Dye removal strategies consist therefore mostly of a combination of different techniques.

1.6.1 Sorption and ion exchange

Pala, Tokat, and Erkaya, (2003) investigated the decolorization of prepared aqueous solutions of three reactive azo dyes used in textile processing by adsorption on different types of powdered activated carbon (PAC). The color removal efficiencies and equilibrium adsorption isotherms for these three dyes [Remazol Gelb 3RS (yellow), Remazol Rb133 (red), Remazol Schwarz B133 (blue)] were investigated using five

commercial powdered activated carbons and two other activated carbons prepared by physical activation of olive wooden stone (OWS), and solvent extracted olive pulp (OWSR). The equilibrium is practically achieved in 60 minutes while most of adsorption took place within the first 20 minutes. The color removal efficiency was found as high as 100% for the commercial activated carbons while 80% efficiency was obtained using the OWS and OWSR. Since OWS and OWSR are waste materials, their use in the synthesis of activated carbon production process will reduce solid waste pollution and raw materials costs.

Albanis *et al.*, (2000) studied adsorption and removal of commercial dyes in aqueous suspension of fly ash mixtures with a sand clay loam soil of low organic matter content. The commercial dyes, Acid orange 7, Acid Yellow 23, Disperse Blue 79, Basic Yellow 288 and Direct Yellow 28 represent the widely used nitro azo structures. Batch and column experiments were carried out at equilibrium condition of concentrations of dyes between 5 and 60ppm. The logarithmic form of Freundlich equation gave a high linearity and the k constants were found to increase with increasing the fly ash content in adsorbent mixtures and the affinity between the adsorbent surface and adsorbed solute. The mean removed amounts of dyes by adsorption batch experiments in soil mixture with 20% fly ash content were up to 53% for Acid Yellow 7, 44.9% for Acid Yellow 23, 99.2% for Direct Yellow 28, 96.8% for Basic Yellow 28 and 88.5% for Disperse Blue 79.

The removal of dye from column experiments decreased with the increase of concentration of the solution. The mean removed amounts of dyes by adsorption of columns of soil mixture with 20% fly ash content and for initial concentration of dye solution 50ppm were up to 33% for Acid

Yellow7, 59.4% for Acid Yellow 23, 84.2% for Direct Yellow 28, 98.2% for Basic Yellow 28 and 60.3% for Disperse Blue 79.

1.6.2 Advanced oxidation processes

Advanced oxidation processes (AOPs) that have been most widely studied are ozonation, UV/H₂O₂, Fenton's reagent (Fe²⁺/H₂O₂) and UV/TiO₂ (Aplin and Wait, 2000). Park and Choi, (2003) demonstrated a new photochemical remediation method for dye-polluted waters. The photodegradation of Acid Orange 7 (AO7) was successfully achieved in the presence of Fe (III) ions only under visible light ($\lambda \geq 420\text{nm}$). Upon adding Fe (III) to AO7 solution, ferric ions formed complexes with AO7 mainly through the azo chromophoric group. The AO7- Fe (III) complex formation was highly pH-sensitive and maximized around pH 3.7. The visible light induced degradation of AO7 was effective only when the complex formation was favored. It is known that Fe (OH)²⁺ species can be photolyzed to produce OH radicals. In order to check if OH radicals were involved in the AO7 degradation, the effect of adding 2-propanol, an OH radical scavenger, on the dye degradation was studied. The degradation rate of AO7 was hardly affected by adding excess 2-propanol, which indicated that OH radicals were not responsible for AO7 degradation in this system.

The proposed mechanism of the dye degradation is the visible light-induced electron transfer from the azo chromophoric group to the iron center in the complex. Therefore, when the formation of AO7-Fe (III) complex was inhibited in the presence of excess interfering anions such as sulfites and sulfates, the photodegradation of the dye was also prevented. The photodegradation of AO7 under visible light produced O-phthalate and

4-hydroxybenzenesulfonate (4-HBS) as major products, but did not reduce the total organic carbon (TOC) concentration. Since this process does not require the addition of hydrogen peroxide, it might be developed into an economically viable method to pretreat or decolorize azo- dye wastewaters using sunlight.

Shu and Huang, (1995) reported a method to oxidize eight non-biodegradable azo dyes by ozonation and photo oxidation process which was studied in a pilot scale photochemical [UV/ozone] reactor. In experiments with ozone bubbling, the degradation of eight azo dyes was found to occur in the absence of UV light. The degradation rate of azo dyes was observed to be first order with respect to both azo dye and ozone concentration. The pH of solution decreased while the azo dyes degraded. UV light did not significantly enhance the degradation ability of the ozonation reaction under various conditions. No degradation was observed when the azo solution was irradiated by UV light alone. Effect of ozone dosage and initial concentration of azo dyes on the rate of degradation were discussed.

Feng, Hu and Yue, (2003) developed a novel nanocomposite of iron oxide and silicate, prepared through a reaction between a solution of iron salt and a dispersion of a laponite clay for the photoassisted Fenton degradation of azo-dye Orange II. It has been found that the H_2O_2 concentration in solution, solution pH, UV light wavelength and power, and catalyst loading are the main factors that have strong influences on the photoassisted Fenton degradation of Orange II.

The optimal H_2O_2 molar concentration is about 4.8mM for 0.1mM Orange II, and the optimal pH of the reaction solution is 3.0. The catalyst exhibits high catalytic activity only under the irradiation of UV light, and

the UV light with a short wavelength is much more effective than the light with a long wavelength. An increase in the UV light power also accelerates the degradation of Orange II. As the catalyst loading increases, the degradation of Orange II also increases until a saturated catalyst loading is achieved. The saturated catalyst loading is about 1.0 g of Fe-nanocomposite catalyst /L (0.1mM Orange II). It was also found that the discoloration of Orange II undergoes a faster kinetic than the mineralization of Orange II, and 75% total organic carbon (TOC) of 0.1mM Orange II can be eliminated after 90 min in the presence of 0.1 g of Fe nanocomposite /L, 4.8mM H₂O₂, and 1X8W UVC.

1.6.3 Biological techniques

Biological dye removal techniques are based on microbial biotransformation of dyes. As dyes are designed to be stable and long-lasting colorants, they are usually not easily biodegraded.

Padmavathy *et al.*, (2003) attempted to degrade some reactive dyes aerobically. The organisms which were efficient in degrading the azo dyes Red RB, Remazol Red, Remazol Blue, Remazol Violet, Remazol Yellow, Golden Yelloe, Remazol Orange, Remazol Black, were isolated from three different sources and were mixed to get consortia. The efficiency of azo dye degradation by consortia was analyzed in presence of various co-substrates, such as glucose, starch, lactose, sewage and whey water, and their effects on dye decolorization have been studied.

It was observed that starch was the best source of carbon for decolorization of reactive azo dyes. In presence of 25 mg/L of starch, all the reactive dyes decolorized within 24 hours with the reduction in chemical oxygen demand (COD) in the range of 75.15-95.9%. The COD

reduction was the maximum in Remazol Orange and Red RB followed by Remazol Yellow, Remazol Violet, Remazol Black, Remazol Red, Golden Yellow and Remazol Blue. The decolorization of the above referred dyes in presence of different wastewaters such as sewage and whey waste showed that whey is the better cosubstrate for aerobic decolorization.

Bell and Buckley, (2003) investigated the decolorization of the dye CI Reactive Red 141 in a laboratory-scale anaerobic baffled reactor (ABR). The results of the physical decolorization tests suggested significant decolorisation due to adsorption to the biomass; however, it is possible that the dye chromophores were reduced due to the low redox potential environment within the test bottles. No dye breakthrough, due to adsorption saturation was observed during operation of the reactor. Chemical oxygen demand (COD) reduction was consistently >90%. Color reductions averaged 86%. The biomass showed acclimation to the dye, with increased methanogenic activity with each increase in dye concentration. The reactor operation was stable, even with increases in the dye concentration. This investigation has shown that successful treatment of a highly colored wastewater is possible in the ABR.

Coughlin, Kinkle and Bishop, (2002) established a stable microbial biofilm community capable of completely mineralizing the azo dye acid orange 7 (AO7) in a laboratory scale rotating drum bioreactor (RDBR) using waste liquor from a sewage treatment plant. A broad range of environmental conditions including pH (5.8-8.2), nitrification (0.0-4.0mM nitrite), and aeration (0.2-6.2 mg O₂/L) were evaluated for their effects on the biodegradation of AO7. Furthermore the biofilm maintained its biodegradative ability for over a year while the effects of these environmental conditions were evaluated.

Reduction of the azo bond followed by degradation of the resulting aromatic amine appears to be the mechanism by which this dye is biodegraded. Complete loss of color, sulfanilic acid, and chemical oxygen demand (COD) indicate that AO7 is mineralized. Two bacterial strains (1CX and SAD4i) originally isolated from the RDBR were able to mineralize, in co-culture, up to 90% of added AO7. During mineralization of AO7, strain 1CX reduces the azo bond under aerobic conditions and consumes the resulting cleavage product 1-amino-2-naphthal. Strain SAD4i consumes the other cleavage product, sulfanilic acid.

1.6.4 Coagulation / Flocculation

Coagulation/ flocculation is often applied in the treatment of textile – processing wastewater, either to partly remove chemical oxygen demand (COD) and color from the raw wastewater before further treatment. The principle of the process is the addition of a coagulant followed by a generally rapid chemical association between the coagulant and the pollutants. The dust formed coagulated or flocs subsequently precipitate or are to be removed from the water phase by flotation. Various inorganic coagulants are used, mostly lime, magnesium, iron and aluminum salts. Coagulation /flocculation with inorganic chemicals generate considerable volumes of useless or even toxic sludge that must be incinerated or handled otherwise. This presents a serious drawback of the process.

1.6.5 Electrolysis

Electrolysis is based on applying an electric current through the wastewater to be treated by using electrodes. The anode is sacrificial metal (usually iron) electrode that withdraws electrons from the electrode material, which results in the release of Fe (II) ions to the bulk solution and

precipitation of $\text{Fe}(\text{OH})_2$ at the electrode surface. The cathode is a hydrogen electrode that produces H_2 gas from water.

Decolorization by electrochemical process is expensive due to large energy requirements (Cooper, 1993) and the limited lifetime of the electrodes (Vandeviver and Bianchi, 1998).

Lorimer, (2001) subjected solutions of both basic and acidic dyes to sonolysis, electrolysis, and sonoelectrolysis. Only basic dyes were decolorized by ultrasound alone. Removal of the acidic dye Sandolan Yellow required the use of an electrooxidation process. The rate of electrochemical decolorization in the absence of ultrasound was dependent on the type of electrolyte, the electrolyte concentration, the reaction temperature and the current density. The sonoelectrooxidation of Sandolan Yellow needed to be performed in a sealed cell to minimize the effects of ultrasonic degassing.

1.6.6 Membrane filtration

Membrane filtration is a quick method with low spatial requirement. Another advantage is that permeates, as well as some of the concentrated compounds, including non- reactive dyes, can be reused. The disadvantages of membrane techniques are flux decline and membrane fouling, necessitating frequent cleaning and regular replacement of the modules.

Gholami *et al.*, (2003) evaluated the effectiveness of two methods for dyestuff removal from textile waste stream. In the first step, different types of dyes used in textile industries were studied in order to determine the types with highest usage rates. In this regard, basic, reactive, disperse and

acidic dyes were selected. In the second type, dye biodegradability was studied through Zahn –Wellens method (ISO-9888 1999). Results showed final chemical oxygen demand (COD) and dye rejected coefficients (R %) of (61%, 57%), (73%, 76%), (25%, 14%), (32%, 8%) for acidic, basic, reactive and disperse dyes, respectively. In the third step, spiral-wound membrane modules nanofilter (NF) with a molecular weight cut off (MWCO) of 300 and 600 dalton (Da) and reverse osmosis (RO) of 50 Da were used. The operating condition in phase 3 were adjusted as: temperature 30 to 35°C, pressure 4 bar for NF membranes and 7.5 bar for RO, flow rate of 10 l/min, and dye concentration of 0.01%. Results showed that COD and dye rejection coefficients for NF with 300 Da and for acidic, basic, reactive and disperse samples of dyes were (6%, 55%), (44%, 70%), (33%, 36%) and (71%, 93%), respectively. These results for NF with 600 Da were (7%, 54%), (64%, 76%), (33%, 29%), (59%, 92%) and for RO were (95%, 99%), (96%, 98%), (45%, 99.6%). Results clearly showed higher removal efficiency for the membrane treatment than for biodegradability studies.

Koyuncu, (2003) investigated the direct filtration of reactive dye house wastewaters by nanofiltration membranes based on permeate flux, and sodium chloride and colour removal. Experiments were performed using both synthetic and industrial dye bath wastewaters with the fluxes of the industrial dye bath wastewaters lower than those of the synthetic solutions. The effects of operating conditions such as pressure and pH were assessed. Studies with DS5 DK type (polysulfone–polyamide) membranes showed that nanofiltration membranes are suitable for direct treatment of wastewaters and the permeate quality was appropriate for reuse in the dyeing process. Pre-treatment and neutralisation were important for

recovery of large amounts of salt and water from the permeate stream. Neutralisation of the solution with HCl rather than H₂SO₄ gave a better permeate from the point of view of the reuse. The highest permeate flux and color removal and the lowest salt removal were achieved with the HCl neutralization.

1.6.7 Removal of textile dyes by metals

Deng *et al.*, (2000) investigated a new method for discoloration of aqueous reactive dyes C.I. Reactive Red 2, C.I. Reactive Blue 4 and C.I. Reactive Black 8 using UV/Fe system. The obtained results showed that the degree of discoloration changes by changing the pH and weight of iron. Correlation analysis showed that the discoloration of dyes were pseudo – zero order reaction. Jawabreh, (2003) studied the degradation kinetics of four Direct diazo dyes; Direct Blue 2, Direct Red 23, Direct Green 1 and Direct Yellow 12 by iron metal in aqueous solution. The results reported showed that the rate of degradation is affected by the acidity, surface area of iron and temperature of the solution. The rates of degradation of the four dyes in aqueous solutions in presence of different metals (Co, Cu, Ni, Mn, Zn, Al and Fe), using UV light were studied. The obtained results showed that the rate of degradation was highest in the presence of aluminum metal and the rate of degradation was found to be higher when degradation was accompanied by exposure to UV light.

Zu'bi, (2003) studied the reducing degradation kinetics of three Acidic azo dyes (Acid Orange 7, Acid Orange 10 and Acid Orange 12) by zero-valent iron in aqueous-solutions. Effective degradation was achieved with rate constants of 0.004, 0.002 and 0.003 mmol/L, and half-lives of 10 min, 22 min and 17 min for Acid Orange 7, Acid Orange 10 and Acid Orange 12 respectively.

1.6.8 Ultra sonic methods

Vinodgopal *et al.*, (1998) studied a new method for degradation of reactive Black dye in oxygen-saturated aqueous solution under high frequency ultrasonic generator. Sonochemical degradation method is relatively new and involves exposing aqueous solutions containing the organic pollutant to ultrasound. The OH radical initiated oxidative degradation of the dye results in 65% mineralization was measured by the decrease in the total organic content. The advantage of using ultrasound rests with the simplicity of its use.

Taicheng, Haofei and Xiong, (2003) investigated the decolorization and COD removal from synthetic wastewater containing Reactive Brilliant Orange K-R (RBOKR) dye using sonophotocatalytic technology. Experimental results showed that this hybrid technology could efficiently remove the color and reduce COD from the synthetic dye-containing wastewater, and that both processes followed pseudo first-order kinetics. At the condition of 0.1 m³/h air flow, 0.75 g/dm³ titanium dioxide and 0.5 mmol/dm³ RBDKR solution, the rate constants of decolorization and COD removal were 0.0750 and 0.0143 min⁻¹, respectively for the photocatalytic process and 0.0005 and 0.0001 min⁻¹, respectively for the sonochemical process. The rate constants of sonophotocatalysis were greater than that the both the photocatalytic and sonochemical process either in isolation or as a sum of the individual process, indicating an apparent synergetic effect between the photo- and sono- processes.

1.7 Aims of this work

The objectives of this work are:

- i. To develop a new method for quantitative determination of four Direct textile dyes, (Direct Red 81, Direct Blue 15, Direct Black 22 and Direct Orange 34) using HPLC technique and spectrophotometric detection.
- ii. To develop a simple and practical method for degradation of these Direct textile dyes.
- iii. To study the kinetic and degradation mechanisms of these Direct textile dyes.
- iv. To determine the concentration of these direct textile dyes in real samples of drinking water and waste water.

Chapter Two

Experimental

PART I : HPLC Analysis

PART II : Degradation of Direct Azo Dyes

2.1 Chemicals and solvents

All chemicals used in this work were of analytical grade and obtained from Aldrich-Sigma, Merck and Riedel-Delhaen. All solvents used were of HPLC grade.

2.2 Standard dyes solutions

Standard solutions of the studied dyes were prepared by weighing out exactly 0.1 g of each dye (Direct Red 81, Direct Blue 15, Direct Black 22, Direct Orange 34) and transferring it into a 1000- ml volumetric flask. The dye was dissolved in water. The pH of the solution was adjusted to pH 6-7 and the volume was completed to the mark. Working solutions were prepared by further dilution of the stock solution of the corresponding dye.

2.3 Mobile phase

The mobile phase for HPLC analysis was prepared (Oxspring, *et al.*, 1996) by weighting out exactly 164 g of N-Cetyl-N,N,N-trimethylammonium bromide (CTAB) and transferring it into a 1000-ml volumetric flask. The CTAB was dissolved in acetonitrile: water (60: 40, v/v). The mobile phase was degassed using JENCONS Scientific LTD Sonicater, and filtered through 0.45 micrometer membrane to remove any particular matter that might clog the system.

2.4 Instrumentation

A. A UV-VIS-NIR SCANNING SPECTROPHOTOMETER UV-3101PC (SHIMADZU) was used for all spectrophotometric measurements. All measurements were carried out using quartz cells 10-mm at room temperature ($25\pm 2^\circ\text{C}$).

- B.** HPLC analysis were carried out using SHIMADZU HPLC chromatograph consists of one pump (model LC-10 AT vp), manual sample injector (Rheodyne 7725i), Diode array detector (model SPD-M 10 Avp) with wavelength in the range (190-800) nm, system controller (model SCL-10 Avp) and class-VP 5.0 Software. Analysis were performed on ZORBAX ODS 4.6 mm x 25cm column, at a flow rate of 0.5 mL/min
- C.** IR analyses were carried out using SHIMADZU FTIR-8201 PC Fourier transform infrared spectrophotometer.
- D.** Other equipments used in the work were: Mechanical stirrer (fluids control division, model 5VB SCR speed control, LEF Corporation), pH meter 3310 JENWAY and Heater with Immersion circulator, mgw LAUDA (MODEL B-1).

2.5 HPLC analysis

Prior to HPLC analysis the visible spectrum of each standard dye was obtained in order to establish its maximum absorbance wavelength. Each dye was chromatographed individually by injecting 20 μ L of 20ppm (Direct Red 81, Direct Blue 15 and Direct Orange 34) and 50ppm of Direct Black 22, then detecting the corresponding peak at its maximum wavelength, in order to determine the retention time of each dye. The calibration curves were constructed by plotting absorbance against concentration of each dye.

2.6 Identification

The dyes were identified by comparison of the retention time in real samples with those of standard solutions under the same conditions (mobile phase, flow rate, temperature, pH and wavelength).

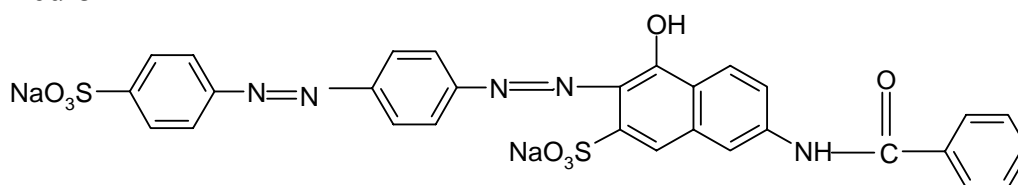
2.7 Degradation of textile dyes using metals

The degradation kinetics of the four Direct dyes (Direct Red 81, Direct Blue 15, Direct Black 22 and Direct Orange 34) using different metals in aqueous solution were studied. A 50mL sample of 20ppm of (Direct Red 81, Direct Blue 15, and Direct Orange 34) and 50ppm of Direct Black 22 was transferred into a 100mL beaker. Fixed amount of metal was added. The pH of the solution was adjusted using dilute HCl (0.1M) and NaOH (0.1 M). The solution was stirred at a speed of 2000 rpm using the mechanical stirrer. The temperature of the solution was adjusted using heater with Immersion circulator.

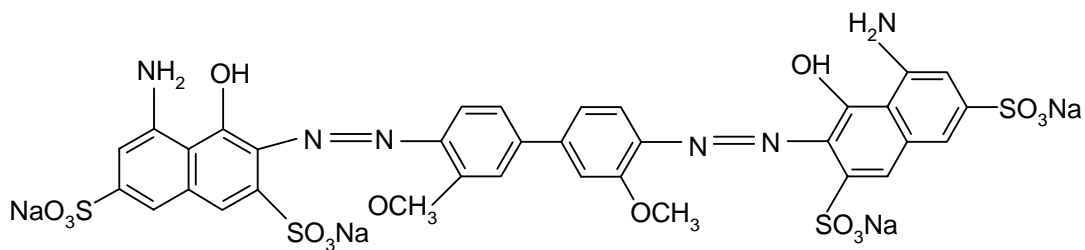
The degradation of the dyes were monitored by measuring the absorbance at the corresponding wavelength (Table page 51) at intervals of 5 minutes for 30 minutes when using Fe and at intervals of 2 minutes for 10 minutes when using Al.

Table 1. Characterisation of dyes studied in this work.

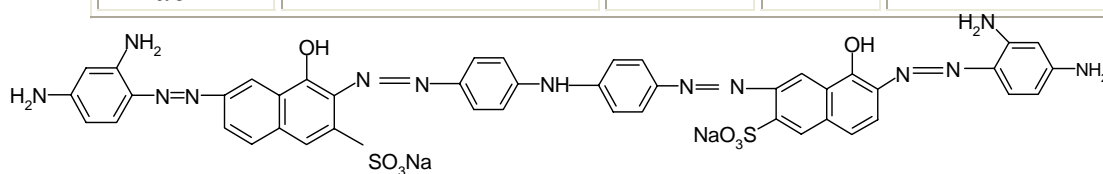
C.I Name	Structural Formula	M.Wt	λ_{\max} (nm)	Chromophore Dye
Direct Red 81	<chem>C29H19N5O8S2Na2</chem>	675.6	510	Diazo



C.I Name	Structural Formula	M.Wt	λ_{\max} (nm)	Chromophore Dye
Direct Blue 15	<chem>C34H24N6O16S4Na4</chem>	992.82	607	Diazo



C.I Name	Structural Formula	M.Wt	λ_{\max} (nm)	Chromophore Dye
Direct Black 22	$C_{44}H_{33}N_{13}O_8S_2Na_2$	981.94	484	Polyazo



C.I Name	Structural Formula	M.Wt	λ_{\max} (nm)	Chromophore Dye
Direct Orange 34	Not available	Not available	411	Not available

Not available in the literature

Chapter Three

Result and Discussion

Part I : HPLC Analysis

Part II : Kinetic Results of Degradation

3.1 Absorption spectra

It is well known that the azo group (-N=N-) of the dye is the basic reason for its visible color. The absorption spectrum of each dye (Direct Red 81, Direct Blue 15, Direct Black 22 and Direct Orange 34) was studied in the wavelength range 200-800 nm. From each spectrum, the maximum absorbance for each dye was selected for the HPLC analysis. The obtained spectra are presented in figure (3.1).

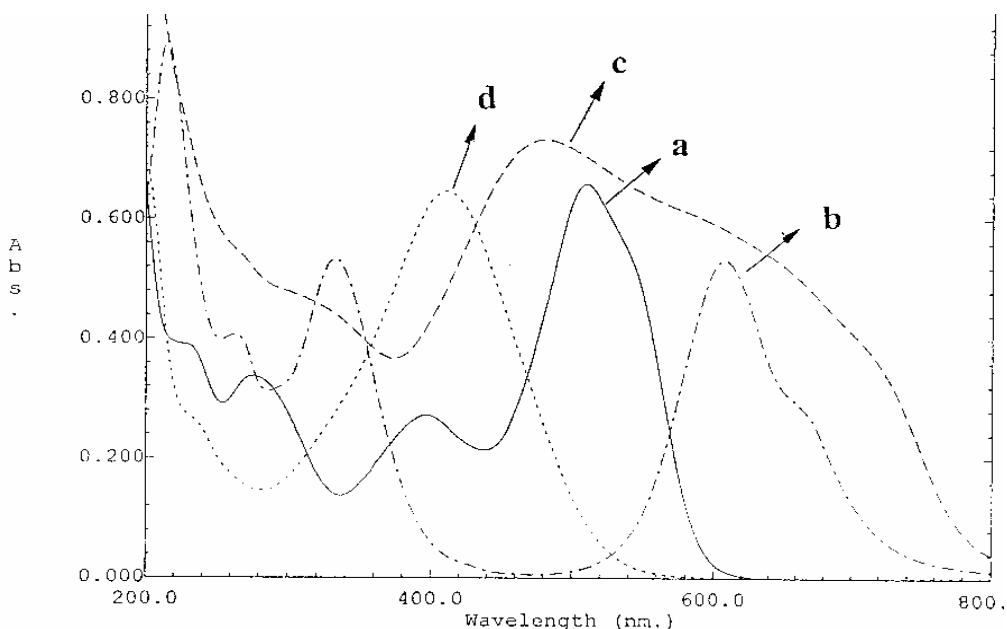


Figure 3.1. Comparison of absorption spectra of 20ppm of (a) Direct Red 81 ($\lambda_{\max}=510$ nm), (b) Direct Blue 15 ($\lambda_{\max}=607$ nm), (d) Direct Orange 34 ($\lambda_{\max}=411$ nm) and 50ppm of (c) Direct Black 22 ($\lambda_{\max}=484$ nm). Conditions: pH = 6.1 and temperature = $5\pm 2^{\circ}\text{C}$.

Part I: HPLC analysis

3.2 HPLC Results

3.2.1 Retention time

The optimum conditions recommended in the experimental part for HPLC analysis were applied to obtain the retention time for each dye. The

obtained results (3.2.1.a, b, c and d) showed retention times of 15.4, 8.8, 5.8 and 12.7 min for Direct Red 81, Direct Blue 15, Direct Black 22 and Direct Orange 34, respectively.

Comparison between the polarities of the four dyes showed that Direct Black 22 has the shortest retention time followed by Direct Blue 15, Direct Orange 34 and Direct Red 81, in that orders. From the retention times, it can be concluded that Direct Black 22 has the highest polarity followed by Direct Blue 15, Direct Orange 34 and then Direct Red 81, in that order. The polarity of each dye refers to the number of functional groups, in each dye as shown in Table 1.

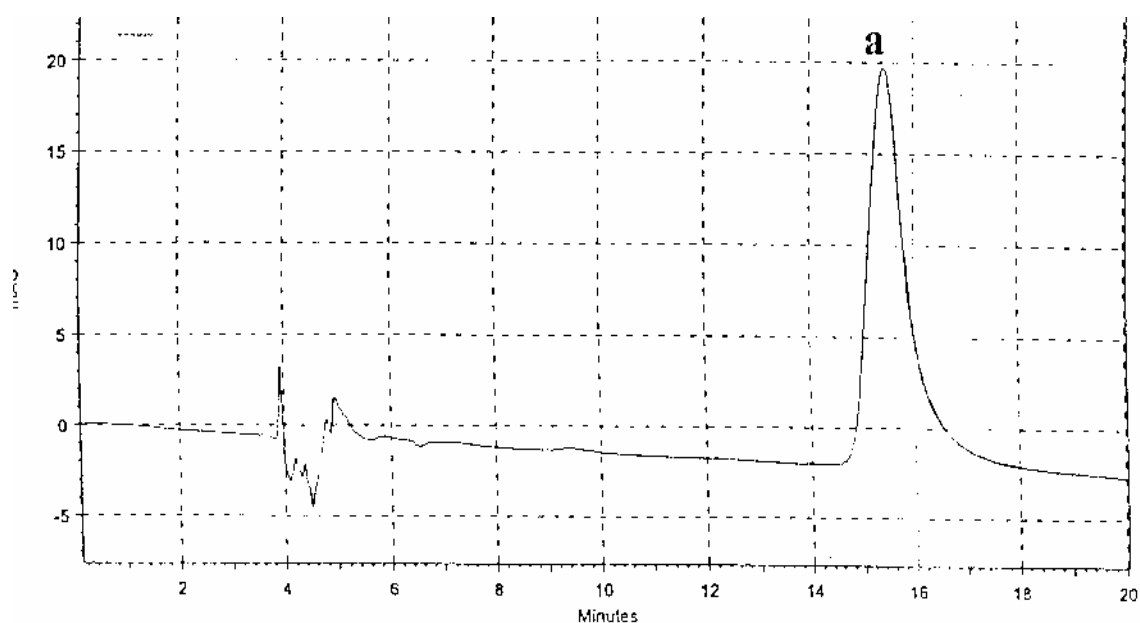


Figure 3.2.1.a. HPLC chromatogram for Direct Red 81 dye with a concentration of 20ppm. Conditions: wavelength = 510 nm, temperature $25\pm 2^\circ\text{C}$, pH 6.1, mobile phase [acetonitrile: water (60: 40, v/v) containing 0.45M CTAB], flow rate = 0.5ml / min and using RP C_{18} column. a: peak for Direct Red 81.

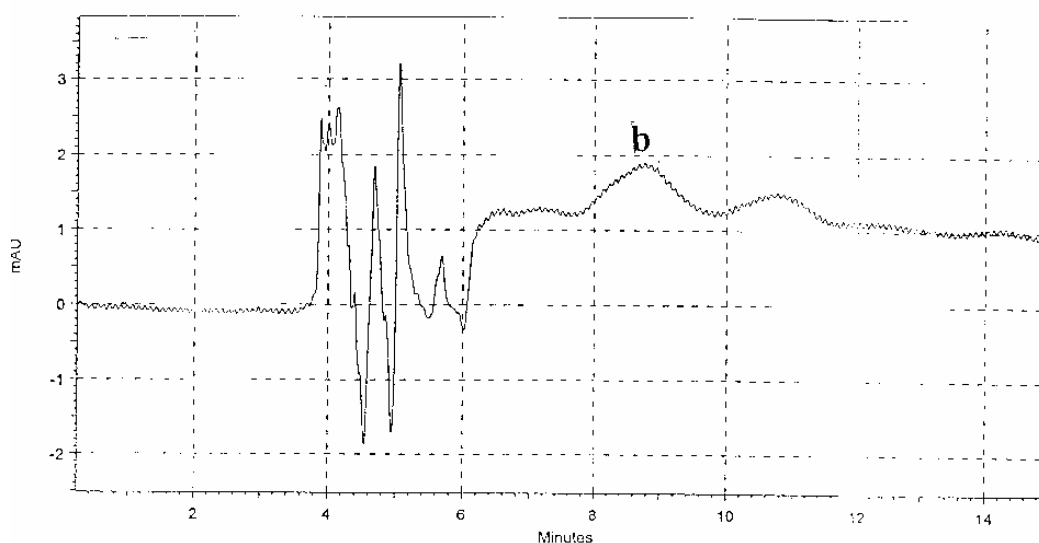


Figure 3.2.1.b. HPLC chromatogram for Direct Blue 15 dye with a concentration of 20ppm. Conditions: wavelength = 607 nm, temperature $25\pm 2^\circ\text{C}$, pH 6.1, mobile phase [acetonitrile: water (60: 40, v/v) containing 0.45M CTAB], flow rate = 0.5ml / min and using RP C₁₈ column. b: peak for Direct Blue 15.

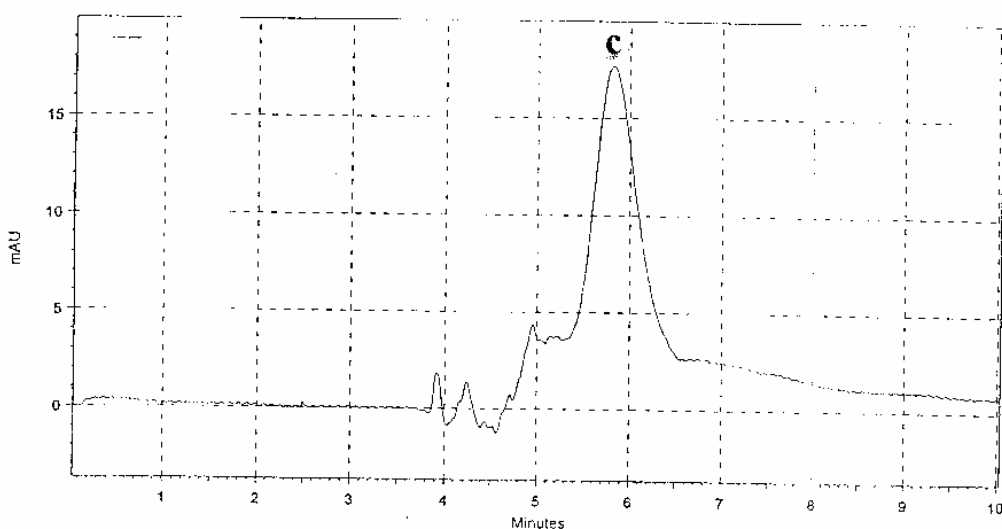


Figure 3.2.1.c. HPLC chromatogram for Direct Black 22 dye with a concentration of 50ppm. Conditions: wavelength = 484 nm, temperature $25\pm 2^\circ\text{C}$, pH 6.1, mobile phase [acetonitrile: water (60: 40, v/v) containing 0.45M CTAB], flow rate = 0.5ml / min and using RP C₁₈ column. c: peak for Direct Black 22.

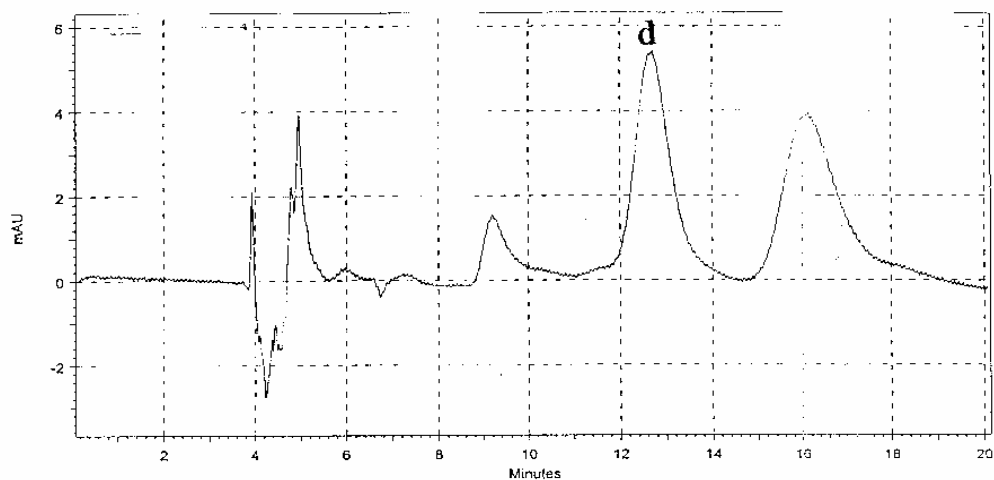


Figure 3.2.1.d. HPLC chromatogram for Direct Orange 34 dye with a concentration of 20ppm. Conditions: wavelength = 411 nm, temperature $25\pm 2^{\circ}\text{C}$, pH 6.1, mobile phase [acetonitrile: water (60: 40, v/v) containing 0.45M CTAB], flow rate = 0.5ml / min and using RP C18 column. d: represents the peak for Direct Orange 34.

3.2.2 Effect of CTAB concentration in the mobile phase on the retention time

The effect of changing the concentration of CTAB in the mobile phase on the retention time of each of the four dyes was studied at pH 6.1, temperature of $25\pm 2^{\circ}\text{C}$, flow rate of 0.5 ml/min and at the selected wavelength. The obtained results are presented in Table (3.2.2). As shown from the results that increasing the concentration of CTAB in the mobile phase resulted a decrease in the retention time of four dyes. At a concentration of 0.15 M no peaks were observed. This might be due to the very long retention time (more than 60 minutes) of the dyes. Therefore, a concentration of 0.45 M was selected for further work since it gives reasonable retention times for the four dyes.

Table 3.2.2. Effect of concentration of CTAB in the mobile phase on the retention time.

Concentration of CTAB (M)	Retention time (min)			
	Direct Red 81	Direct Blue 15	Direct Black 22	Direct Orange 34
0.15	Not observed	Not observed	Not observed	Not observed
0.30	35.7	14.9	10.55	20.22
0.45	15.4	8.8	5.8	12.7

Conditions: pH 6.1, temperature = $25 \pm 2^\circ\text{C}$ and flow rate 0.5 ml/min.

3.2.3 Effect of pH on the retention time

The effect of pH of the mobile phase on the retention time of each dye was studied at the selected wavelength. The obtained results are presented in Table 3.2.3.

Table 3.2.3. Effect of pH of the mobile phase on the retention time.

pH	Retention time (min)			
	Direct Red 81	Direct Blue 15	Direct Black 22	Direct Orange 34
4.0	15.1	8.5	5.5	12.4
6.1	15.4	8.8	5.8	12.7
9.0	15.9	9	6.3	12.7

Conditions: [CTAB] = 0.45 M in acetonitrile : water (60 :40, v/v), and temperature = $25 \pm 2^\circ\text{C}$ and flow rate 0.5 ml/min.

As seen from the results (Table 3.2.3); there is no influence of pH on the retention time of any of the four studied dyes. In the present work pH = 6.1 was selected for further study (normal conditions).

3.2.4 Effect of acetonitrile water ratio (v/v) in the mobile phase on the retention time

The effect of acetonitrile: water in the mobile phase on the retention time of each of the four dyes was studied. The obtained results are presented in Table (3.2.4).

Table 3.2.4. Effect of acetonitrile: water in the mobile phase on the retention time

acetonitrile:water ratio (v/v)	Retention time (min)			
	Direct Red 81	Direct Blue 15	Direct Black 22	Direct Orange 34
60:40	15.4	8.8	5.8	12.7
80:20	17.8	16.6	10.4	22.2

Conditions: [CTAB] = 0.45 M, temperature = 25± 2°C, flow rate 0.5 ml /min and pH =6.1.

It can be seen from the results (Table 3.2.4); that increasing the acetonitrile fraction in the mobile phase (acetonitrile–water mixture) affected an increase in the retention time of the four dyes. This can be attributed to the decrease in CTAB concentration in the mobile phase, which was discussed previously in section 3.2.2.

3.3 Calibration curves

The calibration curves were constructed by plotting the absorbance vs. concentration of each dye. The obtained results are shown in figures (3.3.a, 3.3.b, 3.3.c and 3.3.d). The linear dependence are over the ranges 0.3 – 10ppm , 10 – 30ppm, 0.5 – 10ppm and 1 – 12ppm for Direct Red 81, Direct Blue 15, Direct Black 22 and Direct Orange 34, respectively, with limit of detection 0.3ppm, 10ppm, 0.5ppm and 1ppm. The relative standard deviations (RSD %) were found to be 0.92 %, 0.83 %, 1.13 % and 0.34 %, respectively (n=3) at concentrations of 10ppm for each dye. The optimum conditions for the HPLC determination of dyes as well as the characteristics of the calibration curves are presented in Table (3.3.1).

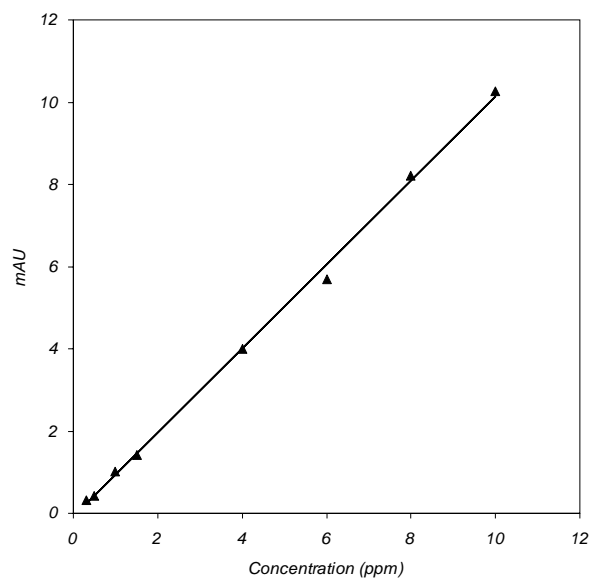


Figure 3.3.a. Calibration curve for HPLC determination of Direct Red 81. Conditions: wavelength = 510 nm, temperature = $25 \pm 2^\circ\text{C}$, pH = 6.1, Mobile phase [acetonitrile: water (60: 40, v/v) containing 0.45 M CTAB], flow rate = 0.5 ml / min.

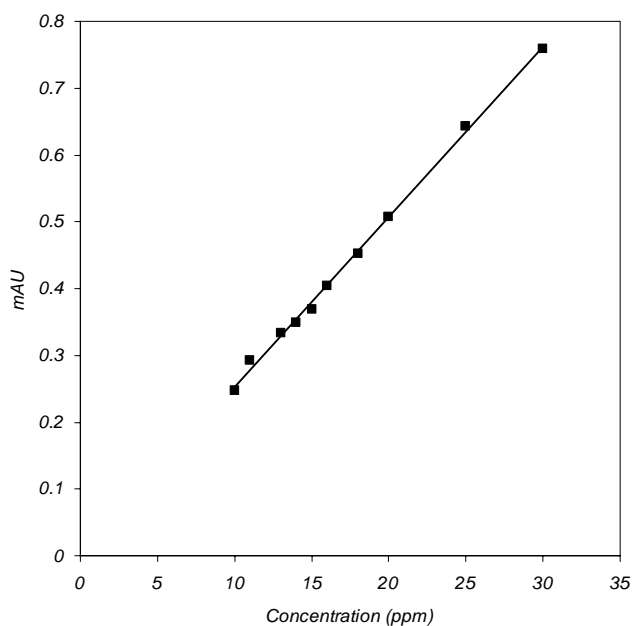


Figure 3.3.b. Calibration curve for HPLC determination of Direct Blue 15. Conditions: wavelength = 607 nm, temperature = $25 \pm 2^\circ\text{C}$, pH = 6.1, Mobile phase [acetonitrile: water (60: 40, v/v) containing 0.45 M CTAB], flow rate = 0.5 ml / min.

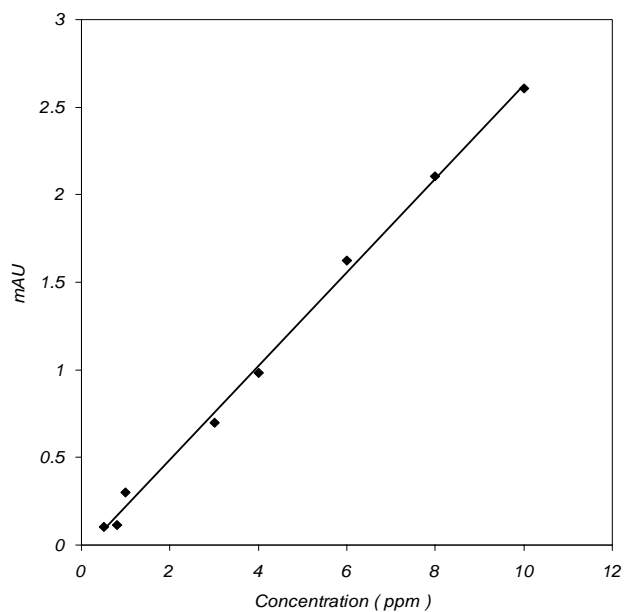


Figure 3.3.c. Calibration curve for HPLC determination of Direct Black 22. Conditions: wavelength = 484 nm, temperature = $25 \pm 2^\circ\text{C}$, pH = 6.1, Mobile phase [acetonitrile: water (60: 40, v/v) containing 0.45 M, CTAB], flow rate = 0.5 ml / min.

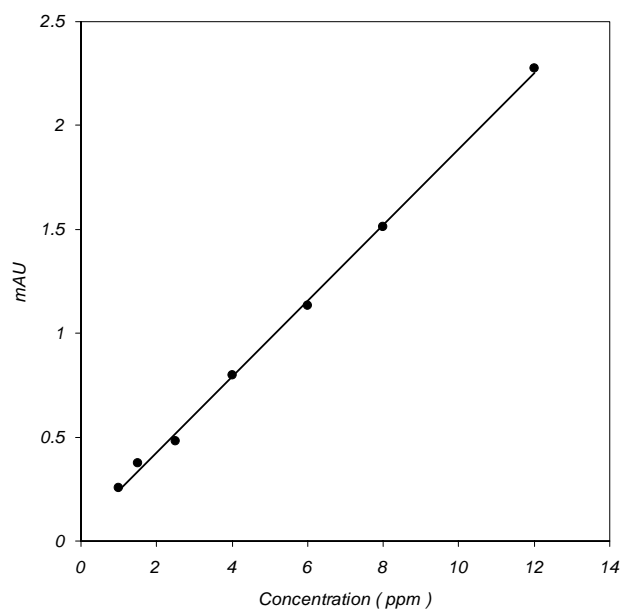


Figure 3.3.d. Calibration curve for HPLC determination of Direct Orange 34. Conditions: wavelength = 411 nm, temperature = $25 \pm 2^\circ\text{C}$, pH = 6.1, Mobile phase [acetonitrile: water (60: 40, v/v) containing 0.45 M, CTAB], flow rate = 0.5 ml / min.

Table 3.3.1. Details of conditions for HPLC analysis.

Parameter	Direct Red 81	Direct Blue 15	Direct Black 22	Direct Orange 34
Detection wavelength (nm)	510	607	484	411
Retention time (min)	15.4	8.8	5.8	12.7
Range of linearity of the calibration curve (ppm)	0.3 - 10	10 -30	0.5 - 10	1 - 12
Limit of detection (ppm)	0.3	10.0	0.5	1.0
RSD* %	0.92%	0.83 %	1.13%	0.34 %

* Average of three measurements. Conditions: temperature 25±2OC, pH 6.1, mobile phase [acetonitrile : water (60 : 40 , v/v) containing 0.45M CTAB], flow rate = 0.5ml / min, using RP C18 column and injection volume of 20 µL.

3.4 Quantitative determination of Direct Red 81, Direct Blue 15, Direct Black 22 and Direct Orange 34 dyes in presence of each other using HPLC technique

As seen from Figures (3.4. a, 3.4.b, 3.4.c and 3.4.d) that it is impossible to identify each dye in the presence of the other three dyes using the conventional spectrophotometer technique due to the overlapping of λ_{\max} of the dyes. Therefore, it is important to separate them from each other before analysis, using HPLC technique.

The conditions for determination of each dye are presented in Table (3.3.1). In order to determine each dye in the presence of the other three dyes the conditions of analysis should be made according to the recommended conditions of the dye. Typical results for the determination of each dye in the presence of the other three dyes are presented in Figures (3.4.e, 3.4.f, 3.4.g and 3.4.h), respectively.

Comparison between the four Figures (3.4.e, 3.4.f, 3.4.g and 3.4.h) showed that it is possible to identify and determine each dye in the presence of the other three dyes without any interference, using the HPLC technique.

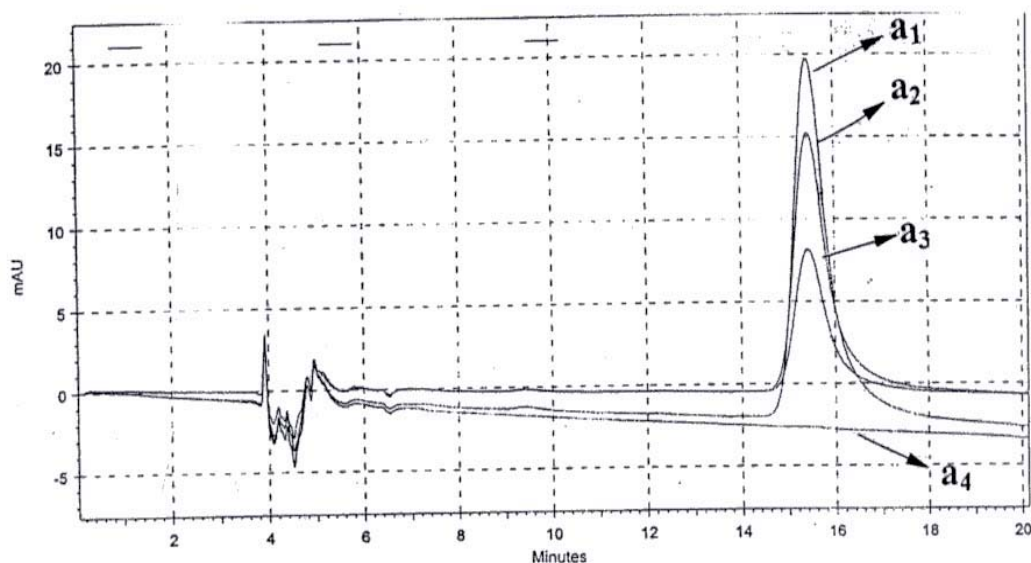


Figure 3.4.a. HPLC chromatograms for Direct Red 81 dye with a concentration of 20ppm at different wavelengths (510 nm, 607 nm, 484 nm and 411 nm). Conditions: temperature $25\pm 2^\circ\text{C}$, pH 6.1, mobile phase [acetonitrile: water (60: 40, v/v) containing 0.45M CTAB], flow rate = 0.5ml / min and using RP C_{18} column. a₁: peak at 510nm; a₂: peak at 484 nm; a₃: peak at 411 nm; a₄: peak at 607 nm.

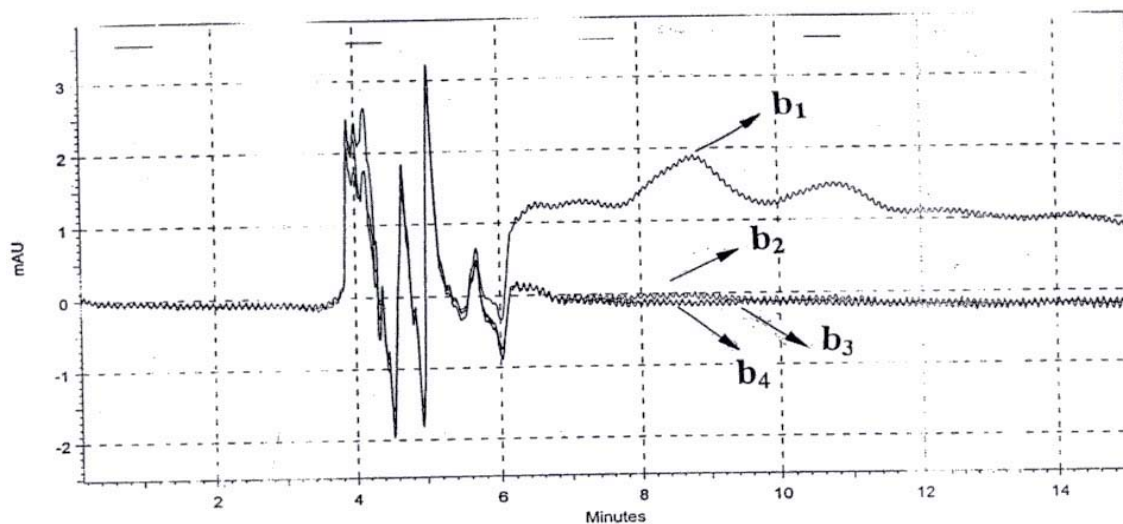


Figure 3.4.b. HPLC chromatograms for Direct Blue 15 dye with a concentration of 20ppm at different wavelengths (510 nm, 607 nm, 484 nm and 411 nm). Conditions: temperature $25\pm 2^\circ\text{C}$, pH 6.1, mobile phase [acetonitrile: water (60: 40, v/v) containing 0.45M CTAB], flow rate = 0.5ml / min and using RP C_{18} column. b_1 : peak at 607 nm; b_2 : peak at 484 nm; b_3 : peak at 411 nm; b_4 : peak at 510 nm.

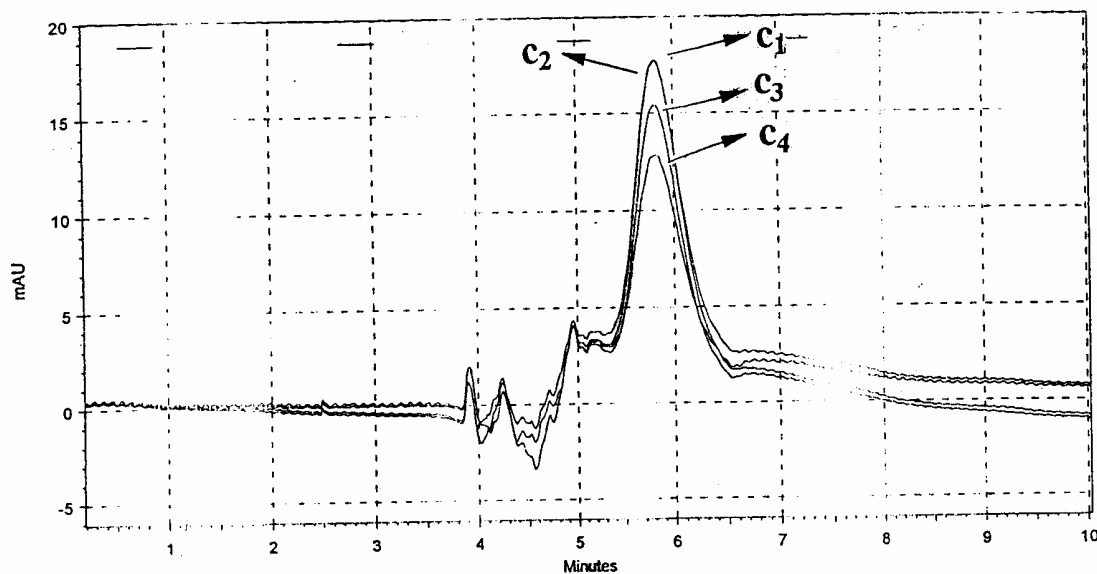


Figure 3.4.c. HPLC chromatograms for Direct Black 22 dye with a concentration of 50ppm at different wavelengths (510 nm, 607 nm, 484 nm and 411 nm). Conditions: temperature $25\pm 2^\circ\text{C}$, pH 6.1, mobile phase [acetonitrile: water (60: 40, v/v) containing 0.45M CTAB], flow rate = 0.5ml / min and using RP C_{18} column. c_1 : peak at 484 nm; c_2 : peak at 510 nm; c_3 : peak at 607 nm; c_4 : peak at 411 nm.

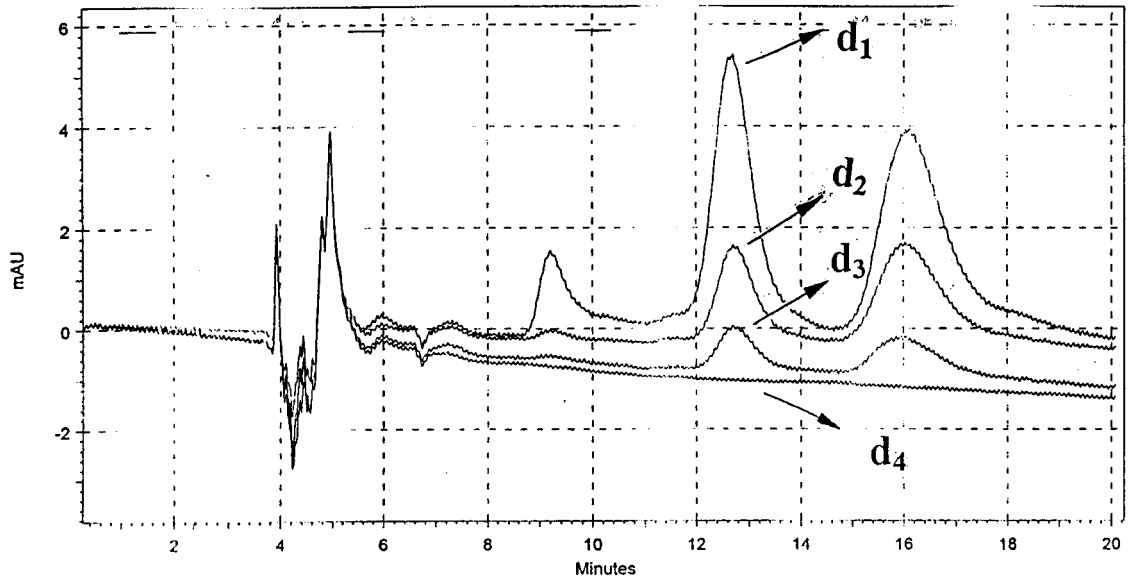


Figure 3.4.d. HPLC chromatograms for Direct Orange 34 dye with a concentration of 20ppm at different wavelengths (510 nm, 607 nm, 484 nm and 411 nm). Conditions: temperature $25\pm 2^\circ\text{C}$, pH 6.1, mobile phase [acetonitrile: water (60: 40, v/v) containing 0.45M CTAB], flow rate = 0.5ml / min and using RP C₁₈ column. d₁: peak at 411 nm; d₂: represents the peak at 484 nm; d₃: peak at 510 nm; d₄: peak at 607nm.

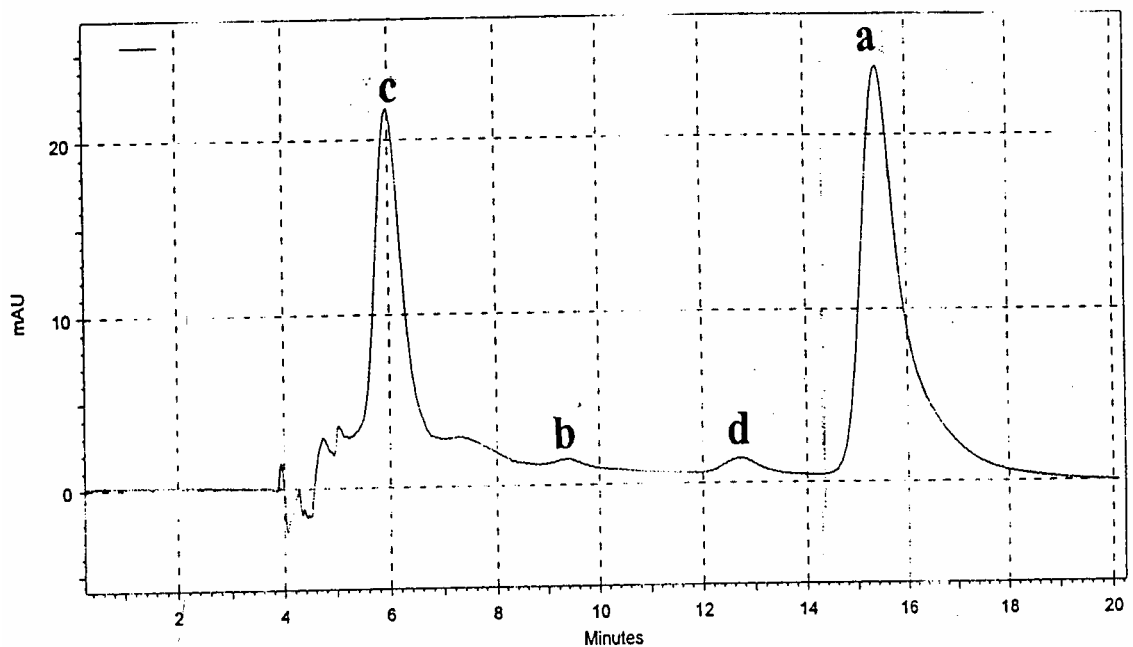


Figure 3.4.e. HPLC quantitative determination of (a) 20ppm Direct Red 81, (b) 20ppm Direct Blue 15, (c) 50ppm Direct Black 22 and (d) 20ppm Direct Orange 34 in the presence of each other at the conditions recommended for Direct red 81.

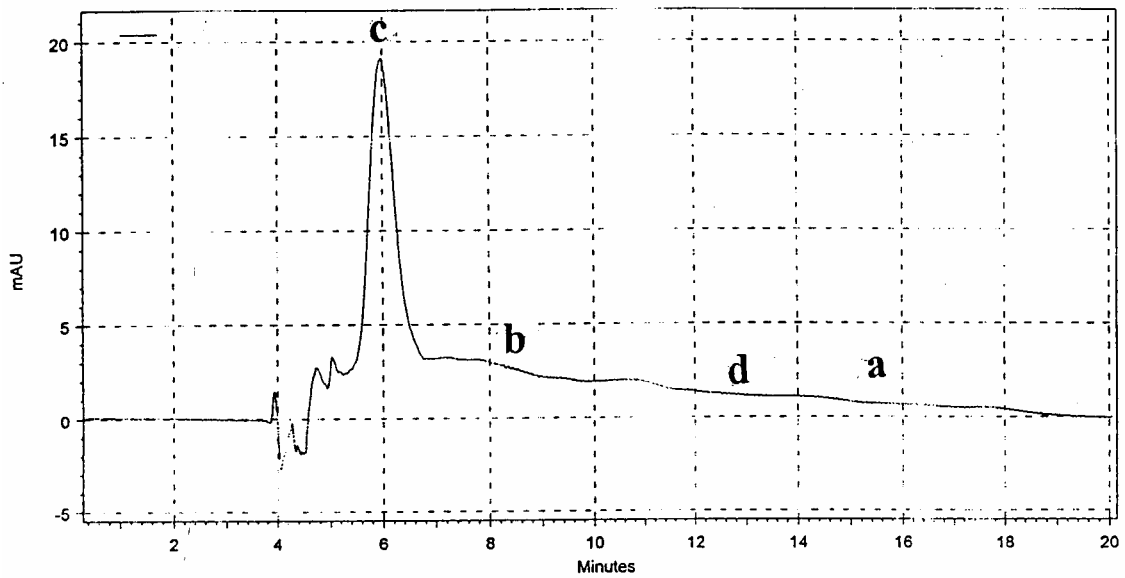


Figure 3.4.f. HPLC quantitative determination of (a) 20ppm Direct Red 81, (b) 20ppm Direct Blue 15, (c) 50ppm Direct Black 22 and (d) 20ppm Direct Orange 34 in the presence of each other at the conditions recommended for Direct Blue 15.

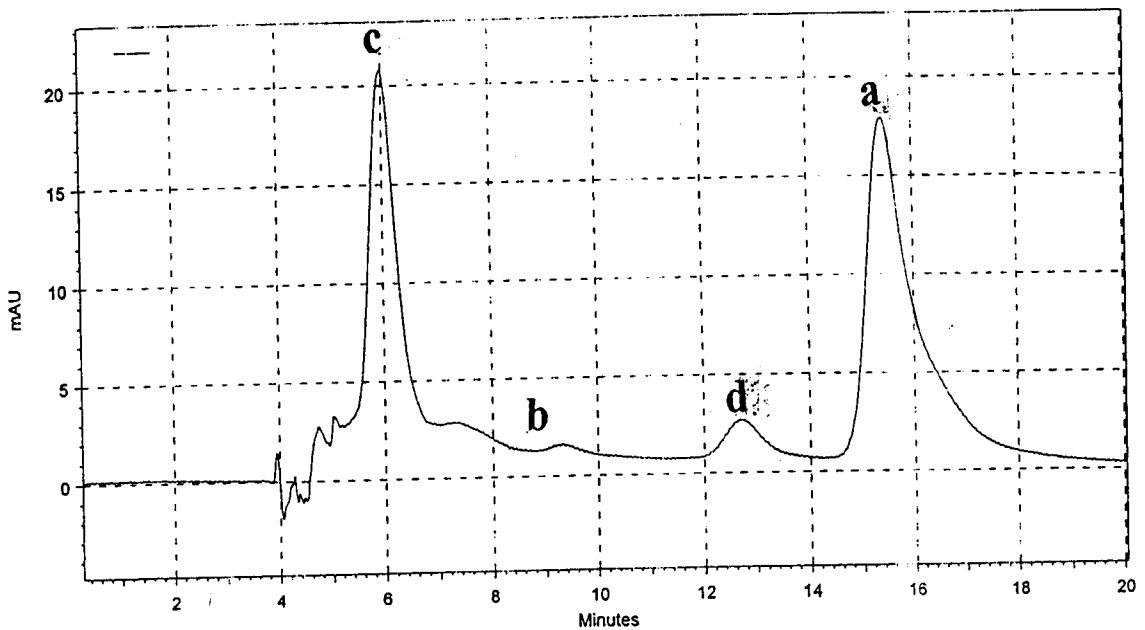


Figure 3.4.g. HPLC quantitative determination of (a) 20ppm Direct Red 81, (b) 20ppm Direct Blue 15, (c) 50ppm Direct Black 22 and (d) 20ppm Direct Orange 34 in the presence of each other at the conditions recommended for Direct Black 22.

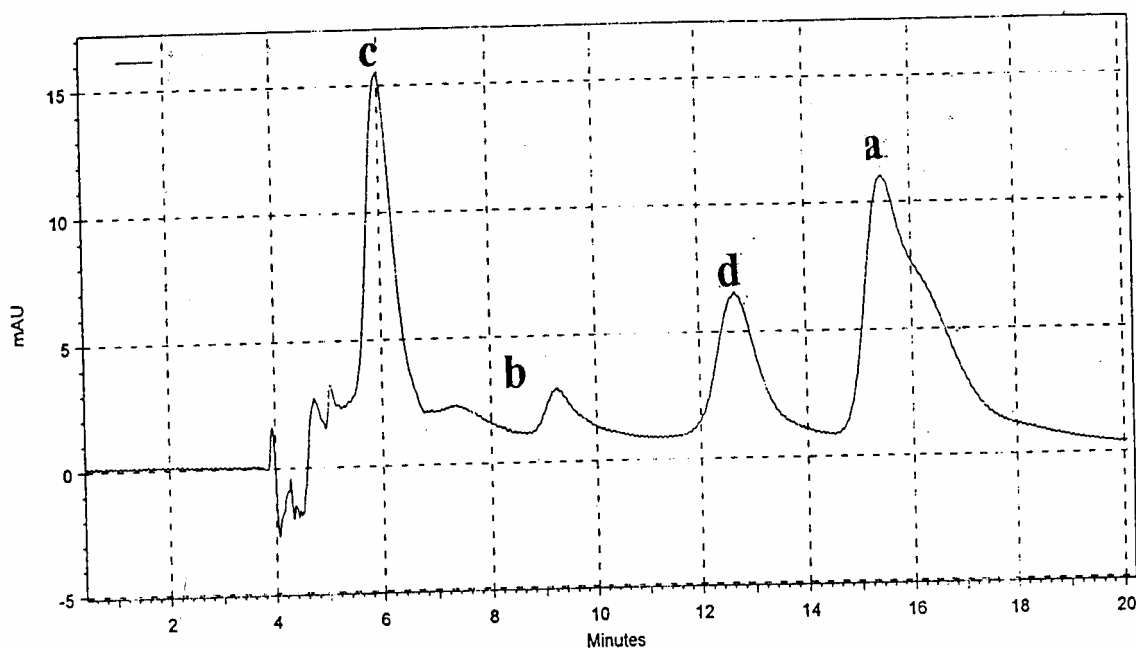


Figure 3.4.h. HPLC quantitative determination of (a) 20ppm Direct Red 81, (b) 20ppm Direct Blue 15, (c) 50ppm Direct Black 22 and (d) 20ppm Direct Orange 34 in the presence of each other at the conditions recommended for Direct Orange 34.

3.5 The resolution (R_s) of the method

The resolution R_s of the method provides a quantitative measure of its ability to separate the components of the mixture. A resolution of 1.5 gives an essential complete separation of the dyes. At a resolution of 1.5, the overlap between two successive dyes is about 0.3%. The resolution can be improved by lengthening the column or by altering the conditions of analysis.

In the present work the resolution between each two successive dyes is calculated. The obtained results (Table 3.5) showed ideal resolutions between the four dyes under the optimum conditions recommended in the experimental part.

Table 3.5. Resolution (R_s) in the separation of the four Direct dyes.

$W_A - W_B^*$	R_s
Direct Black 22— Direct Blue 15	2
Direct Black 22— Direct Orange 34	4.6
Direct Black 22— Direct Red 81	6.4
Direct Blue 15— Direct Orange 34	1.95
Direct Blue 15— Direct Red 81	3.3
Direct Orange 34— Direct Red 81	1.35

* W represents the HPLC characteristic peak of the studied dye. Conditions: temperature 25 ± 20 C, pH 6.1, mobile phase [acetonitrile: water (60: 40, v/v) containing 0.45M CTAB], flow rate = 0.5ml / min and using RP C18 column.

3.6 Analysis of real water samples

The proposed HPLC method was applied for quantitative determination of the four dyes (Direct Red 81, Direct Blue 15, Direct Black 22 and Direct Orange 34) in three real samples of ground water obtained from Wad Assajor, Khallet Asenan and Khallet Issa wells (Nablus city-Palestine). The obtained results are presented in figures (3.6.A, B and C).

It can be seen from the Figures that none of the four Direct dyes was detected in any of the three ground water samples.

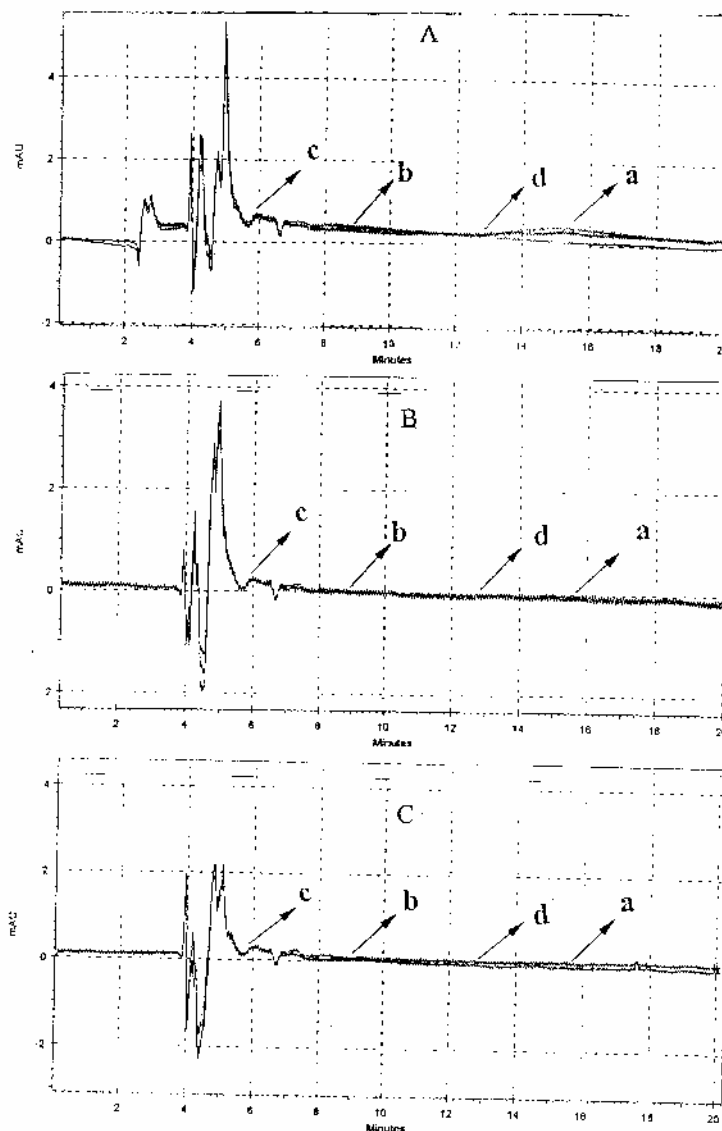


Figure 3.6. A-C. Typical chromatograms for detection and quantitative determination of the four dyes (Direct Red 81, Direct Blue 15, Direct Black 22 and Direct Orange 34) in three real samples of ground water collected from Wad Assajor, Khallet Asenan and Khallet Issa wells, respectively. Conditions: Wavelength (510 nm, 607 nm, 484 nm, 411nm), mobile phase: [0.45 M CTAB in acetonitrile: water (60:40, v / v)], temperature $25\pm 2^\circ\text{C}$, flow rate = 0.5 ml / min, injection volume = 20 μL , pH 6.1 (a, b, c and d): peaks position of Direct Red 81, Direct Blue 15, Direct Black 22 and Direct Orange 34, respectively. Each peak was detected at the corresponding wavelength.

Part II: Kinetic results of degradation

3.7 Kinetic results of degradation

The reducing degradation kinetics of the four Direct dyes in aqueous solutions were studied by investigating the factors that affect the rate of the dye degradation, and these factors include:

- 1- Effect of amount of iron and aluminum.
- 2- Effect of concentration of dye.
- 3- Effect of temperature.
- 4- Effect of pH.
- 5- Effect of agitation speed.

3.7.1 Effect of amount of iron and aluminum on degradation of Direct dyes in aqueous solution

Different amounts of iron and aluminum powder were used to study the effect of relative iron and aluminum surface area on the degradation rate. As seen from figure (3.7.1) that the absorbance of Direct Blue 15 decreases with increasing the time. Several experiments were carried out in which the amount of iron and aluminum was varied while the concentration of dyes and pH were kept constants, these experiments were carried out at constant temperature ($25\pm 2^\circ\text{C}$), and the obtained results are shown in figures (3.7.1.a, b, c and d) for iron and (3.7.1. e, f, g and h) for aluminum. The observations show that the decolorizing rate of the aqueous solution for the four Direct dyes increases as the iron and aluminum amount increases. The results of the iron-mediated and aluminum-mediated reduction of the Direct azo dyes demonstrated that reduction by zero-valent iron and aluminum is a surface mediated process. That is, direct contact of the dye with the iron and aluminum surface is necessary for electron

transfer to occur, so that as the iron and aluminum surface areas increase the rate of the dye decolorization will increase.

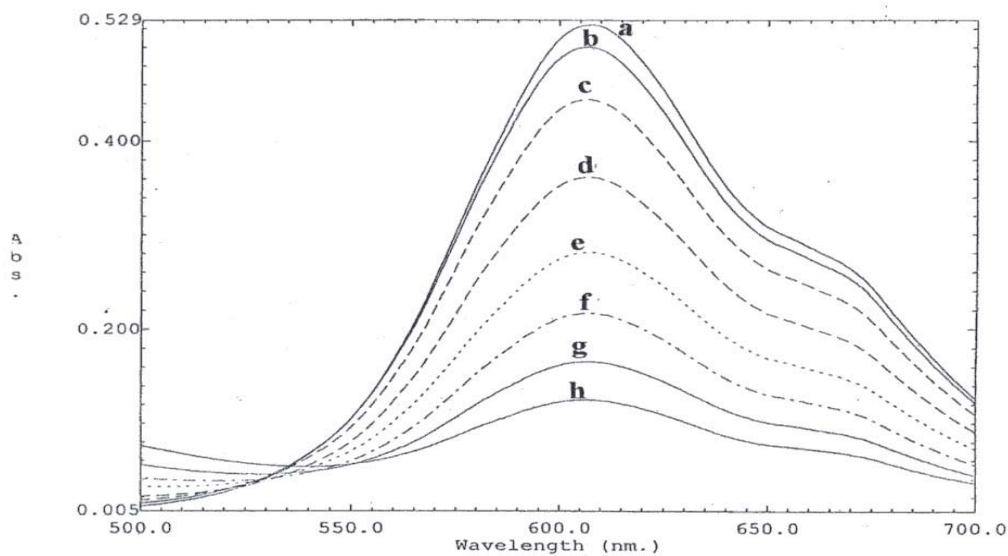


Figure 3.7.1. Absorption spectrum of the degradation solution of 20ppm Direct Blue 15 Conditions: pH= 6.1, amount of iron 1 g/50ml and temperature ($25\pm 2^\circ\text{C}$) at different reaction times curves after (a=0, b=3, c=6, d=9, e=12, f=15, g=18, h=21) min.

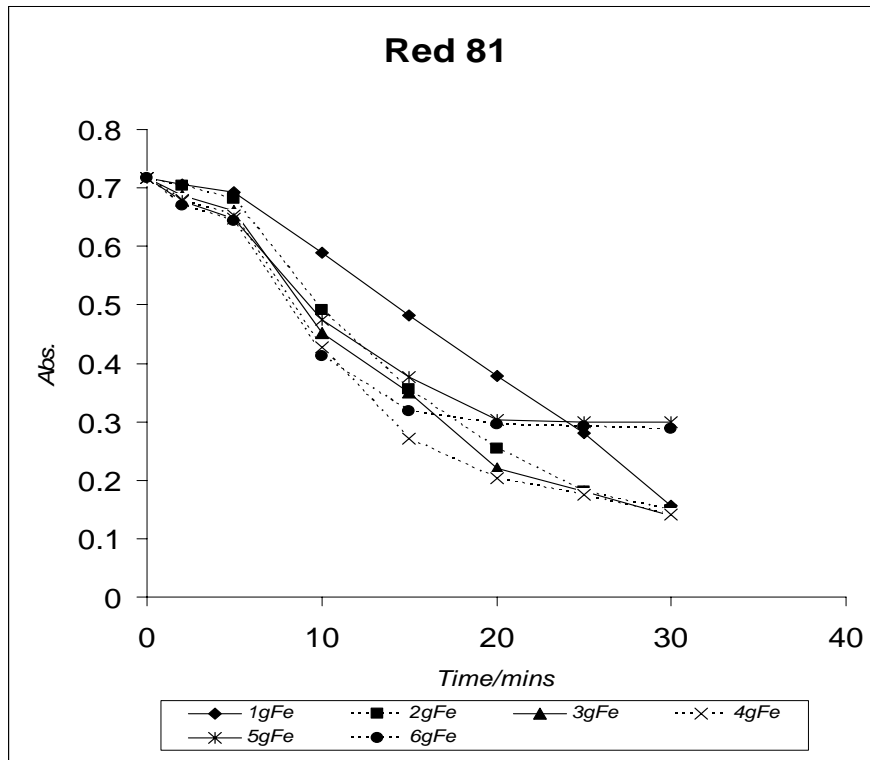


Figure 3.7.1.a. Effect of variable iron amount on degradation of Direct Red 81 dye. Conditions: [dye] = 20ppm, pH = 6.1, temperature ($25 \pm 2^\circ\text{C}$) and $\lambda_{\text{max}} = 510\text{nm}$.

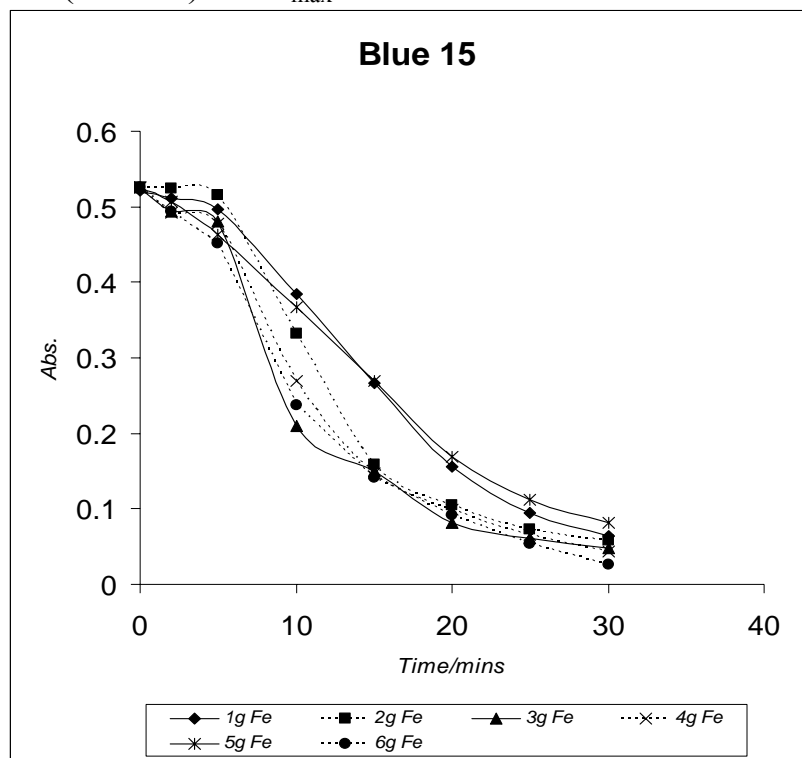


Figure 3.7.1.b. Effect of variable iron amount on degradation of Direct Blue 15 dye. Conditions: [dye] = 20ppm, pH = 6.1, temperature ($25\pm 2^\circ\text{C}$) and $\lambda_{\text{max}}=607\text{nm}$.

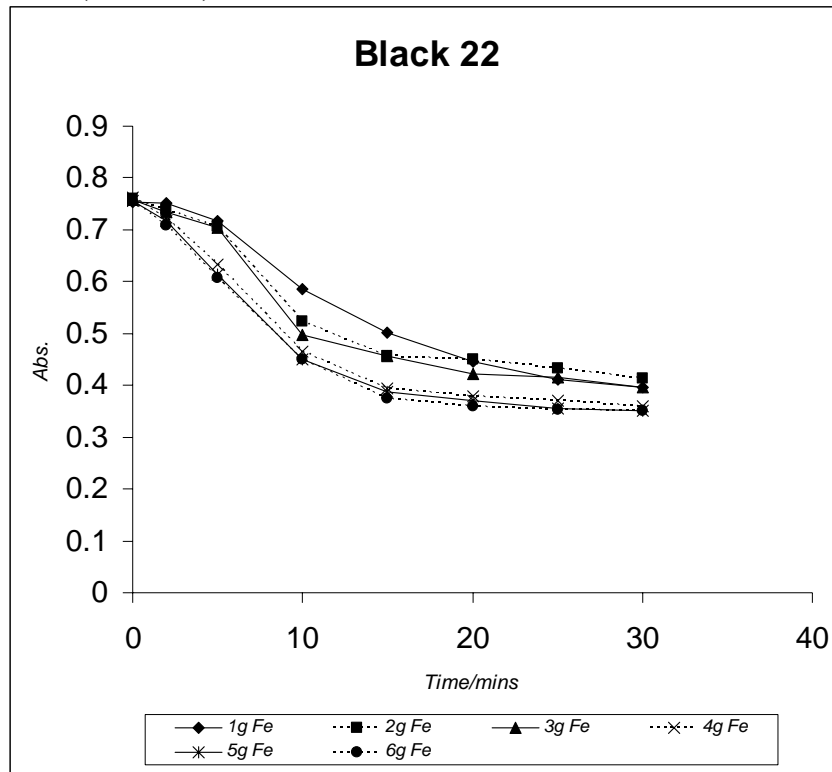


Figure 3.7.1.c. Effect of variable iron amount on degradation of Direct Black 22 dye. Conditions: [dye] = 50ppm, pH = 6.1, temperature ($25\pm 2^\circ\text{C}$) and $\lambda_{\text{max}}=484\text{nm}$.

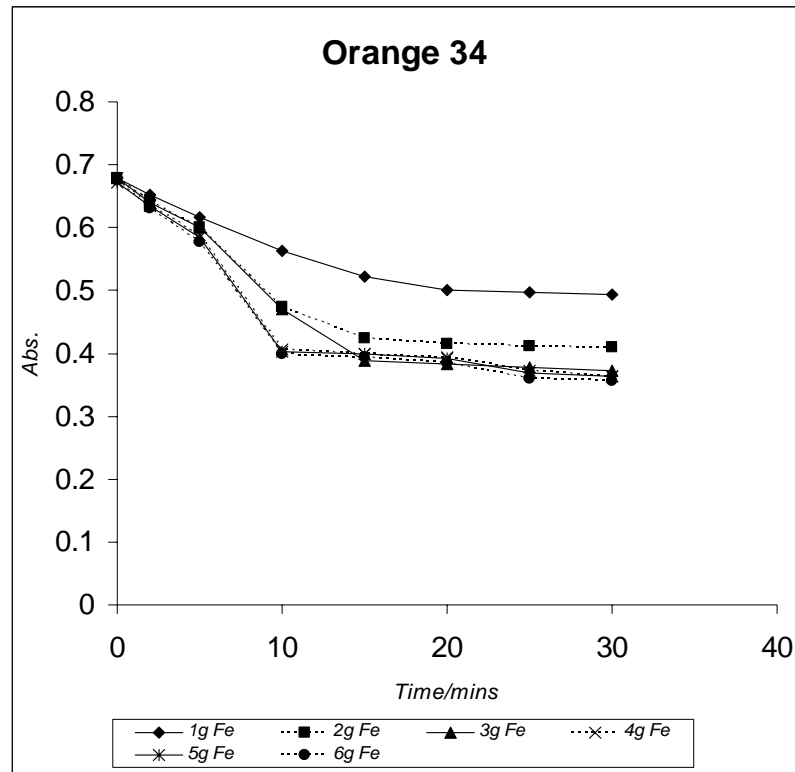


Figure 3.7.1.d. Effect of variable iron amount on degradation of Direct Orange 34 dye. Conditions: [dye] = 20ppm, pH =6.1, temperature ($25\pm 2^\circ\text{C}$) and $\lambda_{\text{max}}=411\text{nm}$.

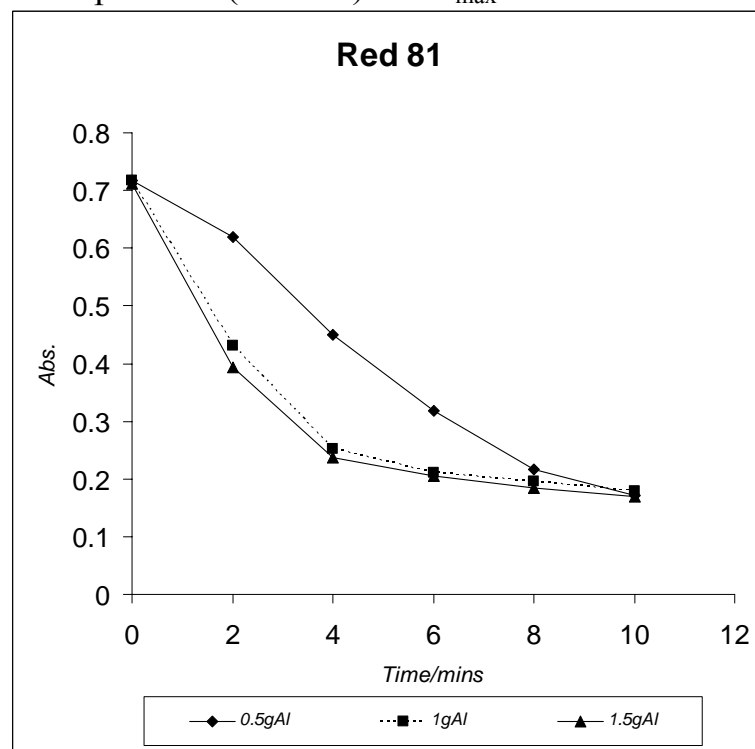


Figure 3.7.1.e. Effect of variable Al amount on degradation of Direct Red 81 dye. Conditions: [dye] = 20 ppm, pH = 6.1, temperature ($25\pm 2^\circ\text{C}$) and $\lambda_{\text{max}}=510\text{nm}$.

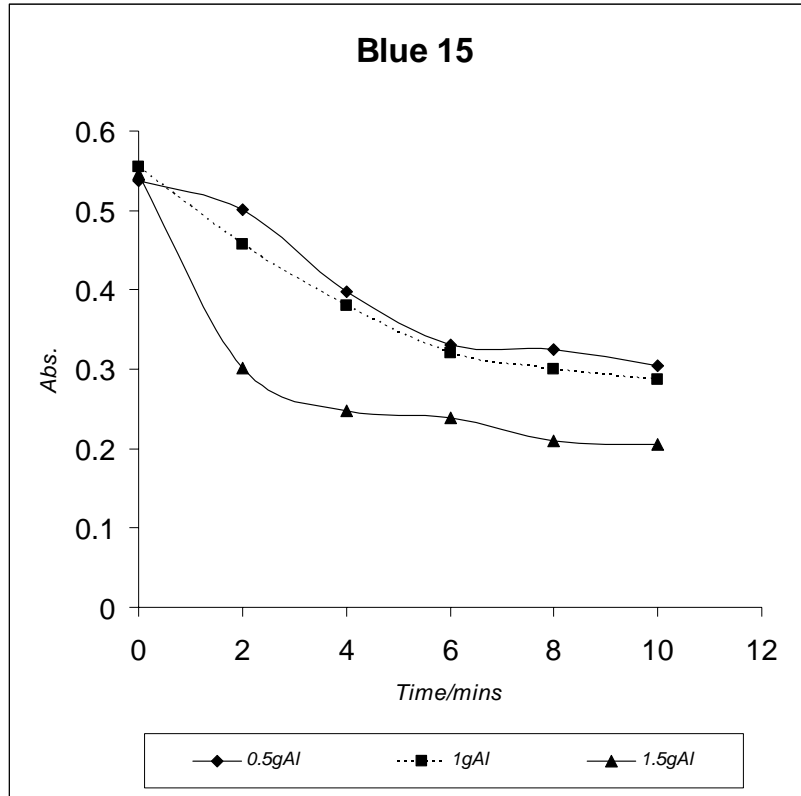


Figure 3.7.1.f. Effect of variable Al amount on degradation of Direct Blue 15 dye. Conditions: [dye] = 20ppm, pH = 6.1, temperature ($25\pm 2^\circ\text{C}$) and $\lambda_{\text{max}}=607\text{nm}$.

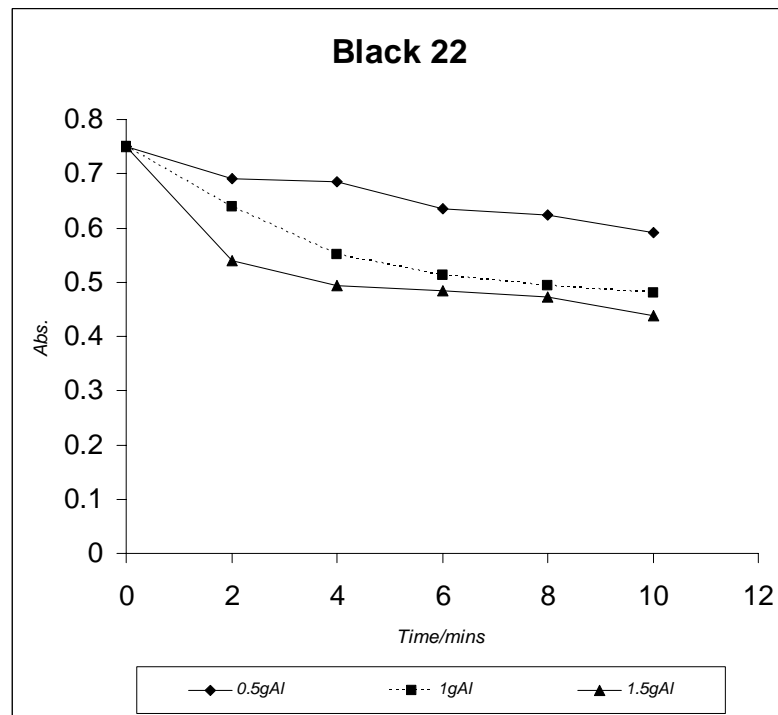


Figure 3.7.1.g. Effect of variable Al amount on degradation of Direct Black 22 dye. Conditions: [dye] = 50ppm, pH = 6.1, temperature ($25\pm 2^\circ\text{C}$) and $\lambda_{\text{max}}=484\text{nm}$.

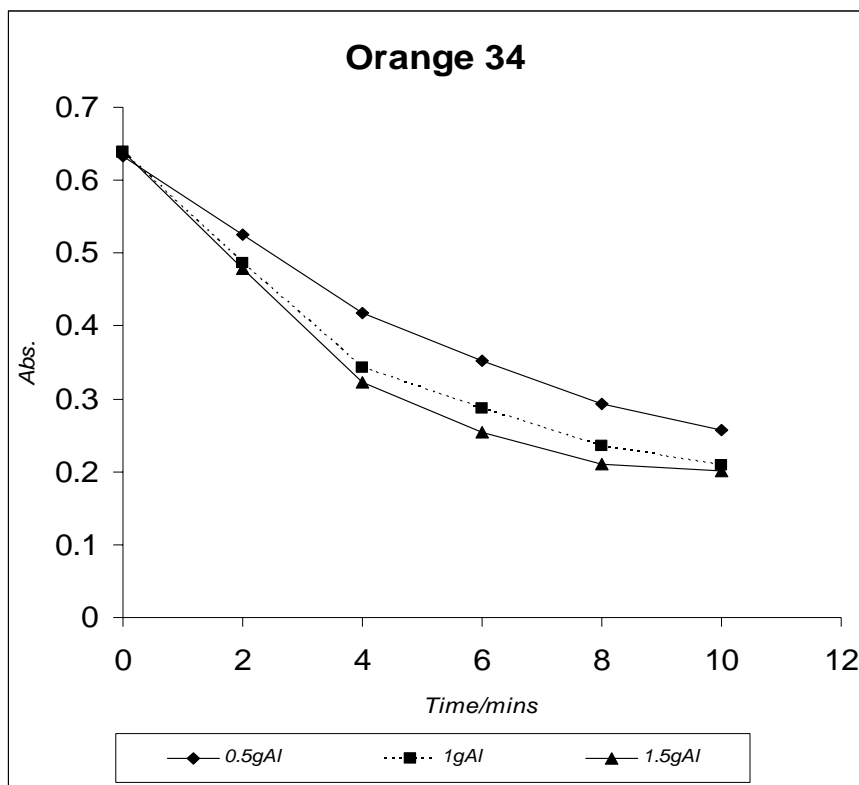


Figure 3.7.1.h. Effect of variable Al amount on degradation of Direct Orange 34 dye. Conditions: [dye] = 20ppm, pH = 6.1, temperature ($25\pm 2^\circ\text{C}$) and $\lambda_{\text{max}}=411\text{nm}$.

3.7.2 Effect of concentration of dye on degradation of aqueous Direct dyes

Several experiments were carried out in which the concentration of the dyes was varied while the amount of iron and aluminum added and pH were kept constants. These experiments were carried out at constants temperature ($25\pm 2^\circ\text{C}$). To obtain the observed rate constant for the degraded dye a plot of natural log absorbance versus time was constructed, the results show a nonlinear regression to the kinetic model for sequential first-order reactions kinetics.

The results of figures (3.7.2.a, b, c, d, e, f, g and h) show that the degradation of the dye fit well with the Langmmir adsorption model as follows:

$$r_L = -dC/dt = k_{obs} \cdot C / (1 + k_{obs} \cdot C)$$

Where r_L is the degradation rate, C is the concentration of the degraded dye, t is the reaction time, k_{obs} is the observed rate constant.

Degradation observed rate constant was calculated from the slope of the plot $1/R_0$ vs. $1/C_0$ figure (3.7.2).

Where R_0 is the initial rate of degradation, C_0 is the initial concentration of the degraded dye.

The obtained results are summarized in Tables (3.7.2.1), (3.7.2.2) and figures (3.7.2.a, b, c and d) for iron and figures (3.7.2.e, f, g and h) for aluminum.

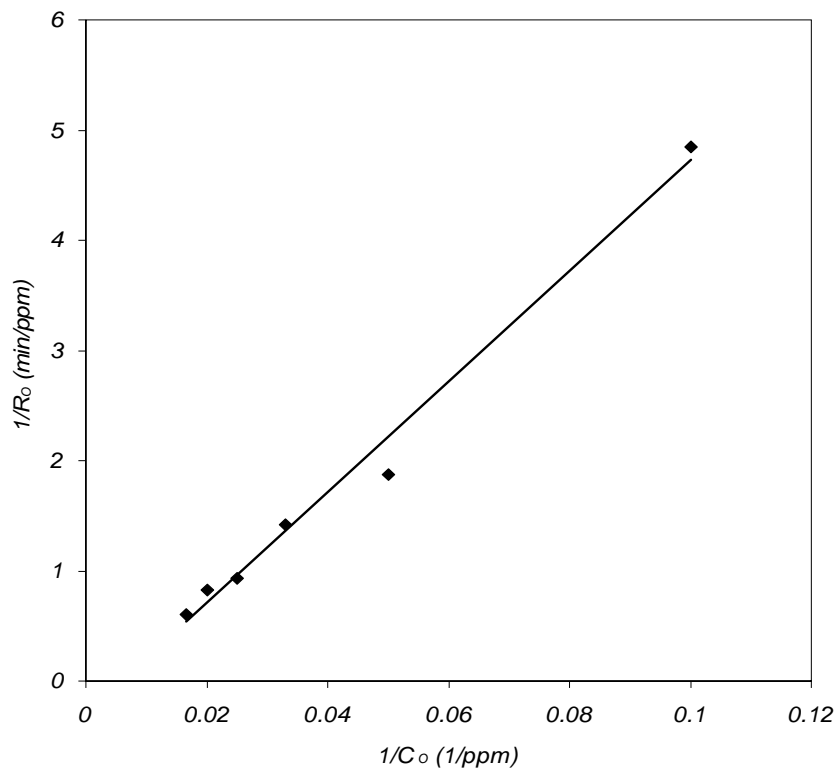


Figure 3.7.2. Langmuir adsorption isotherm plot of Direct Black 22 dye. Conditions: amount of iron = 1g/50ml, pH=6.1 and temperature ($25 \pm 2^\circ\text{C}$).

Table 3.7.2.1. Observed reaction rate constants ($k_{\text{obs.}}$) for the four Direct dyes degradation in $\text{Fe}^0\text{-H}_2\text{O}$ system.

Dye	Amount of iron used g/50 ml	Observed rate constant, $k_{\text{obs.}}$ (mmol/L.min)
Direct Red 81	1	0.0212
Direct Blue 15	1	0.1515
Direct Black 22	1	0.0120
Direct Orange 34	1	0.0160

Conditions: pH = 6.1, temperature ($25 \pm 2^\circ \text{C}$).

Table 3.7.2.2. Observed reaction rate ($k_{\text{obs.}}$) constants for the four Direct dyes degradation in $\text{Al}^0\text{-H}_2\text{O}$ system.

Dye	Amount of aluminum used g/50 ml	Observed rate constant, $k_{\text{obs.}}$ (mmol/L.min)
Direct Red 81	0.5	0.0641
Direct Blue 15	0.5	0.0575
Direct Black 22	0.5	0.0125
Direct Orange 34	0.5	0.0436

Conditions: pH = 6.1, temperature ($25 \pm 2^\circ \text{C}$).

From the observed rate constants, it can be concluded that Direct Black 22 has the highest number of azo groups. The rate of disappearance of color is different in each case with Direct Blue 15 decolorizing the fastest in $\text{Fe}^0\text{-H}_2\text{O}$ system and Direct Black 22 decolorizing the slowest. In general dyes with higher number of -N=N- bonds were slower to degrade (Table 1). Also it can be seen that there is an increase in observed rate constants ($k_{\text{obs.}}$) when using Al metal compared to Fe metal in spite of using less amount of Al, this can be attributed to a higher standard electrode potential (E°) of Al metal. The observed rate constant is different for Direct Blue 15 (less than expected when using Al) this may be explained by the structure. the differences of the observed rate constants between Direct Red 81 and Direct Blue 15 (diazo Direct dyes) can be attributed to the auxochromes (electron-withdrawing or electron-donating substituents

that intensify the color of the chromophore by altering the overall energy of the electron system) of each dye.

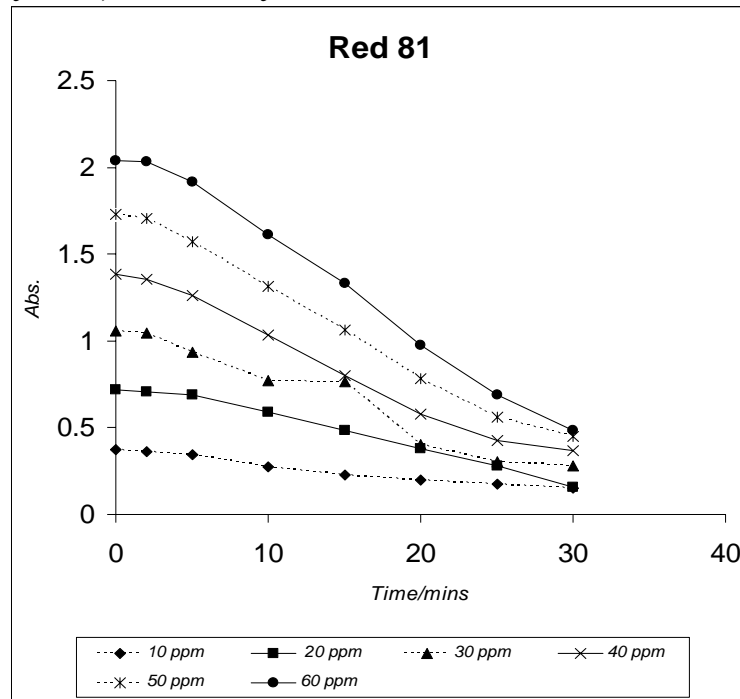


Figure 3.7.2.a. Effect of the dye concentration on degradation of Direct Red 81 dye. Conditions: amount of Fe = 1g/50ml, pH = 6.1, λ_{\max} = 510nm and temperature (25±2°C).

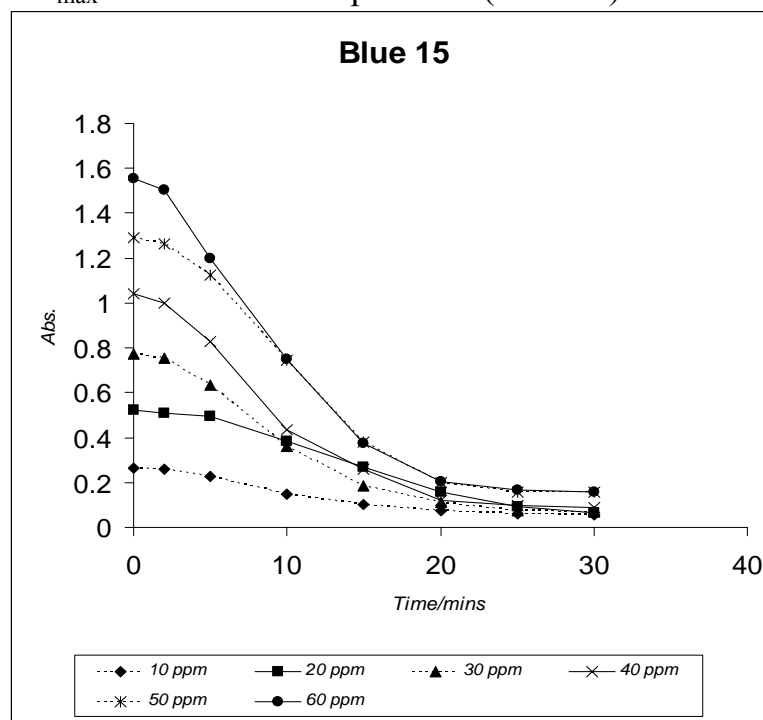


Figure 3.7.2.b. Effect of the dye concentration on degradation of Direct Blue dye. Conditions: amount of Fe = 1g/50ml, pH = 6.1, λ_{\max} = 607nm and temperature (25±2°C).

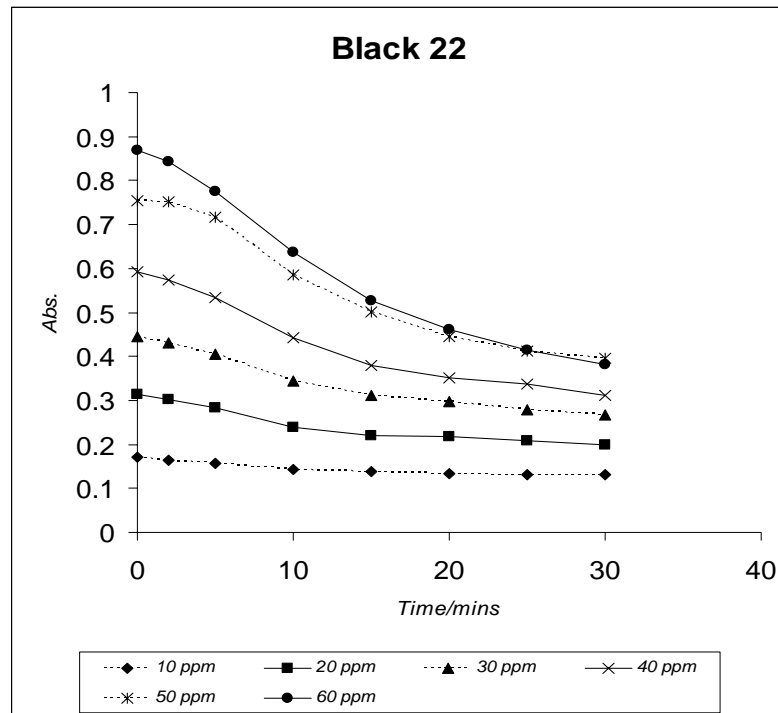


Figure 3.7.2.c. Effect of the dye concentration on degradation of Direct Black 22 dye. Conditions: amount of Fe= 1g/50ml, pH = 6.1, λ_{\max} =484nm and temperature (25±2°C).

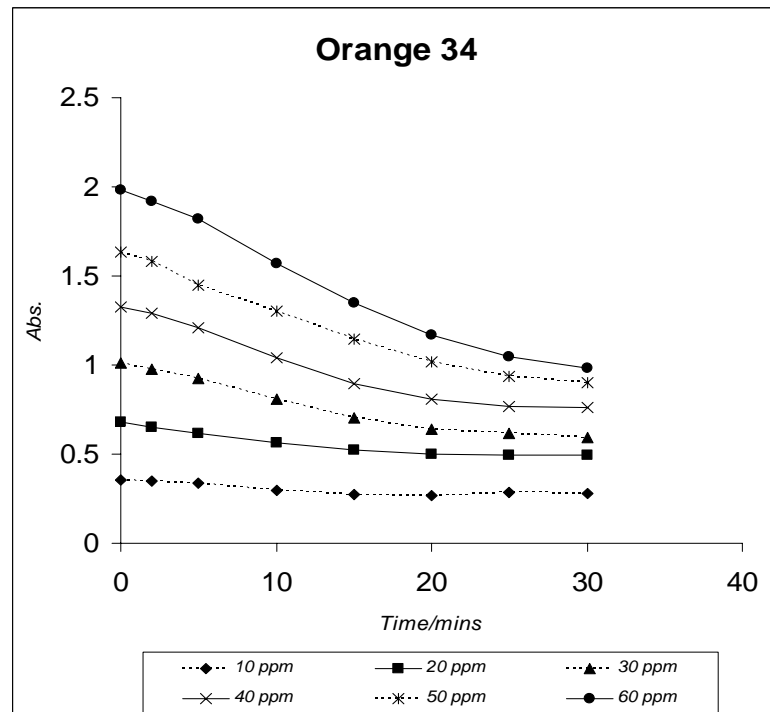


Figure 3.7.2.d. Effect of the dye concentration on degradation of Direct Black 22 dye. Conditions: amount of Fe= 1g/50ml, pH = 6.1, λ_{\max} =411nm and temperature (25±2°C).

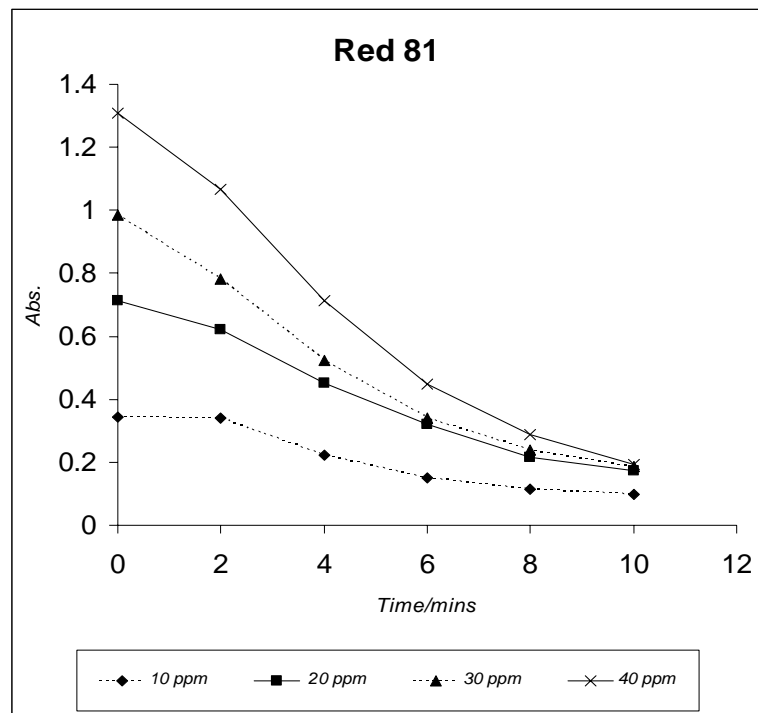


Figure 3.7.2.e. Effect of the dye concentration on degradation of Direct Red 81 dye. Conditions: amount of Al= 0.5g/50ml, pH=6.1, λ_{\max} =510nm and temperature ($25\pm 2^\circ\text{C}$).

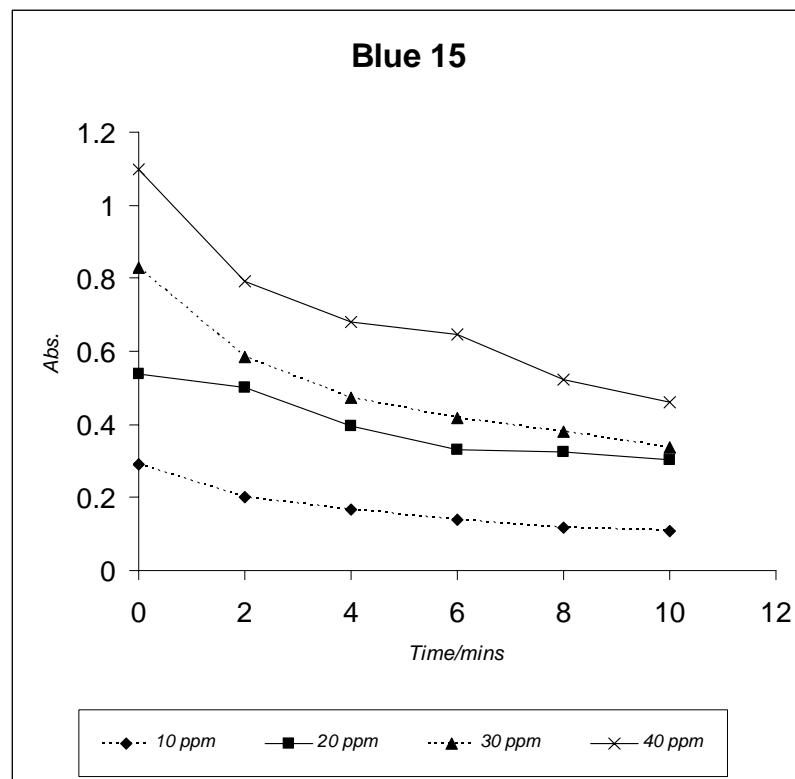


Figure 3.7.2.f. Effect of the dye concentration on degradation of Direct Blue dye. Conditions: amount of Al= 0.5g/50ml, pH=6.1, λ_{\max} =607nm and temperature ($25\pm 2^\circ\text{C}$).

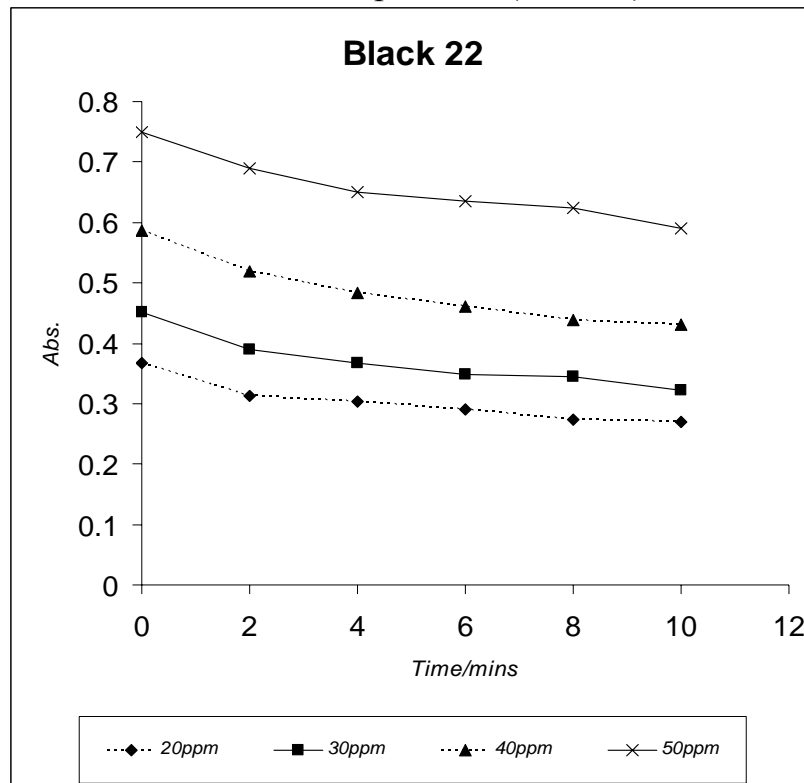


Figure 3.7.2.g. Effect of the dye concentration on degradation of Direct Black 22 dye. Conditions: amount of Al= 0.5g/50ml, pH=6.1, λ_{\max} =484nm and temperature ($25\pm 2^\circ\text{C}$).

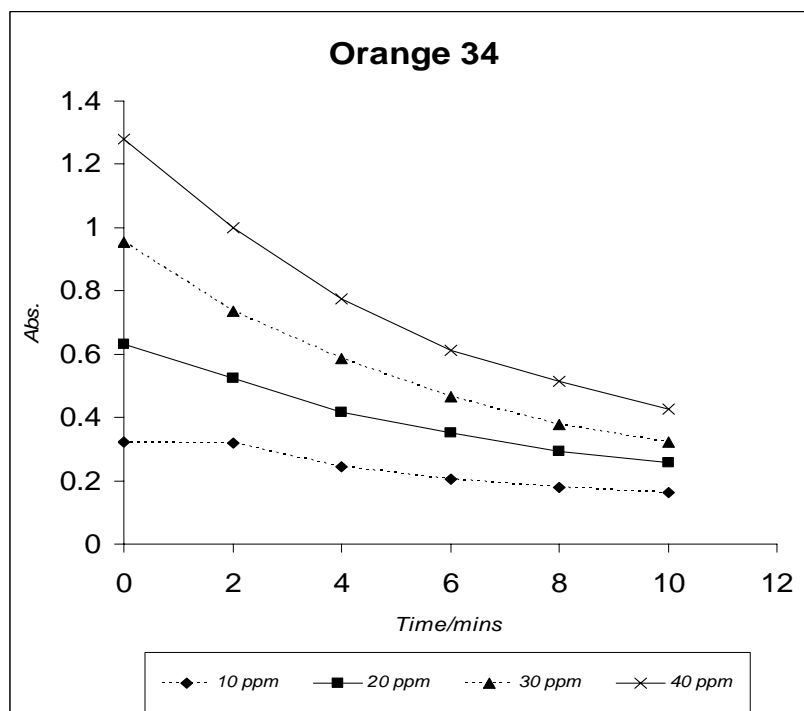


Figure 3.7.2.h. Effect of the dye concentration on degradation of Direct Orange 34 dye. Conditions: amount of Al= 0.5g/50ml, pH=6.1, λ_{\max} =411nm and temperature (25±2°C).

3.7.3 Effect of temperature on degradation of Direct dyes

Several experiments were carried out in which the temperature was varied while the amount of iron and aluminum, the concentrations of the dyes and pH were kept constants. The results are shown in figures (3.7.3.a, b, c and d) for iron and figures (3.7.3.e, f, g and h) for aluminum. The results show that the rate of degradation of each aqueous direct dyes increases with increasing the temperature. The rate constants were assumed to obey the Arrhenius equation:

$$k_{\text{obs}} = A \exp (- E_{\text{act}}^{\#} / RT)$$

Where A is the frequency factor, $E_{\text{act}}^{\#}$ is the activation energy, R is the gas law constant, and T is the temperature in K. This equation was rearranged after taking the natural logarithm of each side to yield

$$\ln k_{\text{obs.}} = \ln A - (E_{\text{act}}^{\#} / R) \times (1/T)$$

Activation energy ($E_{\text{act}}^{\#}$) activation enthalpy ($\Delta H^{\#}$) and activation entropy ($\Delta S^{\#}$) for the four Direct dyes were calculated and presented in Tables (3.7.3.1) and (3.7.3.2).

Table 3.7.3.1. Thermodynamic parameters for degradation of Direct dyes in $\text{Fe}^0 - \text{H}_2\text{O}$ system.

Dye	$E_{\text{act}}^{\#}$ kJ/mol	$\Delta H^{\#}$ kJ/mol	$\Delta S^{\#}$ J/mol
Direc Red 81	12.45	9.98	230.97
Direct Blue 15	6.61	4.14	237.88
Direct Black 22	22.92	20.45	204.18
Direct Orange 34	14.11	11.64	231.55

Conditions: pH = 6.1, amount of Fe = 1 g/50 ml.

Table 3.7.3.2. Thermodynamic parameters for degradation of Direct dyes in Al₂O₃ – H₂O system.

Dye	$E_{act}^{\#}$ kJ/mol	$\Delta H^{\#}$ kJ/mol	$\Delta S^{\#}$ J/mol
Direc Red 81	6.24	4.17	246.33
Direct Blue 15	23.74	21.26	188.70
Direct Black 22	7.47	4.99	256.00
Direct Orange 34	11.15	8.67	233.13

Conditions: pH = 6.1, amount of Al = 0.5 g/50 ml.

Temperature ($25 \pm 2^{\circ}\text{C}$) was selected for further study of the other factors that affect the rate of the dye degradation because it represents the normal conditions of the environment.

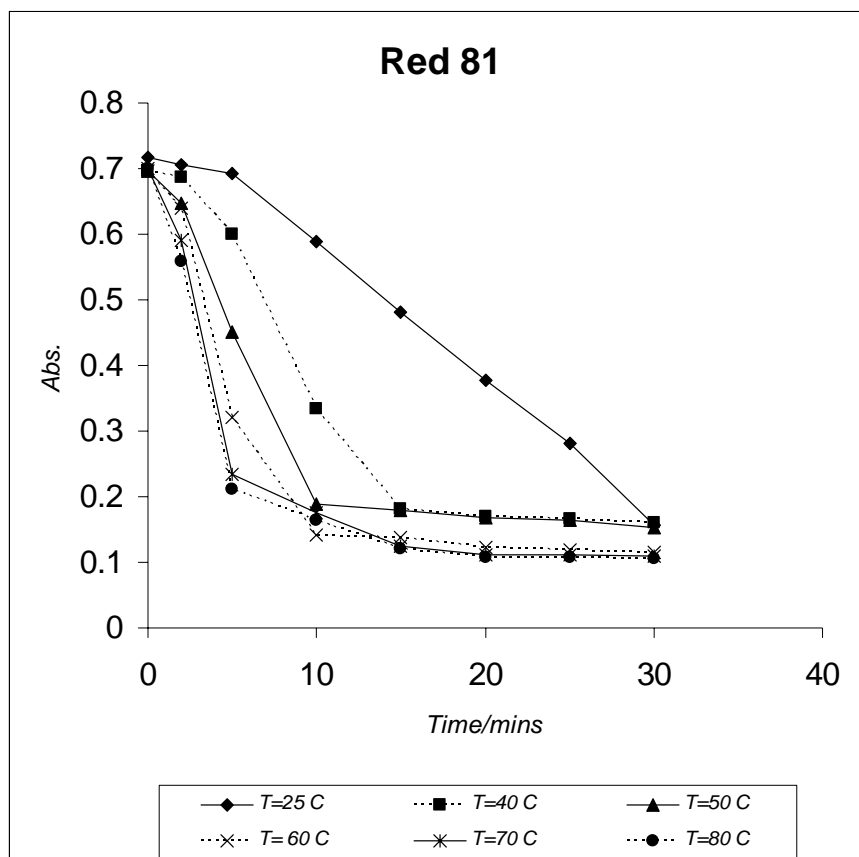


Figure 3.7.3.a. Effect of temperature on degradation of Direct Red 81 dye. Conditions: amount of Fe= 1g/50 ml, [dye] =20ppm, λ_{max} =510nm and pH =6.1.

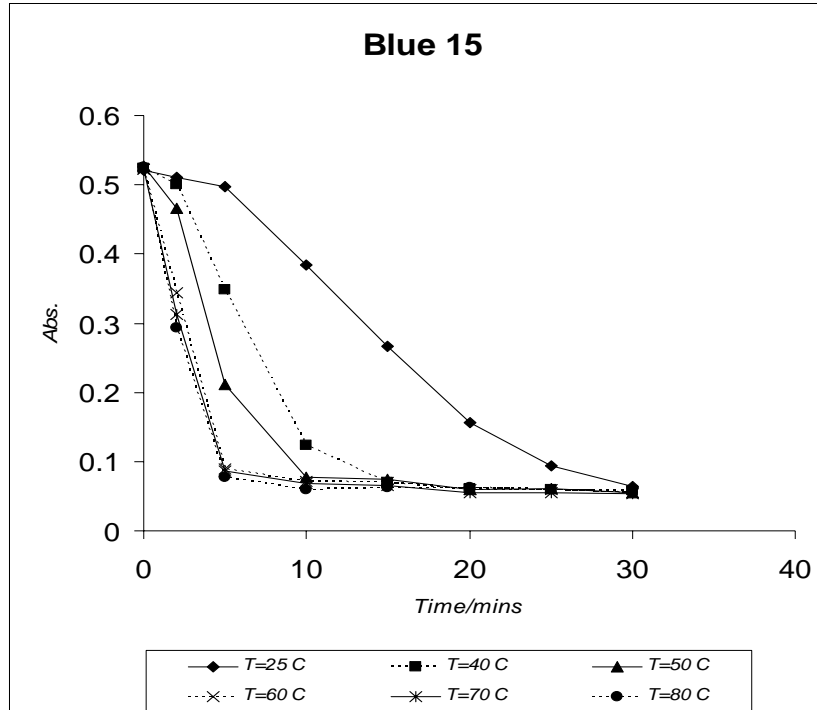


Figure 3.7.3.b. Effect of temperature on degradation of Direct Blue 15 dye.
 Conditions: amount of Fe= 1g/50 ml, [dye] = 20ppm, λ_{\max} =607nm and pH =6.1.

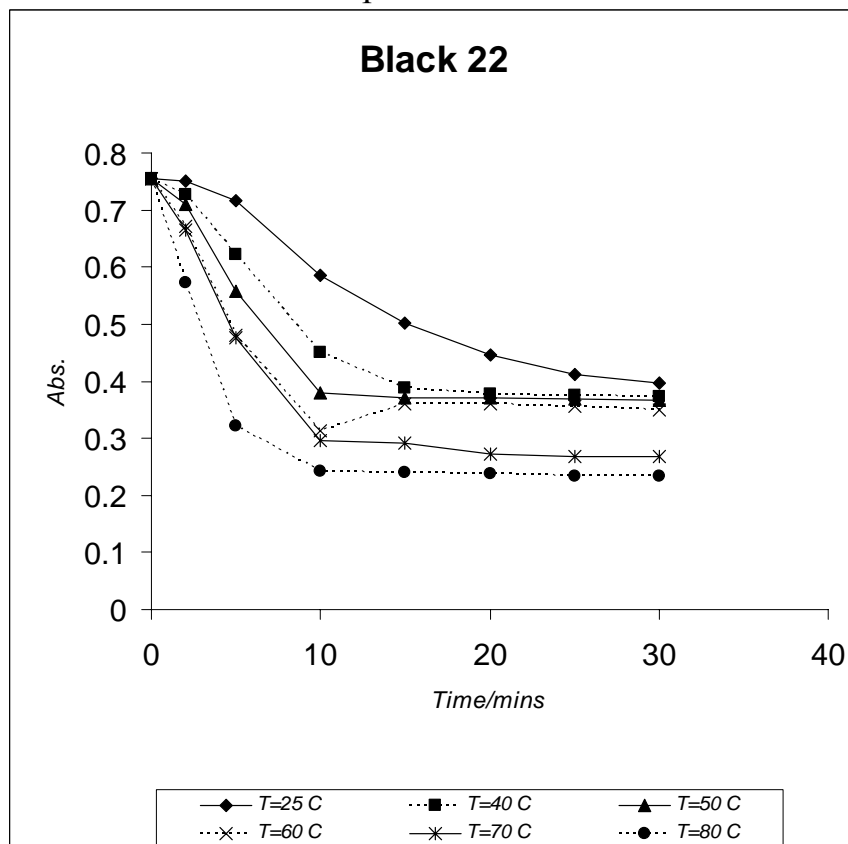


Figure 3.7.3.c. Effect of temperature on degradation of Direct Black 22 dye. Conditions: amount of Fe= 1g/50 ml, [dye] = 50ppm, λ_{\max} =484nm and pH=6.1.

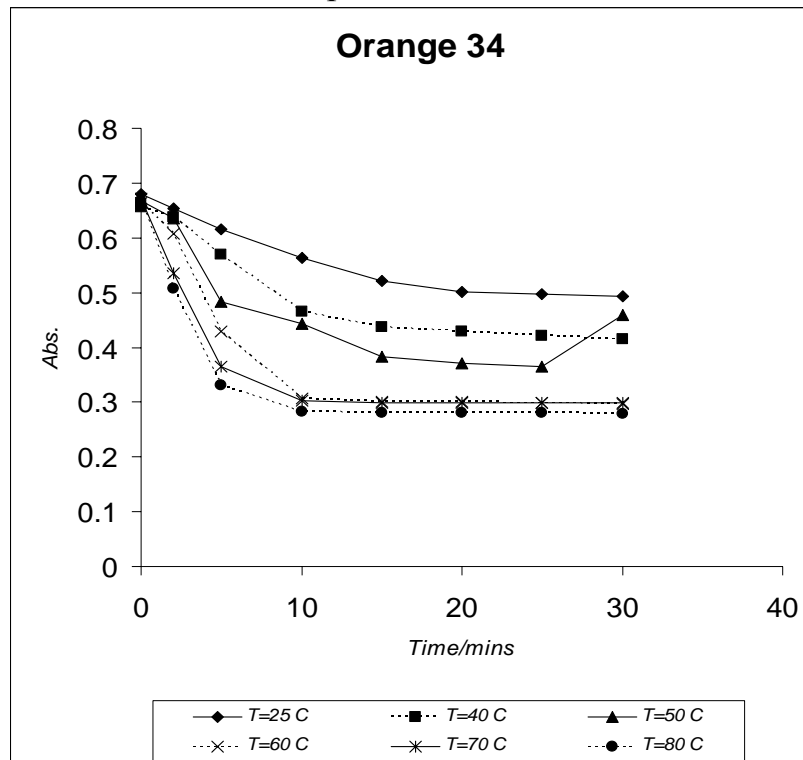


Figure 3.7.3.d. Effect of temperature on degradation of Direct Orange 34 dye. Conditions: amount of Fe= 1g/50 ml, [dye] = 20ppm, λ_{\max} =411nm and pH=6.1.

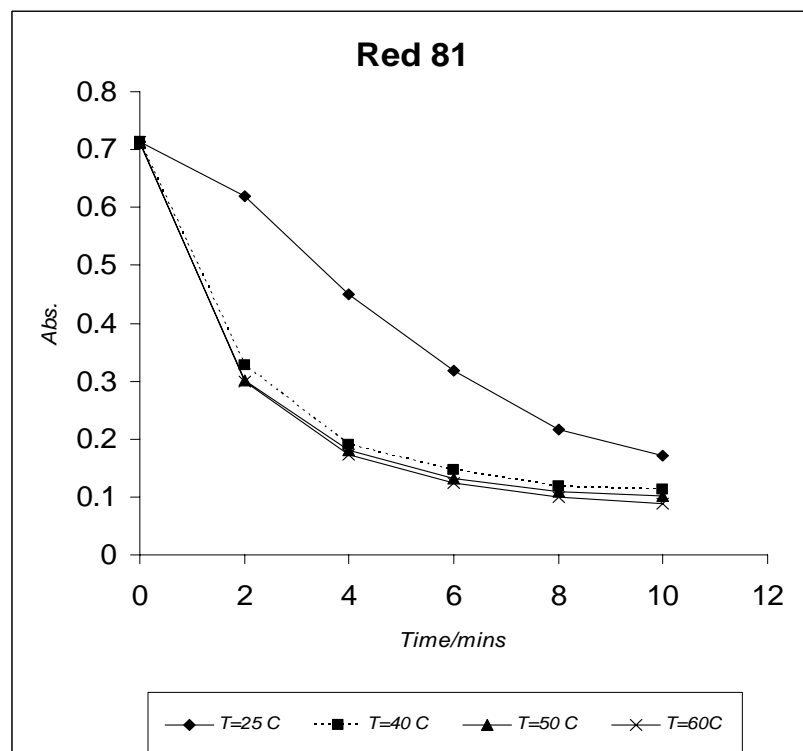


Figure 3.7.3.e. Effect of temperature on degradation of Direct Red 81 dye.
 Conditions: amount of Al= 0.5g/50 ml, [dye] = 20ppm,
 λ_{\max} =510nm and pH =6.1.

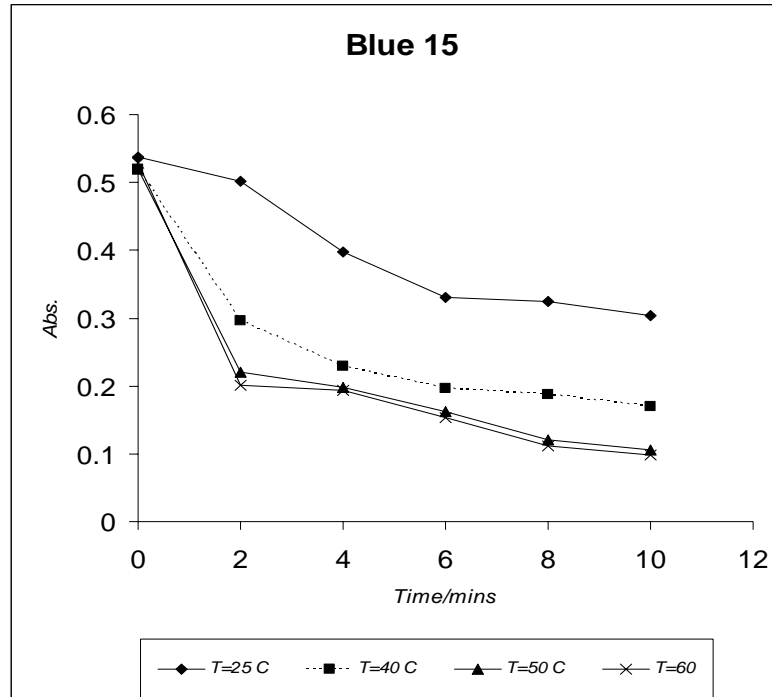
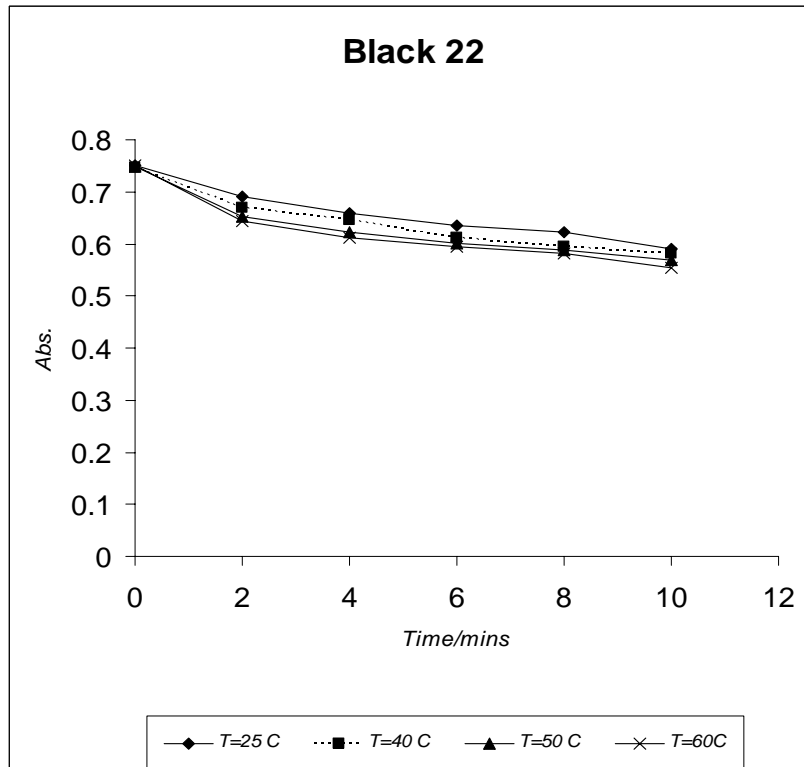


Figure (3.7.3.f. Effect of temperature on degradation of Direct Blue 15 dye.
 Conditions: amount of Al= 0.5g/50 ml, [dye] = 20ppm,
 λ_{\max} =607nm and pH =6.1.



Figure(3.7.3.g. Effect of temperature on degradation of Direct Black 22 dye. Conditions: amount of Al= 0.5g/50 ml, [dye] = 50ppm, λ_{\max} =484nm and pH =6.1.

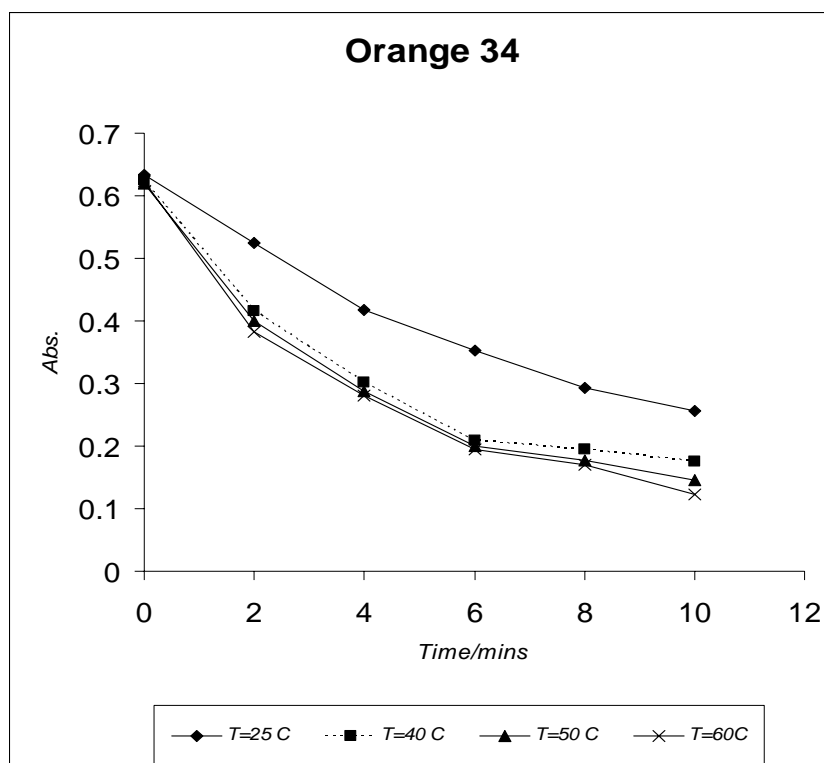


Figure 3.7.3.h. Effect of temperature on degradation of Direct Orange 34 dye. Conditions: amount of Al= 0.5g/50 ml, [dye] = 20ppm, λ_{\max} =411nm and pH =6.1.

3.7.4 Effect of pH on degradation of Direct dyes

Several experiments were carried out in which the pH was varied at room temperature ($25 \pm 2^\circ\text{C}$) while the amount of iron and aluminum, concentration of dyes were kept constants. The results are summarized in figures (3.7.4.a, b, c, d, e, f, g and h). We can see from figures (3.7.4.a, b, c, d, e, f, g and h) that pH strongly affects the degradation rate, when an interaction between dye molecules and iron happens iron as an electron donor, loses electrons, the dye molecule, as an electron acceptor accepts electrons from iron and combined with H^+ and turns into the transition product. This product gets electron from iron and combined with H^+ again,

then it turns into terminal products. So pH would affect the degradation reaction and with acidity increasing, the degradation rate increases of each aqueous Direct dyes that is, the more acid solution is the more rapidly the degradation rate. With more H^+ in acidic solution than that in alkaline solution, the reaction is easier and the reaction rate constant is higher. It is clear that color is much faster removed at a low pH environment. pH =6.1 was selected for further study of the other factors that affect the rate of the dye degradation because it represents the normal conditions of the environment.

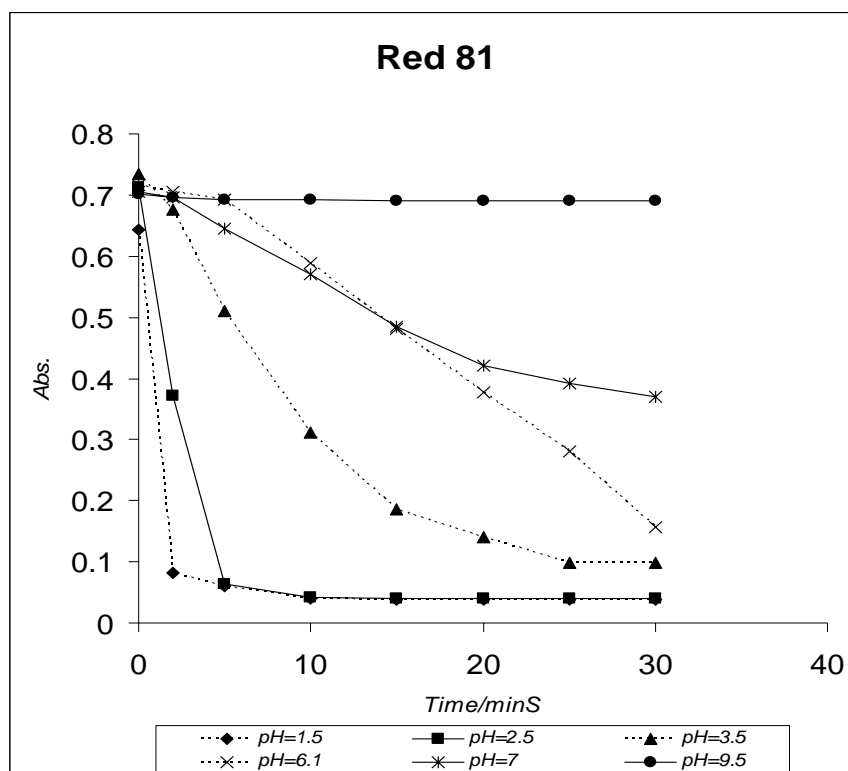


Figure 3.7.4.a. Effect of variable pH on degradation of Direct Red 81 dye. Conditions: amount of Fe= 1g/50 ml, [dye] = 20ppm, λ_{\max} =510nm and temperature ($25 \pm 2^\circ\text{C}$).

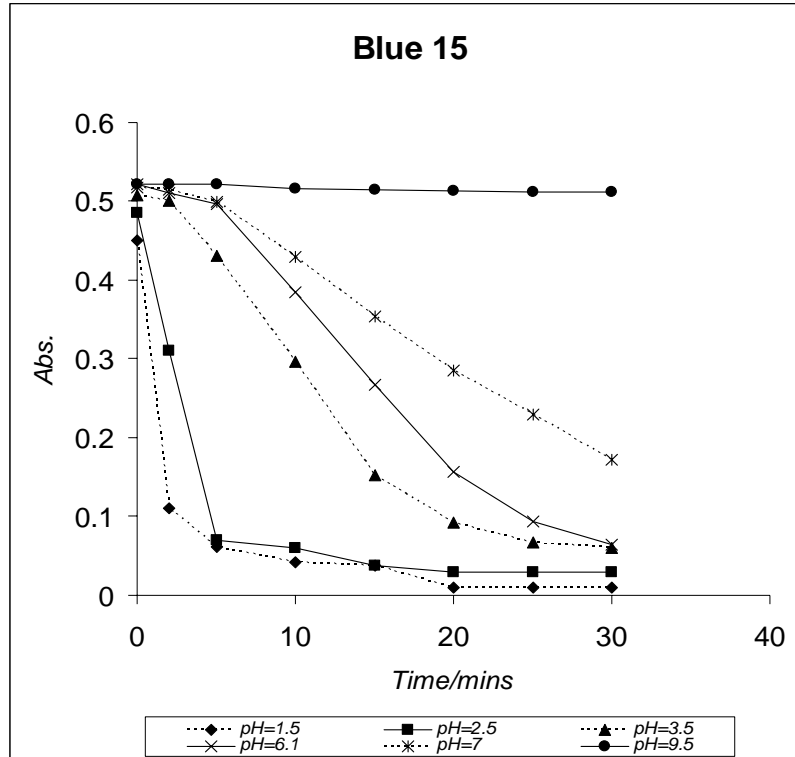


Figure 3.7.4.b. Effect of variable pH on degradation of Direct Blue 15 dye. Conditions: amount of Fe = 1g/50 ml, [dye] = 20ppm, λ_{\max} = 607nm and temperature ($25 \pm 2^\circ\text{C}$).

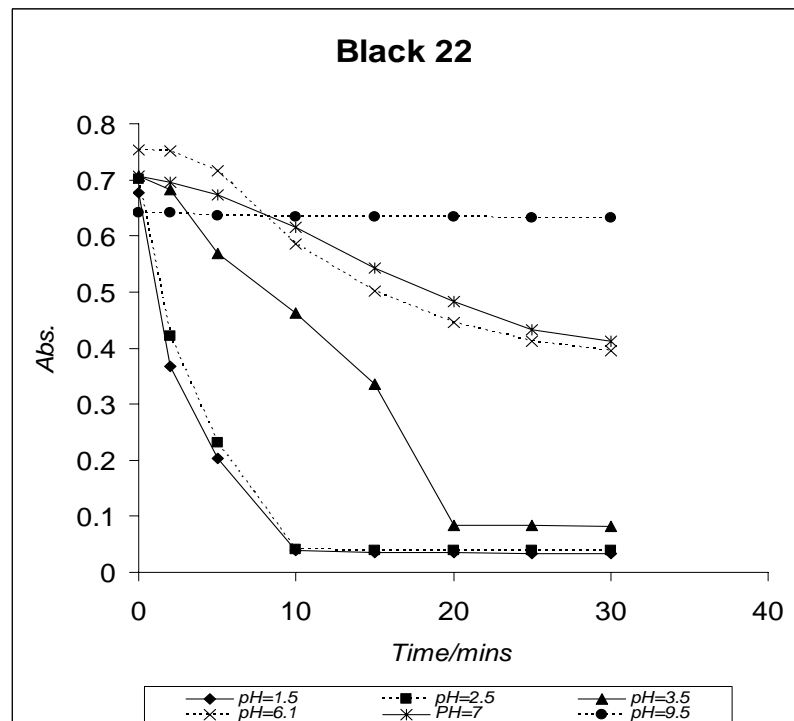


Figure 3.7.4.c. Effect of variable pH on degradation of Direct Black 22 dye. Conditions: amount of Fe = 1g/50 ml, [dye] = 50ppm, λ_{\max} = 484nm and temperature ($25 \pm 2^\circ\text{C}$).

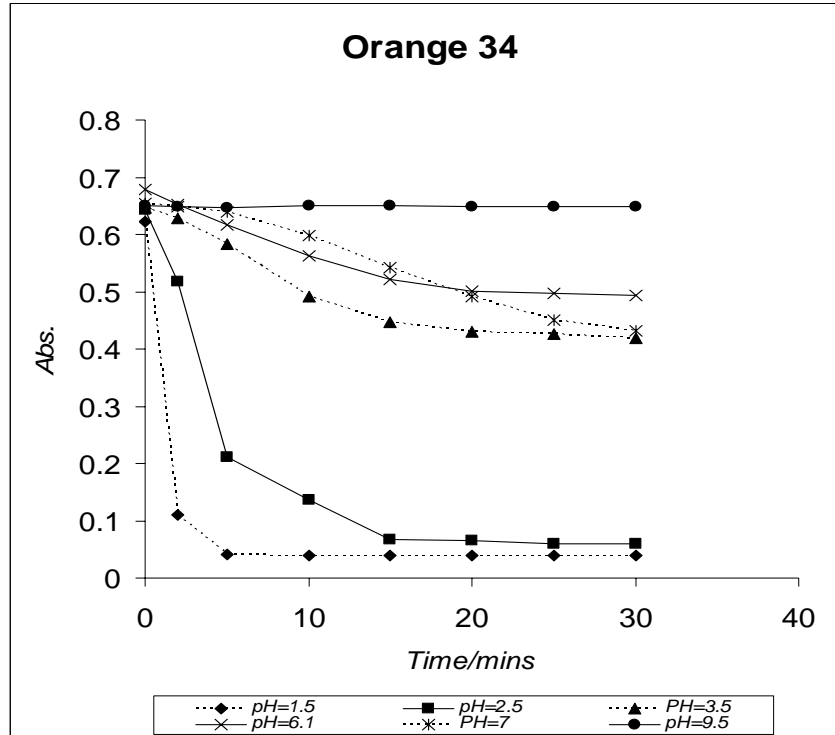


Figure 3.7.4.d. Effect of variable pH on degradation of Direct Orange 34 dye. Conditions: amount of Fe = 1g/50 ml, [dye] = 20ppm, λ_{\max} =411nm and temperature ($25 \pm 2^\circ\text{C}$).

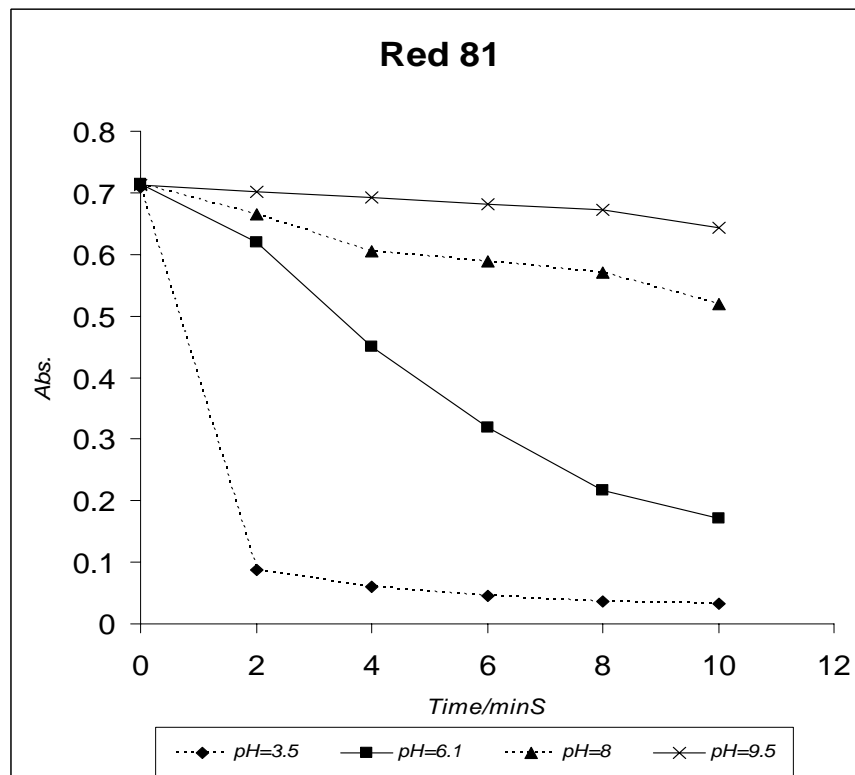


Figure 3.7.4.e. Effect of variable pH on degradation of Direct Red 81 dye. Conditions: amount of Al = 0.5g/50 ml, [dye] = 20ppm, λ_{\max} =510nm and temperature ($25 \pm 2^\circ\text{C}$).

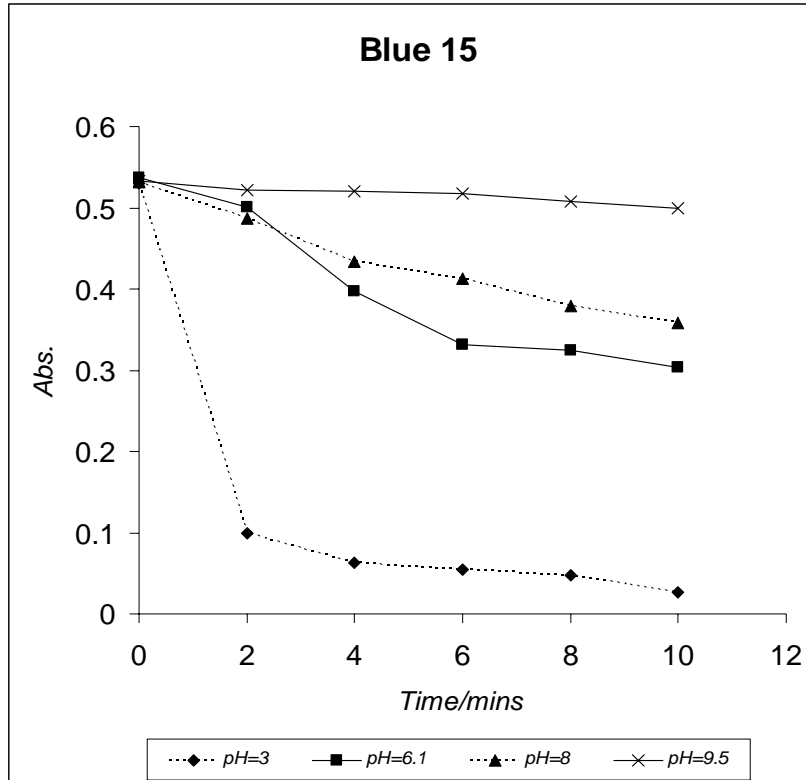


Figure 3.7.4.f. Effect of variable pH on degradation of Direct Blue 15 dye. Conditions: amount of Al = 0. g/50 ml, [dye] = 20ppm, λ_{\max} =607nm and temperature ($25 \pm 2^\circ\text{C}$).

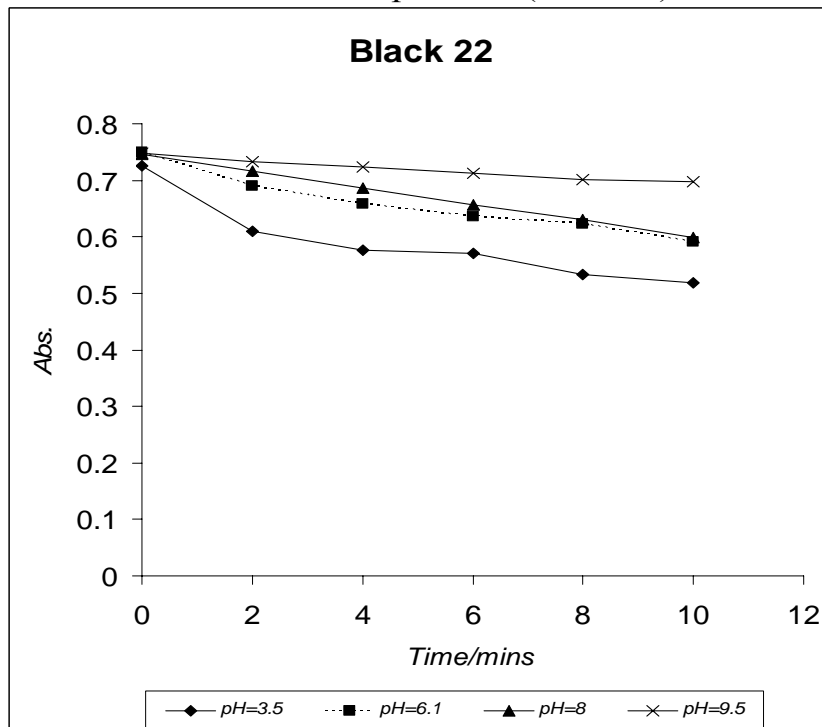


Figure 3.7.4.g. Effect of variable pH on degradation of Direct Black 22 dye. Conditions: amount of Al = 0.5g/50 ml, [dye] = 50ppm, λ_{\max} =484nm and temperature ($25 \pm 2^\circ\text{C}$).

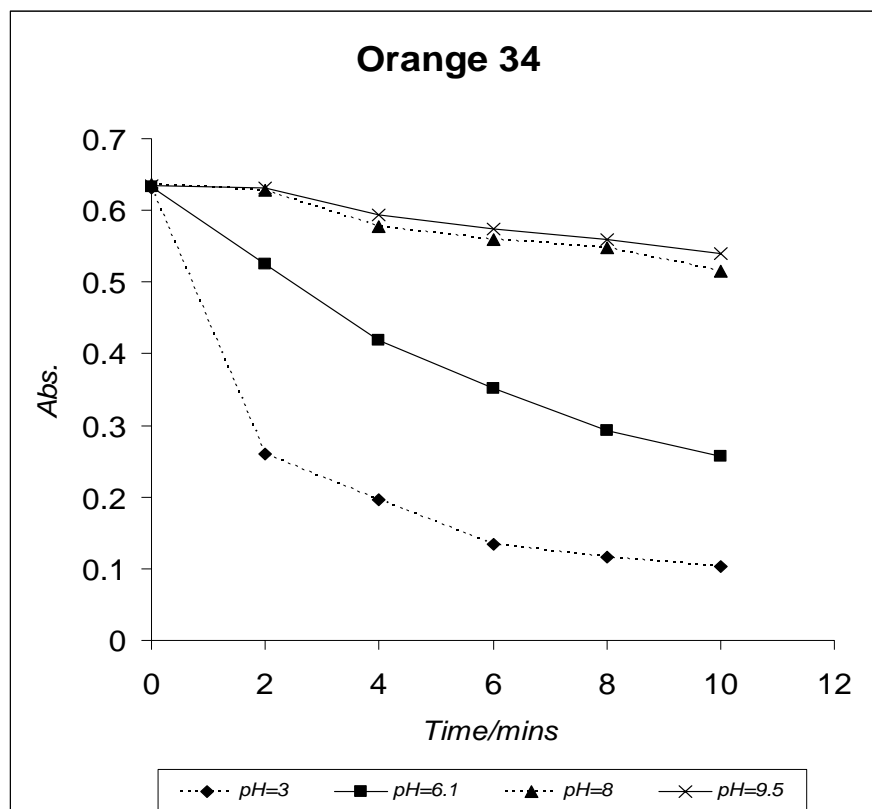


Figure 3.7.4.h. Effect of variable pH on degradation of Direct Orange 34 dye. Conditions: amount of Al = 0.5g/50 ml, [dye] = 20ppm, λ_{\max} =411nm and temperature ($25 \pm 2^\circ\text{C}$).

3.7.5 Effect of agitation speed on degradation of Direct dyes

The effect of the speed of agitation on degradation of Direct azo dyes was studied. Several experiments were carried out in which the speed of agitation was varied (no agitation, 1500 rpm and 2000 rpm) at room temperature ($25 \pm 2^\circ\text{C}$) while the amount of iron and aluminum, concentration of dyes were kept constants. The results are summarized in figures (3.7.5.a, b, c, d, e, f, g and h). It is obviously clear that as the speed of agitation increases, the color is much faster removed.

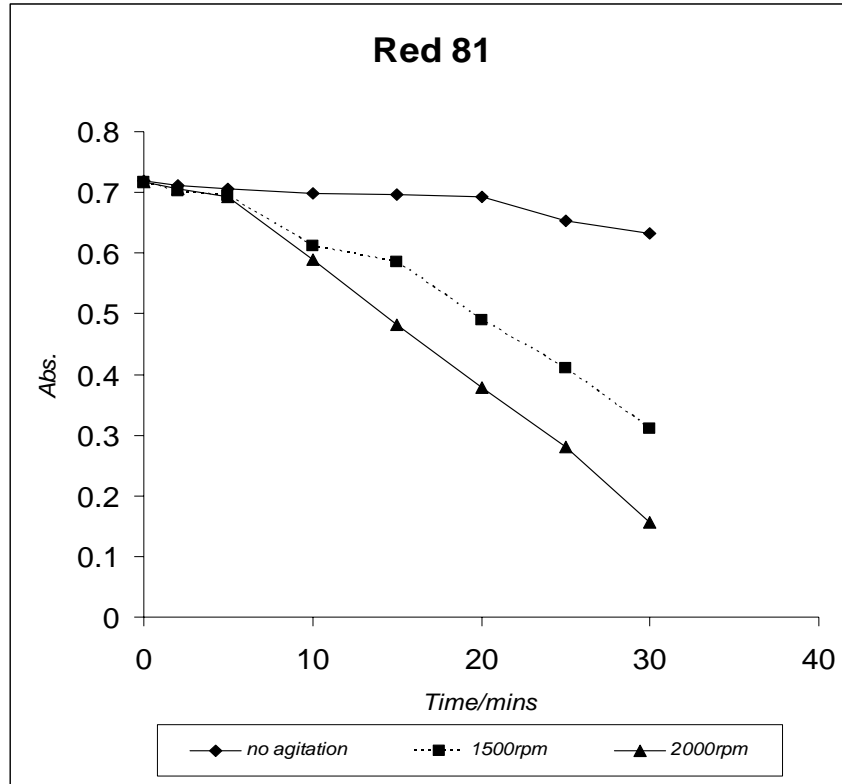


Figure 3.7.5.a. Effect of agitation speed on degradation of Direct Red 81 dye. Conditions: amount of Fe = 1 g/50 ml, [dye] = 20ppm, temperature ($25 \pm 2^\circ\text{C}$), $\lambda_{\text{max}}=510\text{nm}$ and pH= 6.1.

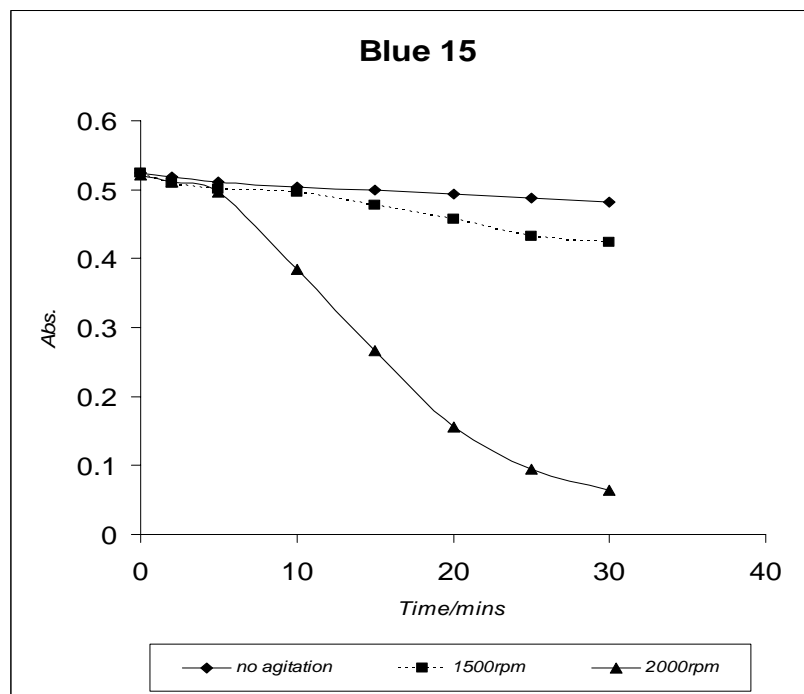


Figure 3.7.5.b. Effect of agitation speed on degradation of Direct Blue 15 dye. Conditions: amount of Fe = 1 g/50 ml, [dye] = 20ppm, temperature ($25 \pm 2^\circ\text{C}$), $\lambda_{\text{max}}=607\text{nm}$ and pH= 6.1.

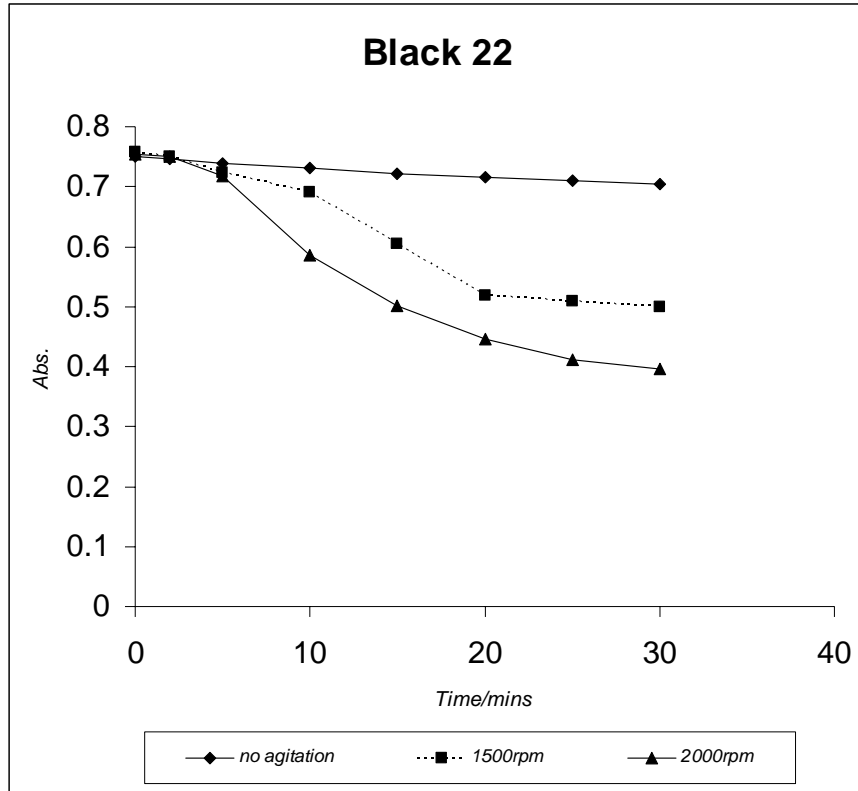


Figure 3.7.5.c. Effect of agitation speed on degradation of Direct Black 22 dye. Conditions: amount of Fe = 1 g/50 ml, [dye] = 50ppm, temperature ($25 \pm 2^\circ\text{C}$), $\lambda_{\text{max}}=484\text{nm}$ and pH= 6.1.

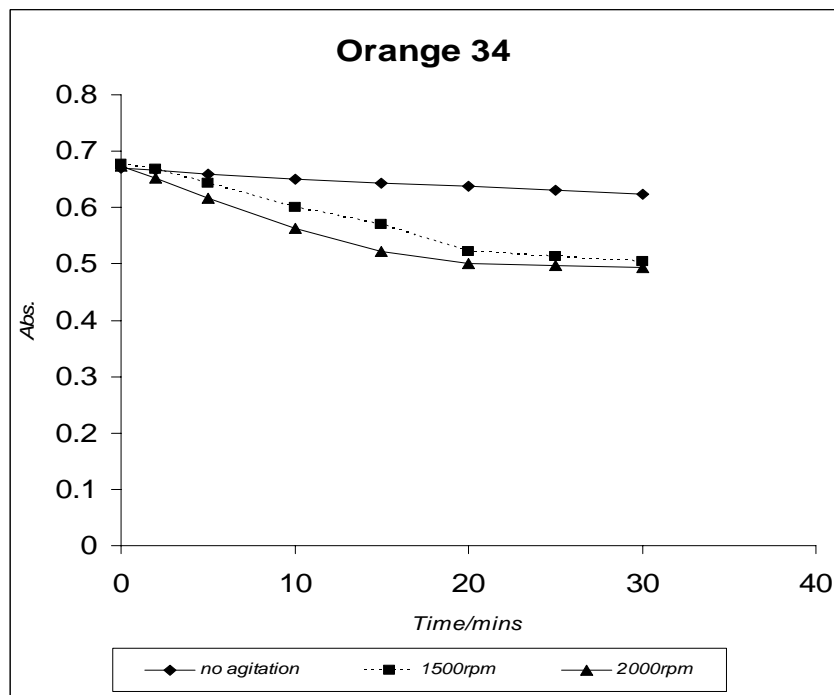


Figure 3.7.5.d. Effect of agitation speed on degradation of Direct Orange 34 dye. Conditions: amount of Fe = 1 g/50 ml, [dye] = 20ppm, temperature ($25 \pm 2^\circ\text{C}$), $\lambda_{\text{max}}=411\text{nm}$ and pH= 6.1.

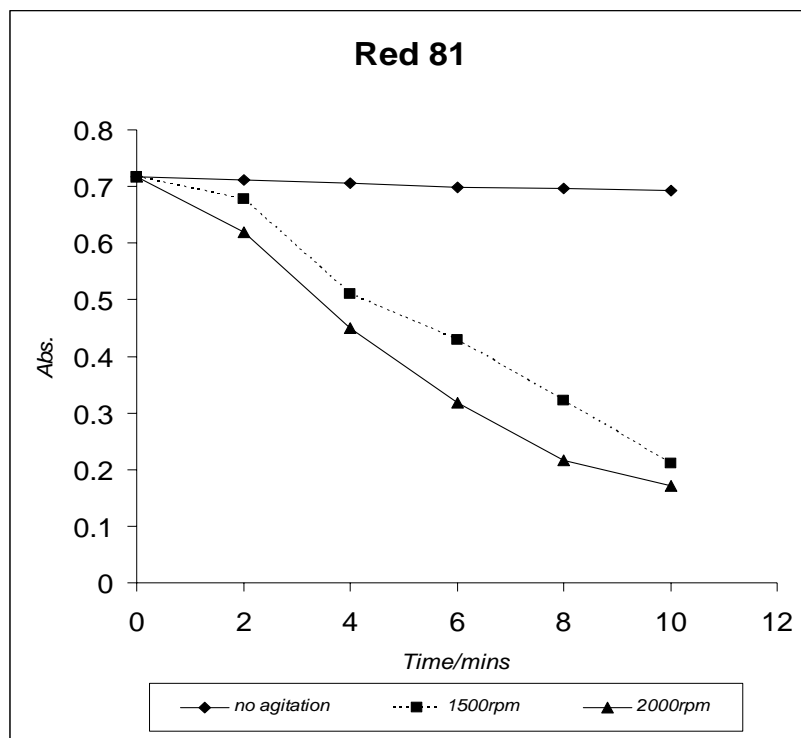


Figure 3.7.5.e. Effect of agitation speed on degradation of Direct Red 81 dye. Conditions: amount of Al= 0.5 g/50 ml, [dye] = 20ppm, temperature ($25 \pm 2^\circ\text{C}$), $\lambda_{\text{max}}=510\text{nm}$ and pH= 6.1.

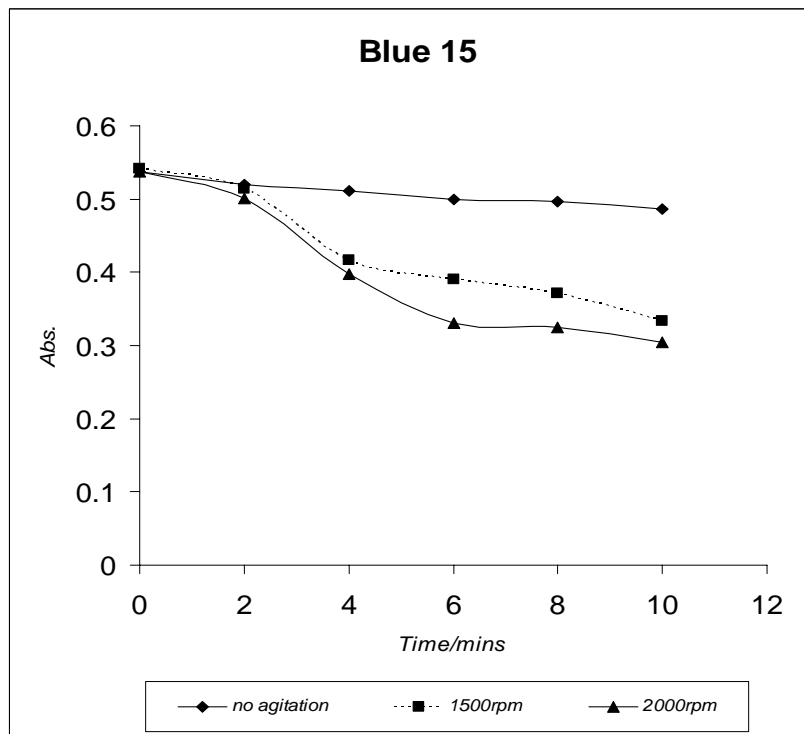


Figure (3.7.5.f). Effect of agitation speed on degradation of Direct Blue 15 dye. Conditions: amount of Al= 0.5 g/50 ml, [dye] = 20ppm, temperature ($25 \pm 2^\circ\text{C}$), $\lambda_{\text{max}}=607\text{nm}$ and pH= 6.1.

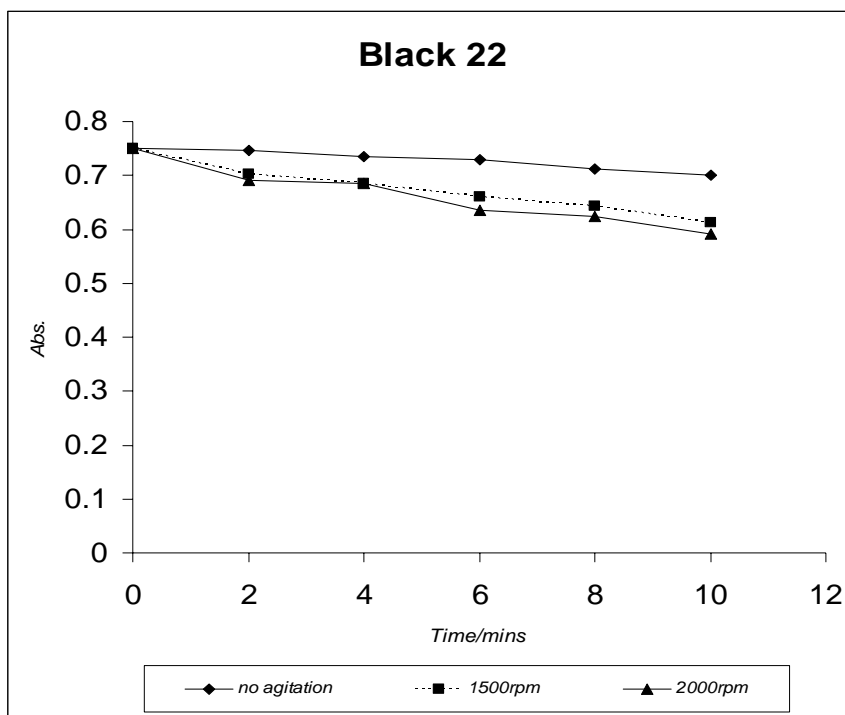


Figure 3.7.5.g. Effect of agitation speed on degradation of Direct Black 22 dye. Conditions: amount of Al= 0.5 g/50 ml, [dye] = 20ppm, temperature ($25 \pm 2^\circ\text{C}$), $\lambda_{\text{max}}=484\text{nm}$ and pH= 6.1.

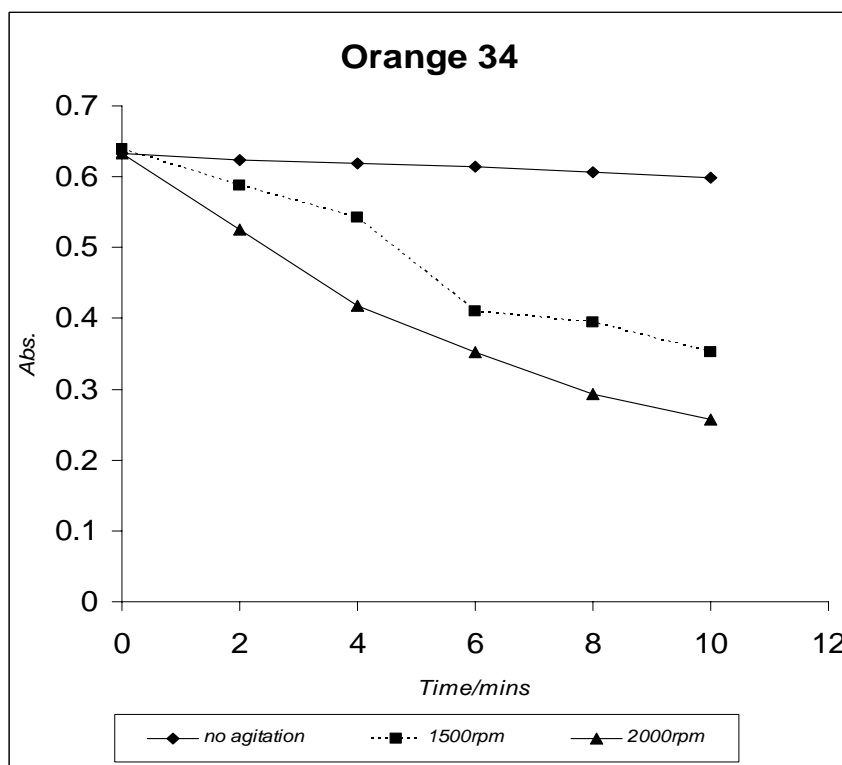


Figure 3.7.5.h. Effect of agitation speed on degradation of Direct Orange 34 dye. Conditions: amount of Al= 0.5 g/50 ml, [dye] = 20ppm, temperature ($25 \pm 2^\circ\text{C}$), $\lambda_{\text{max}}=411\text{nm}$ and pH= 6.1.

3.7.6 Effect of metals nature on degradation of aqueous Direct dyes

The effect of metals nature on degradation was studied. The following metals were used in this study (Mn, Ni, Co, Zn, Mg, and Cu). The experiments were carried out at constant concentration of the dye, time, temperature and pH. The results were presented in figures (3.6.5.a, b, c and d). It can be seen that using Cu do not effect the degradation rate, where using Al, Mg give a higher degradation rate compared to iron. This can be attributed to the standard electrode potential of these elements. There are other factors might affect the degradation rate of each dye; one of them the relative surface areas of the metal.

Table 3.7.6. Standard oxidation potentials (temperature = 25°C)

Half –cell Reaction	E° (volts)
$\text{Mg}_{(s)} \rightleftharpoons \text{Mg}^{2+} + 2e^-$	+ 2.36
$\text{Al}_{(s)} \rightleftharpoons \text{Al}^{3+} + 3e^-$	+ 1.67
$\text{Mn}_{(s)} \rightleftharpoons \text{Mn}^{2+} + 2e^-$	+ 1.18
$\text{Zn}_{(s)} \rightleftharpoons \text{Zn}^{2+} + 2e^-$	+ 0.76
$\text{Fe}_{(s)} \rightleftharpoons \text{Fe}^{2+} + 2e^-$	+ 0.44
$\text{Fe}^{2+} \rightleftharpoons \text{Fe}^{3+} + e^-$	- 0.77
$\text{Fe}_{(s)} \rightleftharpoons \text{Fe}^{3+} + 3e^-$	+ 0.04
$\text{Co}_{(s)} \rightleftharpoons \text{Co}^{2+} + 2e^-$	+ 0.28
$\text{Ni}_{(s)} \rightleftharpoons \text{Ni}^{2+} + 2e^-$	+ 0.24
$\text{Cu}_{(s)} \rightleftharpoons \text{Cu}^{+2} + 2e^-$	- 0.34

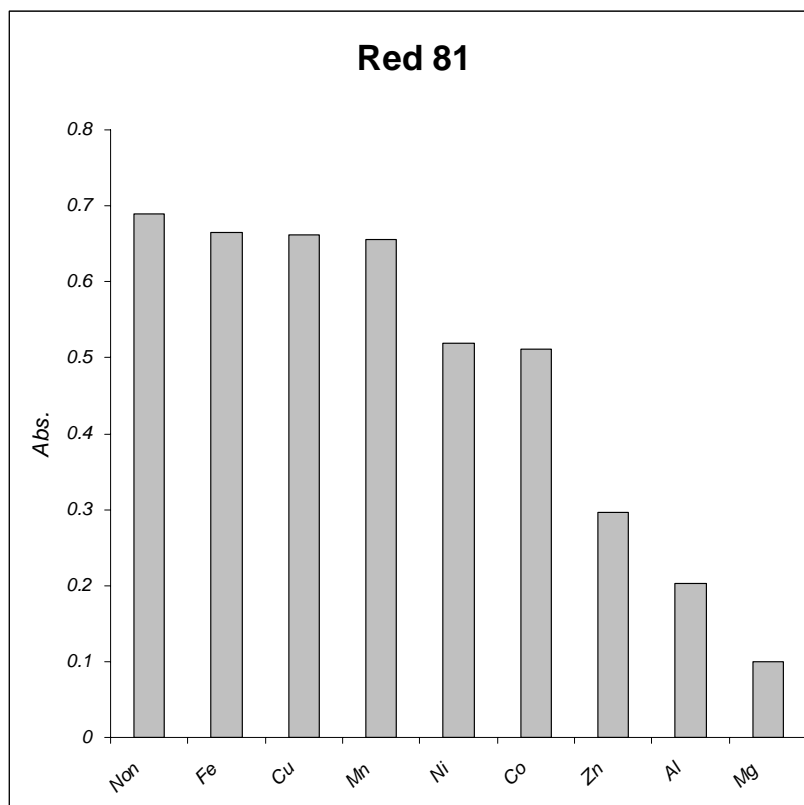


Figure 3.7.6.a. Effect of metals on degradation of Direct Red 81 dye. Conditions: metal amount = 1g/50ml, [dye] = 20ppm, pH = 6.1, time=5 min and temperature ($25 \pm 2^\circ\text{C}$).

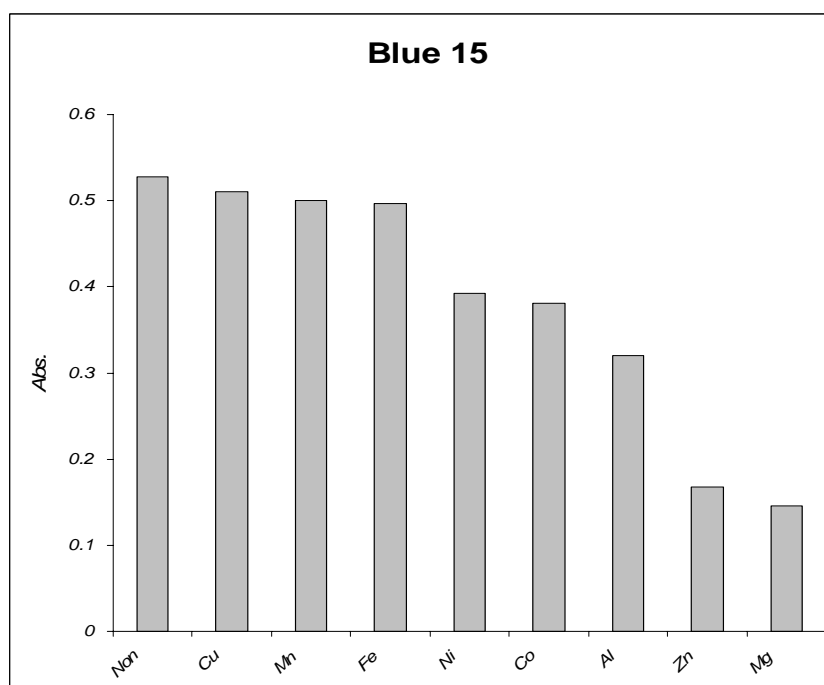


Figure 3.7.6.b. Effect of metals on degradation of Direct Blue 15 dye. Conditions: metal amount = 1g/50ml, [dye] = 20ppm, pH = 6.1, time=5 min and temperature ($25 \pm 2^\circ\text{C}$).

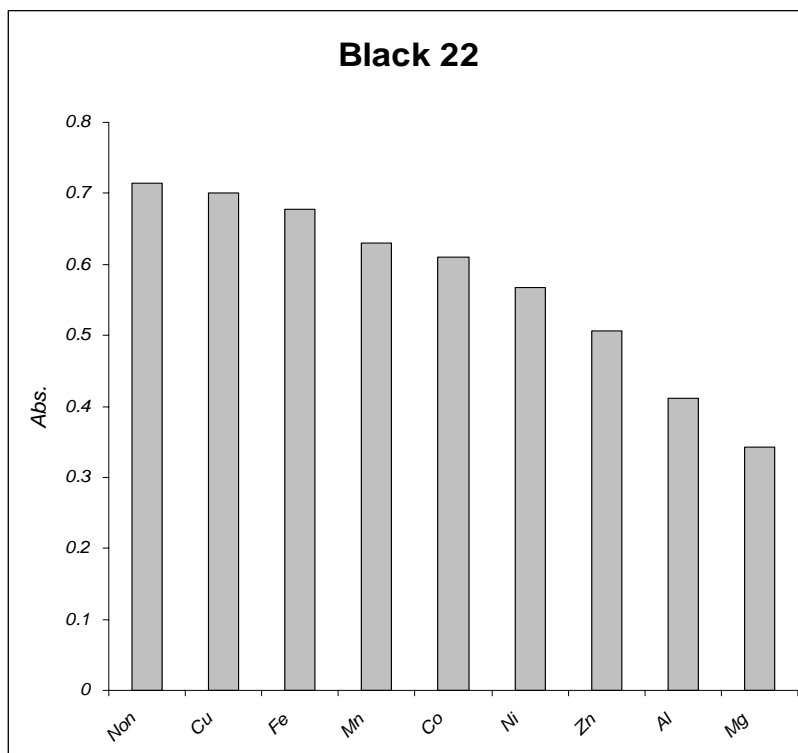


Figure 3.7.6.c. Effect of metals on degradation of Direct Black 22 dye. Conditions: metal amount = 1g/50ml, [dye] = 20ppm, pH = 6.1, time=5 min and temperature ($25 \pm 2^\circ\text{C}$).

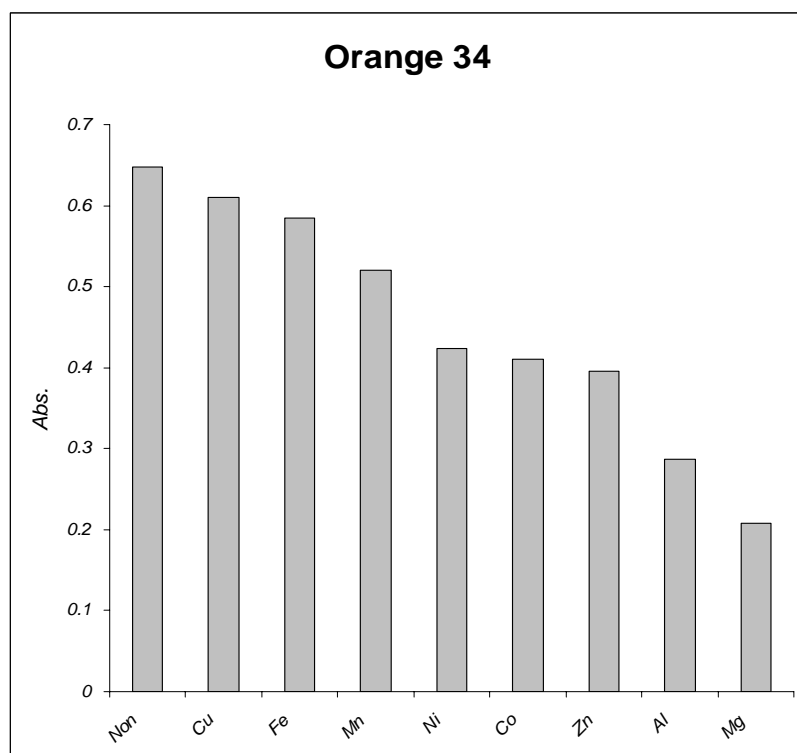


Figure 3.7.6.d. Effect of metals on degradation of Direct Orange 34 dye. Conditions: metal amount = 1g/50ml, [dye] = 20ppm, pH = 6.1, time=5 min and temperature ($25 \pm 2^\circ\text{C}$).

3.8 Degradation mechanism of Direct azo dyes

The primary question concerning the reaction mechanism whether reduction by zero-valent iron is a surface-mediated process. The reaction pathways involve either direct electron transfer from the zero-valent iron at the surface of the iron metal or reaction with dissolved Fe^{2+} or Fe^{3+} , which are products of iron corrosion.

To determine whether reduction by zero-valent iron is surface-mediated, the reaction of a dye molecules was studied in the solution phase of $\text{Fe}(\text{NH}_4)_2(\text{SO}_4)_2 \cdot 6\text{H}_2\text{O}$ and $\text{FeCl}_3 \cdot 6\text{H}_2\text{O}$. An observed lack of reduction argues favorably for a reaction mechanism involving a surface-mediated process. From the kinetic result obtained the following mechanism can be postulated. The mechanism involves the diffusion of the dye to the iron surface where it is adsorbed according to Langmuir adsorption model. The degradation reaction of Direct azo dyes using Fe^0 occurs on the surface of metal iron, when an interaction between dye molecules and iron happens iron as an electron donor loses electrons, the dye molecule as an electron acceptor accepts electrons from iron and combined with H^+ and turns into the transition product. This product gets electron from iron and combined with H^+ again, then it turns into terminal products. So pH and iron amount would affect the degradation reaction. The reaction products specified in the above mechanism were adsorbed.

The mechanism was supported by the disappearance of $-\text{N}=\text{N}-$, the formation of Fe^{2+} ion in the reaction mixture and the increase of the entropy values. Figure (3.8) shows the mechanism of Direct Red 81 dye as an example.

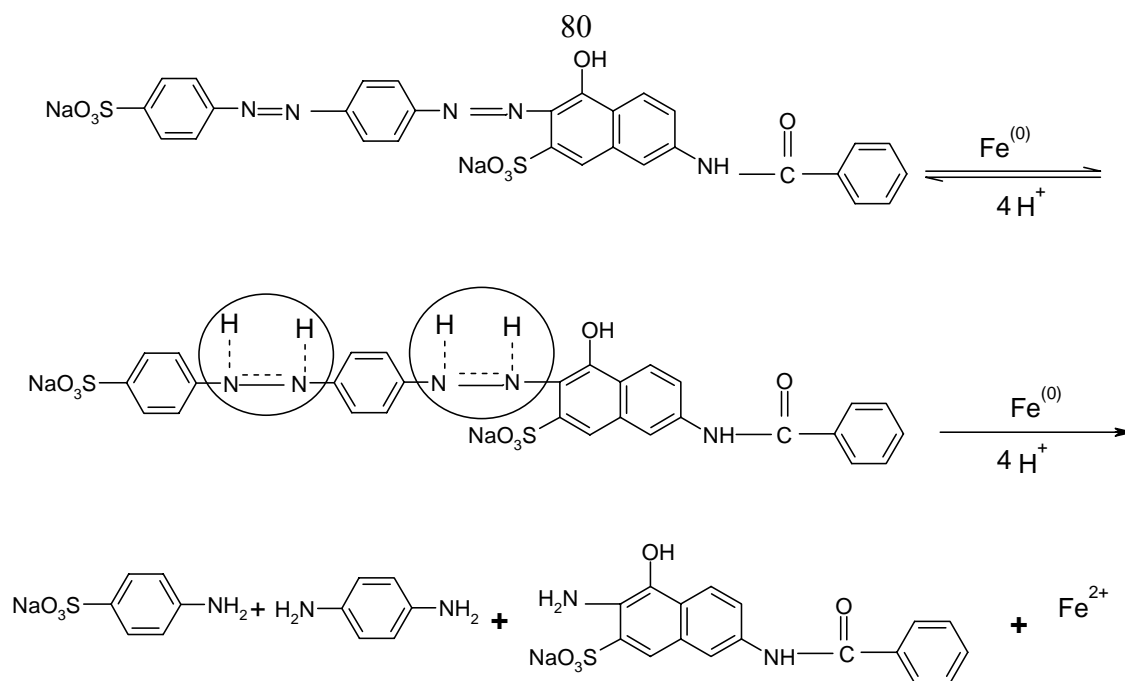


Figure 3.8. Degradation mechanism of Direct Red 81 dye in $\text{Fe}^{(0)} - \text{H}_2\text{O}$ system.

3.9 Results of degradation of Direct dyes

Infrared spectroscopy and absorption spectra were used to confirm the product of the reaction. The $-\text{N}=\text{N}-$ absorption band were followed before and after degradation of each dye. The results were presented in table (3.9) and figures (3.9.a, b, c and d).

Table 3.9. The $-\text{N}=\text{N}-$ absorption band before degradation.

Dye	Wave number of $-\text{N}=\text{N}-$ band
Direct Red 81	1496.7 cm^{-1}
Direct Blue 15	1504.4 cm^{-1}
Direct Black 22	1396.4 cm^{-1}
Direct Orange 34	1350.1 cm^{-1}

Figure (3.9.e) show the absorption spectrum for Direct Red 81 dye before and after degradation by iron. The absorption spectrum of degraded dye show a peak at $\lambda=240 \text{ nm}$ at which 1,4-phenylenediamine (produced from the degradation of the dye) absorbed light.

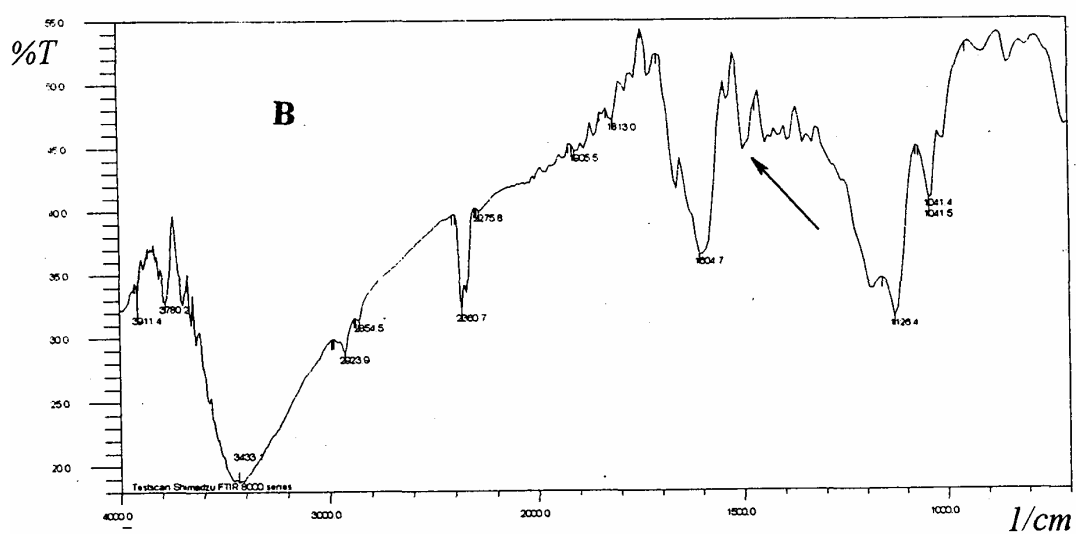
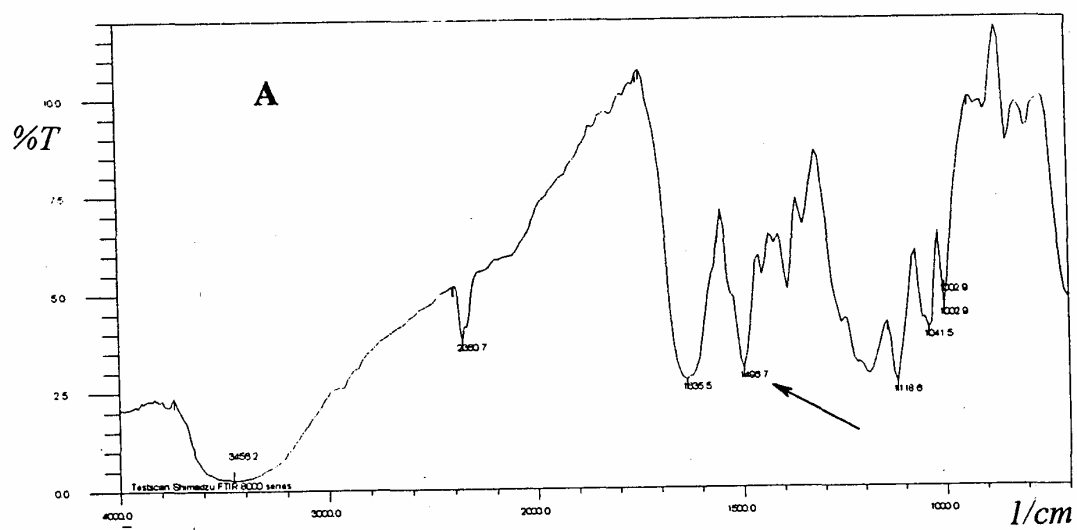


Figure 3.9.a. IR spectrum for Direct Red 81 dye (A) before degradation and (B) after degradation by iron.

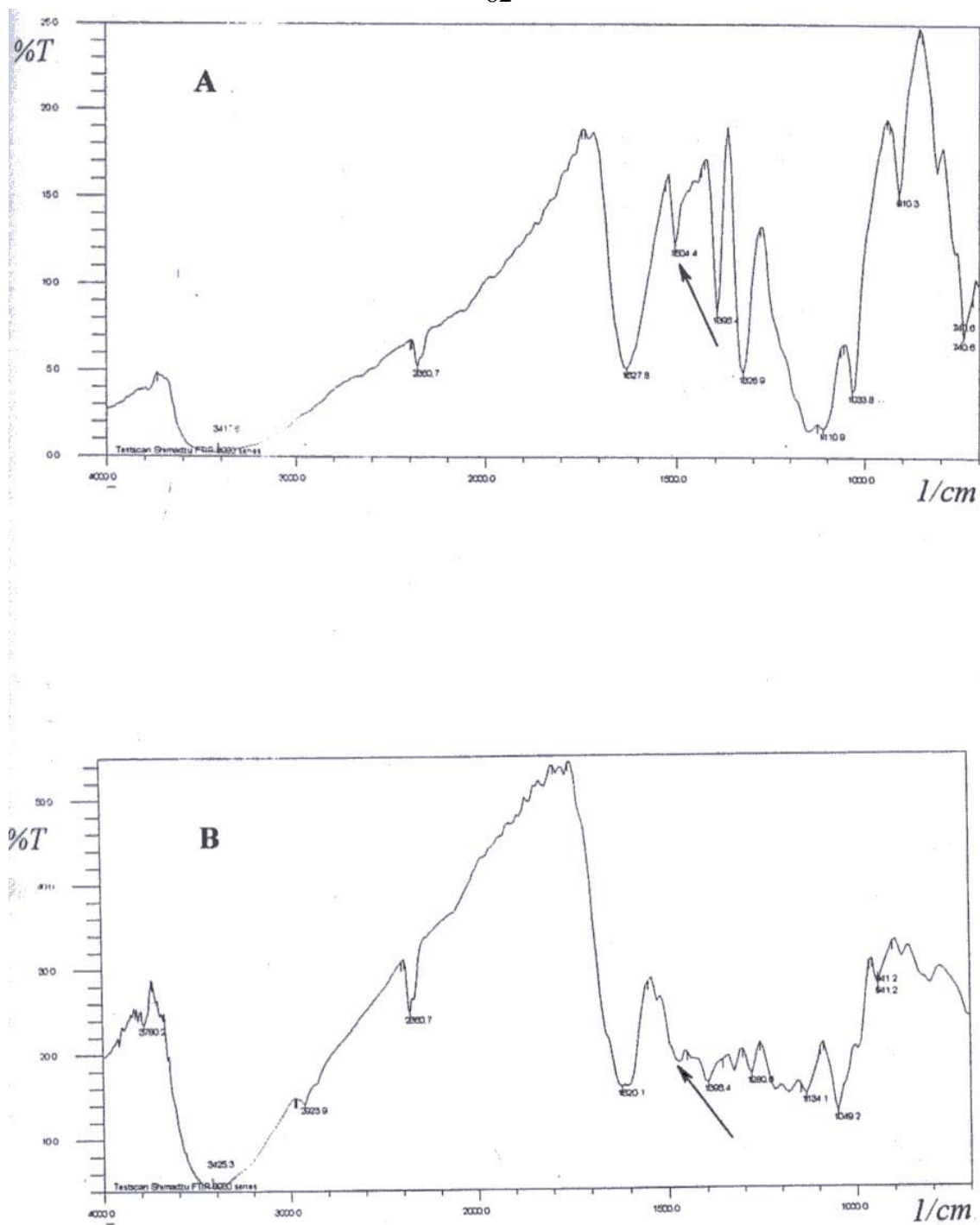


Figure 3.9.b. IR spectrum for Direct Blue 15 dye (A) before degradation and (B) after degradation by iron.

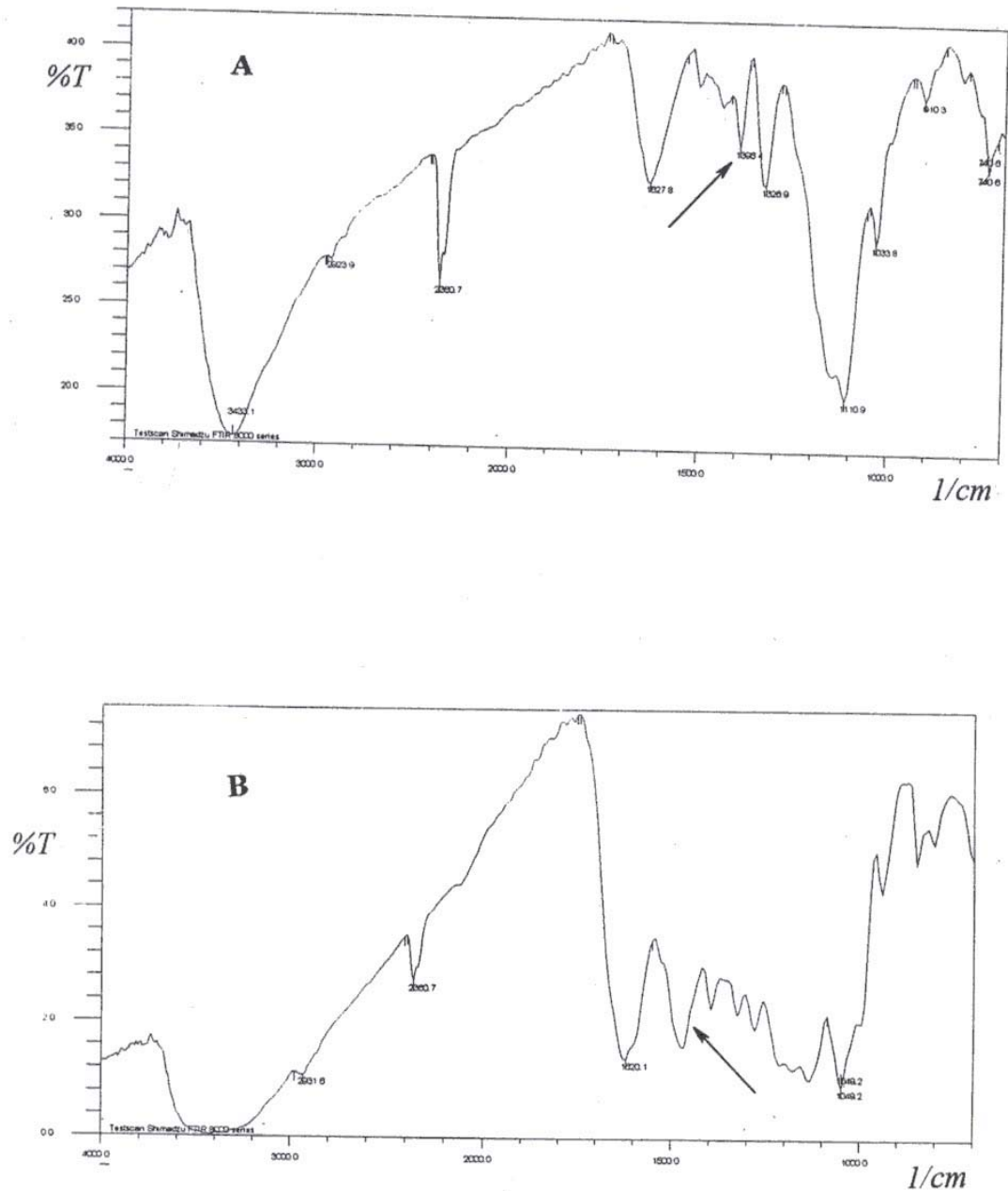


Figure 3.9.c. IR spectrum for Direct Black 22 dye (A) before degradation and (B) after degradation by iron.

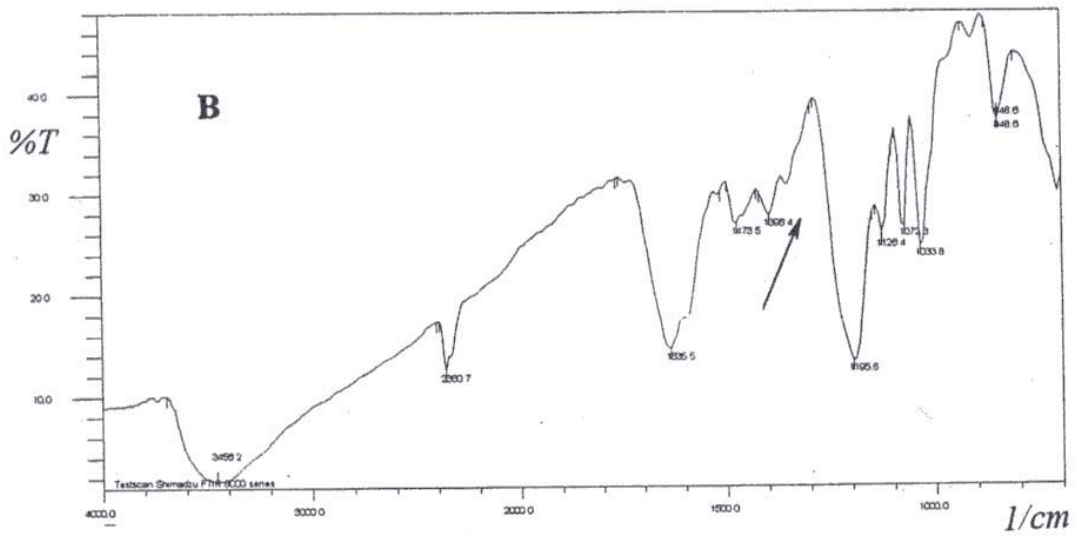
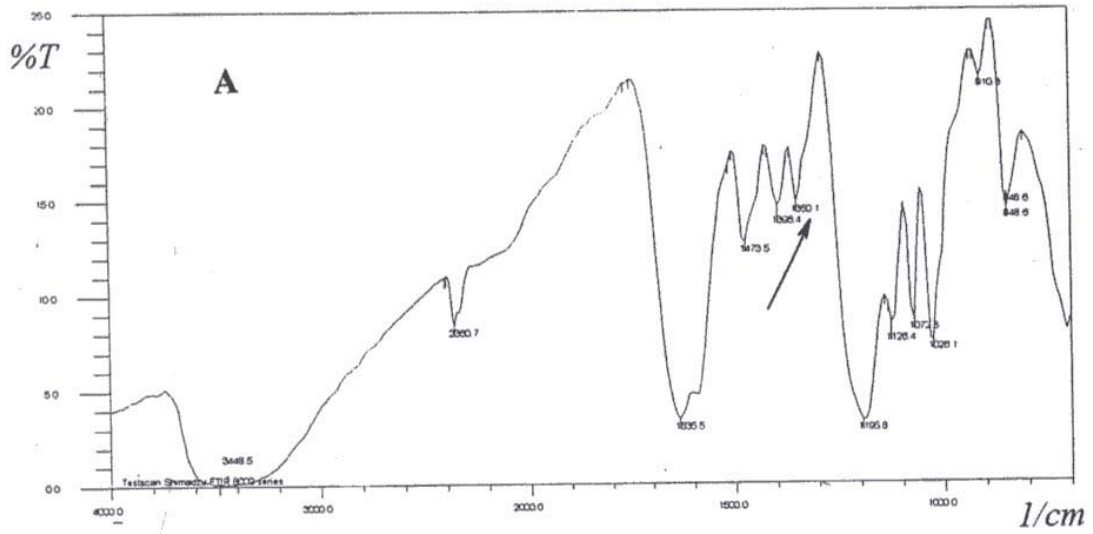


Figure 3.9.d. IR spectrum for Direct Orange 34 dye (A) before degradation and (B) after degradation by iron.

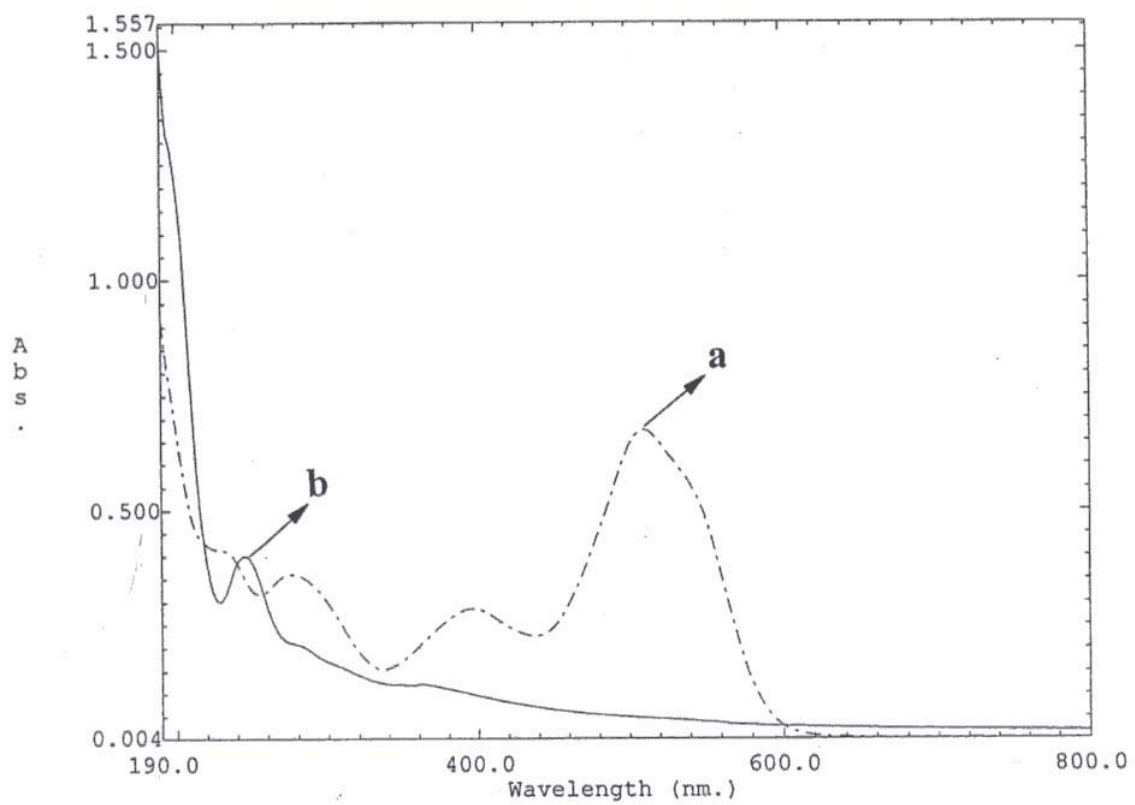


Figure 3.9.e. Absorption spectra for Direct Red 81 dye before degradation (a) and after degradation (b) by iron.

References

- Albanis, T.A., Hela, D.G., Sakellarides, T.M. and Danis T.G. (2000). Removal of dyes from aqueous solutions by adsorption on mixtures of fly ash and soil in batch and column techniques. *Global Nest: the Int. J.* Vol. 2, No. 3, pp. 237-244.
- Anliker, R. and Moser, P. (1987). The limits of bioaccumulation of organic pigments in fish: their relation to the partition coefficient and the solubility in water octanol. *Ecotoxicol. Environ. Saf.*, 13: 43-52
- Anliker, R., Clarke, E. A. and Moser. P. (1981). Use of the partition coefficient as indicator of bio-accumulation tendency of dyestuffs in fish. *Chemosphere*, 10 (263-274).
- Aplin, R. and Wait, T. (2000). Comparison of advanced oxidation process for degradation of textile dyes. *Water Sci. Technol.*, 42: 345-354.
- Bae, S., Motomura, H. and Morita, Z. (1997). Adsorption behavior of reactive dyes on cellulose. *Dyes and Pigments*, Vol. 34, pp. 37-55.
- Bell, J. and Buckley, C.A. (2003). Treatment of a textile dye in the anaerobic baffled reactor. *Water SA* Vol. 29, No. 2, pp.129-136.
- Brown, M.A. and De Vito, S.C. (1993) Predicting azo dye toxicity. *Crit. Rev. Env. Sci. Tec.*, 23: 249-324
- Chippindale, C. and Tacon, P.S.C., *The Archaeology of Rock-Art*. 1998: Cambridge University Press.
- Chung, K.T. and Cerniglia, C.E. (1992) Mutagenicity of azo dyes: Structure-activity relationships. *Mutat. Res.*, 277:201-220.
- Cooper, p. (1993). Removing color from dyehouse wastewaters - a critical review of technology available. *J. Soc. Dyers Col.*, 109: 97-101.
- Correia, V.M., Stephenson, T. and Judd, S.J. (1994). Characterization of textile wastewaters: a review. *Environ. Technol.* 15 (917-919).

- Coughlin, M.F., Kinkle, B.K. and Bishop, P.L. (2002). Degradation of acid orange 7 in an aerobic biofilm. *Chemosphere.*, 46: 11-19
- Davila-Jimenez, M.M., Elizalde-Gonzalez, M.P., Gutierrez-Gonzalez, and Pelaez-Cid, A.A. (2000). Electrochemical treatment of textile dyes and their analysis by high-performance liquid chromatography with diode array detection. *Journal of Chromatography A*, 889 (253-259).
- Deng, N., Luo, F., Wu, F., Xiao, M. and Wu, X. (2000). Discoloration of aqueous reactive dye solutions in the UV/Fe⁰ system. *Wat. Res.* Vol. 34, No. 8, pp. 2408-2411.
- ETAD (1997). German ban of use of certain azo compounds in some consumer goods. ETAD Information Notice No. 6, (Revised).
- Feng, J., Hu, X. and Yue, P., (2003). Degradation of Azo-dye Orange II by a photoassisted fenton reaction using a novel composite of iron oxide and silicate nanoparticles as a catalyst. *Ind. Chem. Res.*, 42:2058-2066.
- Fewson, C.A. (1998). Biodegradation of xenobiotic and other persistent compounds: causes of recalcitrance. *Trends Biotechnol.*, 6 (148-153).
- Fisher, Ch.-H., Bischof, M. and Rabe, L.G. (1990). Identification of natural and early synthetic textile dyes with HPLC and UV/VIS-spectroscopy by diode array detection. *Journal of Liquid Chromatography.*, 13(2), 319-331.
- Gholami, M., Nasser, S., Alizadehfard, M.R. and Mesdaghinia, A. (2003). Textile dye removal by membrane technology and biological oxidation. [www.cciwca/waric/38-2/38-2-379 htm](http://www.cciwca/waric/38-2/38-2-379.htm).
- Govert, f., Temmerman, E. and Kiekens P. (1999). Dvelopment of voltammetric sensors for the determination of sodium dithionite and indanthrene/indigo dyes in alkaline solutions. *Analytica Chimica Acta.*, 385:307-314.

- Grierson, Su. *Dyeing and Dyestuffs*. Aylesbury, Bucks: Shire Album 229, Shire Publications Ltd. 1989.
- Harbin D.N., Going J.E. and Breen J.J. (1990). A spectrophotometric method of estimating total levels of textile dyes on air monitoring filters. *American Industrial Hygiene Association*. 51 (4):185-193.
- Jaskot, R.H. and Costa D.L. (1994). Toxicity of an anthraquinone violet dye mixture following inhalation exposure, intratracheal instillation gavage. *Fundam. Appl. Toxicol.*, 22 (103-112).
- Jawabreh, M., (2003). Chromatographic and spectrophotometric determination of some Direct textile dyes before and after their degradation. Msc. Thesis. An-Najah National University, Nablus-Palestine.
- Jung, R., Steinle, D. and Ankliker, R. (1992) A compilation of genotoxicity and carcinogenicity data on aromatic aminosulphonic acids. *Food Chem. Toxicol.*, 30: 635-660.
- Koyuncu, I., (2003). Direct filtration of Procion dye bath wastewaters by nanofiltration membranes: flux and removal characteristics. *Journal of Chemical Technology & Biotechnology* , Vol. 78, No. 12, pp. 1219-1224.
- Krupa, N.E. and Cannon, F.S., (1996). Pore structure versus dye adsorption. *Am. Water Works Ass. J.*, 88: 94-108.
- Lorimer, J.P., Mason, T.J., Plattes, M., Phull S. S. and Walton, D. J. (2001). Degradation of dye effluent. *Pure Appl. Chem.*, Vol. 73, No. 12, pp. 1975-1968.
- Nikulina, G.L., Deveikis, D.N and Pyshnov, G. (1995). Toxicity dynamics of anionic dyes in air of a work place and long term effects after absorption through skin. *Med. Tr. Prom. Ekol.*, 6 (25-28).

- Novotna, P., Pacakova, V., Stulik, K. and Bosakova, Z. (1999). High-performance liquid chromatographic determination of some anthraquinone and naphthoquinone dyes occurring in historical textiles. *Journal of Chromatography A*, 863 (235-241).
- Ollgaard, H., Frost, L., Galster, J. and Hasen, O.C.(1998). *Survey of azo-colorants in Denmark: Consumption, use, health and environmental aspects.*, Ministry of Environment and Energy, Denmark.
- O'Neill, C., Hawkes, F.R., Hawkes, D.L., Lourenco, N.D., Pinheiro, H.M. and Delee, W. (1999) Colour in textile effluents-sources, measurement, discharge consents and simulation: a review. *J. Chem. Technol. Biotechnol.*, 74: 10009-10018.
- Oxpring, D.A., McMullan, G., Smyth, W.F. and Marchant, R. (1996). Decolourisation and metabolism of the reactive textile dye. Remazol Black B, by an immobilized microbial consortium. *Biotech. Lett*, 18:527-528.
- Padmavathy, S., Sandhya, S., Swaminathan, K., Subruhmanyam, Y.V., Chakrabarti, T. and Kaul, S. N. (2003). Aerobic decolorization of Reactive azo dyes in presence of various cosubstrates. *Chem Biochem. Eng. Q.* 17(2) 147-151.
- Pala, A., Tokat, E. and Erkaya, H. (2003) Removal of some Reactive Dyes from Textile Processing Wastewater Using Powered Activated Carbon. *Proceedings of the First International Conference on Environmental Research and Assessment Bucharest, Romania.*
- Park, H. and Choi, C. (2003). Visible light and Fe(III)-mediated of Acid Orange 7 in the absence of H₂O₂ . *Journal of Photochemistry and Photobiology A: Chemistry* 159:241-247.

- Perez-Urquiza M., Part M.D. and Beltran J.L. (2000). Determination of sulphonated dyes in water by ion-interaction high-performance liquid chromatography. *Journal of Chromatography A*, 871 (227-234).
- Perez-Urquiza, M., Ferrer, R. and Beltran, J.L., (2000). Determination of sulfonated azo dyes in river water samples by capillary zone electrophoresis. *Journal of Chromatography A*, 883(277-283).
- Prakash, A. AND Solank, S. (1993). Sorption and desorption behavior of phenol and chlorophenols on guar derivatives: *reclamation of textile effluents, Research and Industry*, 38 (35-93).
- Preiss, A., Sanger, U., Karfich, N. and Levsen, K. (2000) Characterization of dyes and other pollutants in the effluent of a textile company by LC/NMR and LC/MS. *Anal. Chem.*, 72:992-998.
- Rafi, F., Franklin, W. and Cerniglia, C.E. (1990). azoreductase activity of anaerobic bacteria isolated from human intestinal microflora. *Appl. Environ. Microbiol.*, 56:2146-2151.
- Rafols, C. and Barcelo, D. (1997). Determination of mono- and disulphonated azo dyes by liquid chromatography-atmospheric pressure ionization mass spectrometry. *Journal of Chromatography A*, 777 (177-192).
- Shu, H. and Huang, C.R., (1995). *Chemosphere*, Vol. 31, No. 8, pp. 3813-3825.
- Siren, H. and Sulkava, R. (1995). Determination of black dyes from cotton and wool fibers by capillary zone electrophoresis with UV detection: application of marker technique. *Journal of Chromatography A*, 717 (149-155).
- Su, J.C. and Horton, J.J. (1998). Alergic contact dermatitis from azo dyes. *Australas. J. Dermatol.*, 39 (1) 48-49.

- Taicheng, A., Haofei, G. and Xiong, Y. (2003). Decolourization and COD removal from reactive dye-containing wastewater using sonophotocatalytic technology. *Society of Chemical Industry.*, 78:1142-1148.
- Tayem, N. (2002). Behaviour and determination of some textile dyes in soil, sewage and drinking water. Msc. Thesis. An-Najah National University, Nablus-Palestine.
- Vandevivere, P.C., Bianchi R. (1998). Treatment and reuse of wastewater from the textile wet –processing industry: Review of emerging technologies. *J. Chem. Technol. Biotechnol.*, 72: 289-302.
- Vinodgopal, K., Peller, J., Makogon, O. and Kamat, V. (1998). Ultrasonic mineralization of a Reactive textile azo dye, Remazol Black B. *Wat. Res.* Vol. 32, No. 12, pp. 3646-3650.
- Welham, A. (2000) The theory of dyeing (and the secret of life). *J. Soc. Dyers Colour.*, 116: 140-143.
- Yinon, J. and Saar, J. (1991). Analysis of dyes extracted from textile fibers by thermospray high-performance liquid chromatography-mass spectrometry. *Journal of Chromatography*, 568 (73-84).
- Zanoni, M.V.B., Fogg, A.G., Berek, J. and Zima, J. (1997). Electrochemical investigations of reactive dyes; cathodic stripping voltammetric determination of anthraquinone-based chlorotriazine dyes at a hanging mercury dropelectrode. *Analytica Chimica Acta.*, 349:101-109.
- Zee, F.P. (2002). Anaerobic azo dye reduction . Ph.D. thesis. Wageningen University, Wageningen-Netherlands.

- Zhang, Y., Hou, W., and Tan, Y. (1997). Structure and Dyeing Properties of some Anthraquinone Violet Acid Dyes. *Dyes and Pigments*, Vol. 34, No. 1, pp. 25-35.
- Zollinger, H. (1987) Color Chemistry- Synthesis, Properties and Application of Organic Dyes and Pigments. VCH New York, PP. 92-102.
- Zu'bi, A. (2003). Voltammetric and HPLC determination of some textile dyes. Msc. Thesis. An-Najah National University, Nablus-Palestine.

.

..

J.

.
..

-:

(Direct Red 81, Direct Blue 15, Direct Black 22 and Direct Orange 34)
(HPLC)

.(RPC₁₈)

N-Cetyl-N,N,N-trimethylammonium bromide (CTAB)-:

acetonitrile: water :

CTAB

-:

0.5–10ppm

10–30ppm

0.3–10ppm

% RSD

1–12

ت
1.13 % 0.83 % 0.92 % :
10 ppm (n=3) 0.34 %